ISBN 978-82-326-6378-1 (printed ver.)
ISBN 978-82-326-5910-4 (electronic ver.)
ISSN 1503-8181 (printed ver.)
ISSN 2703-8084 (electronic ver.)

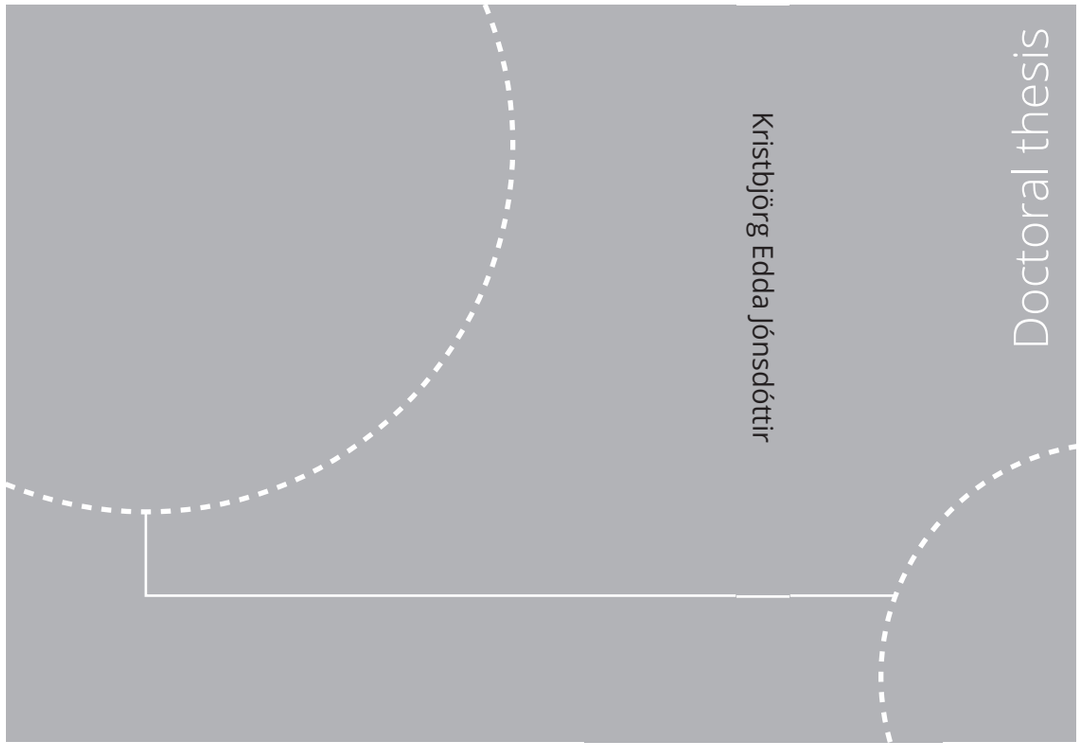

Doctoral theses at NTNU, 2021:133

Kristbjörg Edda Jónsdóttir

Current flow processes at full-scale Atlantic salmon farm sites

NTNU
Norwegian University of
Science and Technology

Doctoral theses at NTNU, 2021:133

NTNU
Norwegian University of
Science and Technology
Thesis for the degree of
Philosophiae Doctor
Faculty of Information Technology
and Electrical Engineering
Department of Engineering Cybernetics

NTNU
Norwegian University of
Science and Technology

Kristbjörg Edda Jónsdóttir

Current flow processes at full-scale Atlantic salmon farm sites

Thesis for the degree of Philosophiae Doctor

Trondheim, April 2021

Norwegian University of Science and Technology
Faculty of Information Technology
and Electrical Engineering
Department of Engineering Cybernetics

NTNU
Norwegian University of Science and Technology

Thesis for the degree of Philosophiae Doctor

Faculty of Information Technology
and Electrical Engineering
Department of Engineering Cybernetics

ISBN 978-82-326-6378-1 (printed ver.)
ISBN 978-82-326-5910-4 (electronic ver.)
ISSN 1503-8181 (printed ver.)
ISSN 2703-8084 (electronic ver.)

Doctoral theses at NTNU, 2021:133
ITK-report: 2021-2-W

Printed by Skipnes Kommunikasjon AS

Summary

The aquaculture industry has grown exponentially the last 30 years. In Norway the Atlantic salmon is the dominant species and the rapid growth of the industry has led to both challenges and controversy. The issues faced by the industry are multifaceted and two of the most pressing issues that hinder expansion of the industry are lack of space and salmon lice. Several different solutions are employed to reduce the salmon lice infestation. Some argue that prevention based methods such as the lice shielding skirt may be the solution, while others suggest that both issues can be solved by moving to more exposed farm sites.

Independently of farm design all production units at sea must take into consideration the impact of the ocean currents. This holds particularly true for exposed sites where the ocean current is expected to have periods of stronger and more persistent water flow. For cages based on the traditional "Grøntvedt" design that utilises nets to keep the fish, the current flow plays a vital role in how dissolved oxygen, nutrients, waste and food pellets and transported through and downstream of the cage. As the current passes through the net the speed is reduced and a portion of the current is diverged around the cage. At exposed sites, this reduction may be beneficial with regards to the wellbeing of the fish. However, at more sheltered sites weak currents may lead to poor water exchange resulting in low dissolved oxygen levels which are necessary for the fish to thrive. The use of lice shielding skirts to fend off the salmon lice can further reduce the current flow and result in an unhealthy environment for the fish.

The main objective of this thesis was to gain new insight into the current flow at full-scale sites and inside the cages. Specifically the interest was how current conditions at exposed sites could be evaluated using fish welfare criteria, and how lice shielding skirts influenced the current conditions. As the current flow at individual sites depend on many factors such as topography, hydrography, farm layout, cage design and more, this was

studied through collecting existing long-term data sets from five sites along the Norwegian coastline, as well as designing and executing three full-scale experiments.

A classification scheme based on the swimming capacities of Atlantic salmon was developed and applied on the current flow data from the five sites to evaluate if fish welfare was maintained for Atlantic salmon and lumpfish. Only one of the five sites was found acceptable for lumpfish, while four were found acceptable for small salmon post-smolt. The full-scale experiments investigated different aspects of the interaction between lice shielding skirts and current flow. The first studied the impact of a non-permeable tarpaulin skirt on the current flow field inside the cage, while the second established the characteristic current flow field around a conical sea cage equipped with a permeable skirt. The results indicated that the influence of the conical cage on the downstream current disappeared as the diameter of the cage decreased with depth. The reduction in current speed was established for both of these cages and were higher than reduction through non-shielded cages. Finally, the impact of shielding skirt on dissolved oxygen levels inside cages were determined at two hydrographically different sites, revealing a complex interaction between dissolved oxygen level, skirt, ocean currents and local stratification.

Preface

This thesis is submitted in partial fulfilment of the requirements for the degree of Philosophiae Doctor (Ph.D.) at NTNU – the Norwegian University of Science and Technology.

This work has been performed at the department of Engineering Cybernetics (ITK) under the supervision of Associate Professor Jo Arve Alfredsen, Dr. Zsolt Volent at Sintef Oceans and Associate Professor Morten Omholt Alver.

Funding has been provided by the RACE research grant program funded by SINTEF Ocean through the research project "Water currents in fish farms at site scale". The enclosed work was undertaken from 2016 to 2020.

The focus of this thesis is on the Atlantic salmon farming industry in Norway and builds heavily on full-scale experimental work carried out in Norway. The details of each study will not be recited in its entirety in this thesis, instead the interested reader is referred to the enclosed papers for a more comprehensive description of the experiments. As the marine aquaculture industry is multi-disciplinary the thesis will consider several topics ranging from biology, oceanography, instrumentation and policy. It is my hope that for those new to marine aquaculture this thesis can function as an introduction to the many relevant research issues of the industry, and for those more informed as a brief and useful review.

Acknowledgments

First and foremost, I would like to extend my gratitude to Jo Arve Alfredsen for his input, guidance and support through these four years. The many good discussions have been both informative and uplifting when my motivation faltered. I would also like to underline my gratitude to Zsolt Volent for not only facilitating the execution of full-scale measurements, but his patience in carrying them out with me in addition to our many discussions. This thesis

would not have come to fruition had it not been for the collaboration with Zsolt and SINTEF Ocean.

On that note, there are many at SINTEF Ocean whose input and collaboration has been much appreciated. I would specifically like to mention Pascal Klebert for discussions about the data and data processing, Magnus Oshaug Pedersen, Birger Venås and Terje Bremvåg for support at carrying out the full-scale measurements at Hosnaøyan (2018), Siri Vassgård for support at Soløya and Fornes (2019), and Eleni Kelasidi and Andreas Hagemann for providing images for the thesis. I'd also like to thank SINTEF ACE for access to equipment, and SalMar AS, Ellingsen Seafood AS, Nordlaks Oppdrett AS and SinkabergHansen AS for access to their sites, and the support from their on-site staff when we were carrying out our studies.

There are many at ITK who have been essential for the execution of my PhD, and especially during my time as teaching assistant and lecturer. Firstly, I would like to thank Terje Haugen, Stefano Bertelli, Glenn Angell and Gunnar Aske for being ever helpful and cheerful. Secondly, I would like to thank Rune Mellingseter and Knut Anders Reklev for solving all my course related issues. And lastly, Tove Kristin Blomset Johnsen, Eva Løfshus Amdahl and Lill Hege Pedersen for always having a solution at hand.

To mention the many fellow PhD candidates which have made an impact through the years would take far too much space, hence I will only mention two by name, but know that there are many and they have all contributed to the shared effort of keeping my spirits high. Firstly, Linn Danielsen Evjemo, I am forever grateful that we ended up sharing an office. Despite not working on anything remotely similar, you have been a pivotal part for the completion of this thesis. With outrageous amounts of coffee and a willingness to always lend an ear, you have had to endure my rants and moments of poor concentration. I pity anyone who's office was near ours, for our many discussions have certainly been a disturbance. Secondly, Waseem Hassan, one of the few marine aquaculture PhD candidate at ITK. I am truly grateful for the academic discussions and coffee breaks we've had the last four years. It has been highly beneficial to have someone to talk to that knows the frustrations of full-scale experimental work.

I'd also like to extend my gratitude to my many friends in Trondheim, Oslo and elsewhere. To mention some: Ada, Andrea, Ida, Kristina, Marit, and Synne, thank you for our mandatory cabin trips and Christmas dinners, and encouraging words when I've been down in the dumps. And of course my family, especially my parents Katrín and Jón, and my brother Siggi, for general enthusiasm regarding my PhD and support in life. Also

my grandparents, Amma Bogga, Amma Edda and Afi Siggi, for their continuous interest in my work, and my grandfather's many stories of life at sea.

Lastly, I'd like to thank Sunny, not only for introducing me to the necessity of having a dog in one's life, but his unwavering support and encouragement throughout the years. Covid-19 may have halted some of our planned adventures, but I'm confident we'll have many more to come, and I look forward to all of them.

This work would not have been completed without the combined support from all of those mentioned above and many more. To all of you I would like to express a most heartfelt thank you.

Contents

Chapter 1

Introduction

1.1 Atlantic salmon farming in Norway

By 2050 the current world population of 7.7 billion is predicted to increase to 9.7 billion (UN, 2019). To avoid food shortage it is necessary to enhance food production. Increased production from the ocean is suggested as a solution as an expansion in agriculture is not feasible due to limited available arable land and freshwater sources (Marra, 2005; Duarte et al., 2009). Food production from the ocean comprises fisheries and aquaculture industry. Global fisheries can not be expected to meet the raising demands of the future population as an increase in production would mean forfeiting sustainable fishing levels (FAO, 2020). Aquaculture on the other hand has increased production by 527% from 1990 to 2018 with a total of 114 mill tonnes in 2018, where 31 mill tonnes were aquatic animals from marine aquaculture (Fig. 1.1) (FAO, 2018, 2020). Since 2014 the aquaculture industry has provided more than half of the fish and shellfish consumed by humans (FAO, 2020).

Aquaculture is the breeding, rearing and stock raising of fish, crustaceans, molluscs, and cultivating of aquatic plants in marine and freshwater. Freshwater fish is the largest sector in the industry (Fig. 1.1), however an expansion within this sector is limited by the same factors as agriculture. It is instead the marine aquaculture sector that has the greatest potential for expansion and increased production (Marra, 2005; Duarte et al., 2009).

The Norwegian aquaculture production consists mainly of Atlantic salmon (Fig. 1.1). Globally 2.4 mill tonnes Atlantic salmon were produced in 2018, with 53% produced in Norway (FAO, 2020). Aquaculture in Norway has a long history, with the earliest record of cultivating fish in freshwaters written on a runestone sometime around 1050-1100 stating: “Eiliv Elg carried fish

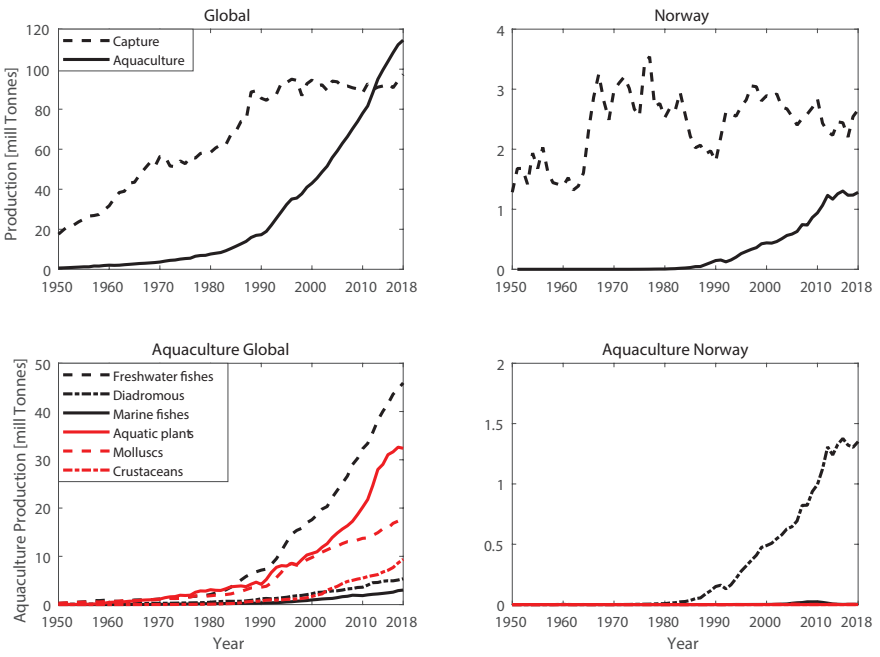

Figure 1.1: Production from capture and aquaculture industries globally and in Norway from 1950 to 2018. The second row shows the production of the main aquaculture industries globally and in Norway. Atlantic salmon are included in the diadromous fish. Data from FAO (2018).

to Raudsjø" (Hesthagen and Kleiven, 2016). Breeding and hatching of fish started in the 1850's, but the production of Atlantic salmon in Norway did not start until the 1960s (Tilseth et al., 1991; Nash, 2011). Before the 1960s there had been several trials at rearing Rainbow Trout, but Atlantic salmon quickly became the dominating species due to technical advancements in the rearing of anadromous fish combined with the higher market price and greater marketing potential (Tilseth et al., 1991; Nash, 2011).

The Atlantic salmon is an anadromous fish, meaning it is born in freshwater, but spends most of its adult life in saltwater. The production of Atlantic salmon is therefore divided into two phases. The first phase takes place on land in freshwater tanks, and the second phase takes traditionally place in cages out at sea. When the fertilized egg is hatched, the salmon is known as an alevin. From there it develops into fry and then parr. The parr then goes through the process of smoltification where it turns into a smolt

Figure 1.2: Picture of SINTEF ACE facilities Rataren, Frøya, Norway, consisting of 8 cages arranged in a 2x4 matrix. (Photo: Magnus Oshaug Pedersen, SINTEF Ocean, shared with permission).

by going through a number of physiological changes to adapt to a life in seawater (Thorstad et al., 2011; Bjelland et al., 2015). For farmed Atlantic salmon it takes roughly 10-16 months from being hatched to smoltification takes place, however through selective breeding there are now smolts which are ready after 8 months (Asche and Bjørndal, 2011). For the wild salmon this process can take anywhere between 1 and 8 years (Thorstad et al., 2011). After the process of smoltification, the salmon is adapted to sea water and can be transferred to the fish cages out at sea. This phase is known as the grow-out phase.

The grow-out phase has traditionally occurred in fish farms located within fjords and along the coastline, sheltering the farm from extreme weather conditions. The farm usually consists of several cages, where the number of cages and how these are arranged varies between farms (see Fig. 1.2 for an example of a 2x4 farm organisation). There are many cage designs available, and these can be categorized based on three main properties: position in the water column (floating, submersible, submerged), type of net (rigid or flexible) and containment method (open or closed) (Lekang, 2020; Chu et al., 2020).

Since 2015 there has been a rapid development of new designs in Norway spurred on by the Norwegian government's development permits. These permits were awarded by the Fisheries Directorate to farms that had developed new concepts with substantial innovation. Currently most cages in Norway are in principle modelled after the "Grøntvedt cage" created by the brothers

Sivert and Ove Grøntvedt in the late 1960s (Nash, 2011), and can be categorised as open net floating flexible cages (Lekang, 2020; Chu et al., 2020). These cages consist of a surface collar structure from which a net is hung (Fig. 1.3). The net is weighed down, often by a sinker ring resulting in the net having a cylindrical shape above this ring, and a conical beneath it (see Fig. 1.4).

Each cage is allowed to hold up to 200 000 fish. During the grow-out phase farming operations consist of tasks like feeding and size grading, but also monitoring water quality, fish welfare and fish density in each cage (Bjelland et al., 2015). The grow-out phase lasts 12 to 18 months (Asche and Bjørndal, 2011). Following the grow-out phase the salmon are transported to shore for slaughtering, processing and packaging. How fast and how successful the grow-out phase is depends on controllable variables such as smolt quality, feeding and light (Asche and Bjørndal, 2011), and uncontrollable variables such as water temperature, current conditions and seasonable variability among others.

Since 2012 the near exponential growth in Atlantic salmon farming in Norway has leveled off (FAO, 2018, 2020), and in recent years the salmon farming has consolidated with fewer farmers and locations. The number of locations decreased from around 1900 in 1991 to 1000 in 2011 while production doubled (Gullestad et al., 2011). This intensification of the production has led to both controversy and challenges related to the grow-out phase which must be solved for further growth of the industry (Marra, 2005; Troell et al., 2014).

Figure 1.3: Cage at SINTEF ACE facilities Rataren, Frøya, Norway, with a diameter of 50 m showing the floating collar, feeding system and the cage net strung up on the inside (green net). (Photo: Magnus Oshaug Pedersen, SINTEF Ocean, shared with permission).

1.2 Overview of challenges and developments in marine aquaculture

Two of the main challenges the marine aquaculture industry must tackle to become a sustainable industry is its reliance on terrestrial crops and wild fish for feed, and its impact on the aquatic ecosystem (Marra, 2005; Duarte et al., 2009; Troell et al., 2014; Röcklinsberg, 2015). As cages are placed out at sea the stock are affected by the environment, but the production can also influence the wider environment as illustrated in Fig. 1.4 (Lekang et al., 2016).

The presence of a fish farm influences the local and regional ecosystem through the discharge of nutrients, excess feed and faeces (Grefserud et al., 2019). The consequences of the interaction between farm and ecosystem depend on several factors such as the size of the farm, water depth, water current and more (Holmer et al., 2005). Salmon releases nitrogen and phosphorus through its gills as a by-product of its metabolism. As Norwegian coastal waters are mainly nitrogen-limited an increase in nitrogen can alter the local ecosystem, however the risk for regional eutrophication is considered low (Grefserud et al., 2019). A more pressing concern is the impact salmon farms have on the wild salmonid population. There are serious conflicts between the rapid expanding aquaculture industry and the desire to

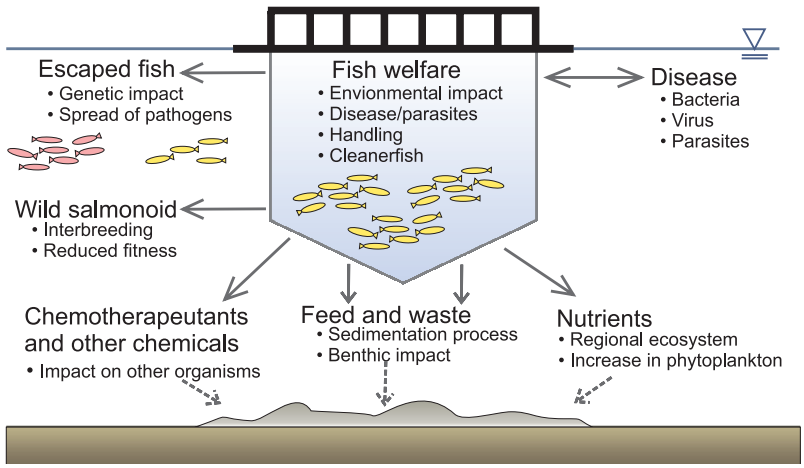

Figure 1.4: Overview over challenges related to the internal cage environment and the cage's interaction with the nearby ecological system (modified from Svåsand et al., 2017).

keep a healthy and sustainable wild salmon population (Liu et al., 2011). The largest issues are parasites, diseases and escape of fish (Lekang et al., 2016).

The main concern regarding escaped fish is its interaction with the wild salmon population. Wild salmon spawn and spend their juvenile years in freshwater rivers. Once smoltification occurs they migrate to the open ocean, avoiding prolonged stays in estuaries and fjords, and after 1-5 years at sea return to the rivers to spawn (Thorstad et al., 2011). Escaped farmed salmon that migrate to the same rivers and breed with the wild population can cause changes in genotype and loss of genetic variation in the wild population (Roberge et al., 2008), with the hybrid fish displaying reduced fitness and survival (McGinnity et al., 2003). It is theorized that the cumulative reduction of fitness could cause extinction of vulnerable wild populations (McGinnity et al., 2003).

In addition to interbreeding, escaped fish could increase the spread of diseases, such as the infectious salmon anaemia (ISA), amoebic gill disease (AGD) and pancreas disease (PD). Extensive farming has also resulted in an increase in sea lice infestation pressure, both in salmon farms and on the wild population (Barrett et al., 2020).

1.2.1 Salmon lice (Lepeophtheirus salmonis)

The salmon lice *Leopeophtheirus salmonis* is a host-specific parasite that attaches itself to Atlantic Salmon (Fig. 1.5). The first description of salmon lice was probably that written by the Danish-Norwegian bishop Erik L. Pontoppidan (1698 – 1764) (Berland and Margolis 1983, cited in Torrissen et al., 2013). Louse have historically been observed in low numbers (Finstad et al., 2011), and there was little scientific interest before the lice became an issue for aquaculture in the 1970s (Pike and Wadsworth, 1999; Torrissen et al., 2013).

The life cycle of the salmon lice consists of five phases and 10 stages. The first two stages are the planktonic nauplius stages, followed by one infective copepodid stage, four attached chalimus stages, two mobile pre-adult stages and one adult stage (Pike and Wadsworth, 1999). During the first three stages the louse are non-feeding and depend on internal stored reserves for nutrients, but during its third stage the louse starts to search for and infest hosts. It therefore positions itself in the water column to optimize contact with hosts (Harris et al., 2011).

Once it has attached itself to a host the copepodids moults into the

Figure 1.5: Close up of adult female salmon lice (Photo: Andreas Hagemann, SINTEF Ocean, shared with permission.)

first of the four sessile chalimus stages and can now feed on mucus, skin and body fluids (Harris et al., 2011; Torrissen et al., 2013). It is first after the lice moults into the larger movable stages (pre-adult and adult) that the lice can cause lesions to the skin (Finstad et al., 2000; Harris et al., 2011; Svåsand et al., 2017). As the lesions increase in size they can cause problems with dehydration, disturbed electrolyte balance and physiological functioning of the fish, increasing the risk of bacterial infection (Svåsand et al., 2017), and can in extreme cases be fatal (Finstad et al., 2000; Costello, 2006).

Unfortunately for the marine aquaculture industry the high density of potential hosts in farms all year is optimal for the salmon lice. The lice are natural parasites of fish, but due to the extensive farming, there has been an increased infestation pressure on both salmon farms and the wild population (Barrett et al., 2020). Although the quantitative impact of the salmon farming on lice infestations on the wild populations remains controversial, there is an agreement that salmon farms have effect on the local abundance of salmon lice (Heuch and Mo, 2001; Torrissen et al., 2013; Finstad et al., 2011; Barrett et al., 2020).

To reduce the infestation pressure the Norwegian Ministry of Trade and Industry (2012) has enforced strict regulations regarding permissible lice levels on farmed salmon with stricter requirements during the out-migrating period for wild salmon smolts. As of March 2017 the maximum number of mature female lice per salmon could not exceed 0.2 during this period, and 0.5 for the rest of the year (Norwegian Ministry of Trade and Industry,

2012). If this level is exceeded measures must be initiated to reduce the lice levels.

In 2017 the "Traffic light" system was also introduced in Norway. The system divides the coastline into 13 regions which are graded as either open for increased production (green), can continue with same level of production (yellow) or must decrease production (red). This grading is based on the impact aquaculture has had on lice infestations on the wild salmonid population over the last two years (Norwegian Ministry of Trade and Industry, 2017). Salmon lice has a significant economic impact through this system as it can restrict the regional growth of the industry, but also through the cost of lice removal operations.

Lice removal, or delousing, is one of the costliest operations in the industry (Liu and Bjelland, 2014; Abolofia et al., 2017; Iversen et al., 2017). Delousing treatments can be divided into three main groups: chemical, non-chemical and preventative (Svåsand et al., 2017). Chemotherapeutants, either used in bath treatments or as in-feed additives, has for the last four decades been the main treatment (Overton et al., 2019). Although effective against lice there have been massive accidents such as when the use of hydrogen peroxide lead to mass death of 136 000 salmon in one cage (NTB, 2016). Using chemotherapeutants can also slow down the growth of salmon (Liu and Bjelland, 2014), have an adverse impact on the environment by harming the nearby shrimp populations (Bechmann et al., 2019, 2020), and there are also several reports of treatment-resistant lice (Aaen et al., 2015).

The use of chemotherapeutants to remove lice has decreased in recent years indicating that the industry has changed strategy, instead applying other non-chemical methods such as thermal, fresh water and mechanical removal (Folkehelseinstituttet, 2019; Overton et al., 2019). Due to the financial cost of the salmon lice issue new methods and commercial products are continuously introduced to the industry, resulting in a disparity between the rapid rate of development and scientific validation of these new solutions (Bui et al., 2020a). Many of the new methods require handling of the fish, such as crowding, pumping and moving the fish in and out of the cages which can stress the fish and cause injuries to the gills, skin, fins and snout (Svåsand et al., 2017; Noble et al., 2018). A review of delousing from 2012 to 2017 revealed that there was an increase in mortality after using certain removal methods (Overton et al., 2019). Handling of fish also increase the probability of escapes and lice removal operations are by farm operators perceived to be particularly risky with regards to salmon escapes (Thorvaldsen et al., 2015). As was confirmed when the data from 2014 to 2019 revealed

delousing operations and transportation of fish as the two main causes of escapes during this period (Norwegian Directorate of Fisheries, 2020a).

Another non-chemical solution are cleaner fish which feed on the lice. The use of cleaner fish has increased exponentially since 2008 (Powell et al., 2018). Cleaner fish were introduced as a preventative, economic and non-medical solution to the lice (Bjordal, 1988; Liu and Bjelland, 2014; Imsland et al., 2014). Compared to the other lice treatments where handling of the fish are required, cleanerfish have the advantage of not inducing stress in the salmon (Imsland et al., 2018). The practice of using cleaner fish started with the use of wrasses (labridae) in the late 1980s (Bjordal, 1988), but the lumpfish (*Cyclopterus lumpus L.*, Fig. 1.6) quickly became the dominant species. Unlike the wrasses which are unfit for water temperatures below 6 °C, the lumpfish remains active during the winter months (Imsland et al., 2014; Powell et al., 2018). In Norway alone, the use of lumpfish increased from 10.3 million in 2015 to 42.7 million in 2019 (Norwegian Directorate of Fisheries, 2020b).

Figure 1.6: Image of a lumpfish. (Photo: Stine W. Dahle, SINTEF Ocean, shared with permission.)

The lumpfish has proven efficient at reducing the number of pre-adult, mature male and mature female lice per fish in full-scale experiments (Imsland et al., 2014, 2018). Its effectiveness is however disputed as there is a lack of replicated experiments and salmon farmers have reported varying success (Overton et al., 2020). There are also serious concerns regarding the welfare of cleanerfish given the reports of mortality rates as high as 40% (Norwegian Food and Safety Authority, 2020; Overton et al., 2020), and some suggesting that there is a lack of registration and the real mortality

rates are closer to 100% (Poppe, 2017; Berglihn, 2019).

Due to the many issues related to delousing, there has been a plea for a shift to more prevention-focused louse management (Barrett et al., 2020). Preventative measures are methods that aim to reduce contact between lice and fish, and reduce the need for both chemical and non-chemical treatments. These are methods such as barrier technology, geographic spatiotemporal management, manipulation of swimming depth, functional feeds, repellents and host cue masking (Barrett et al., 2020). Preventative measures also include solutions such as moving the entire grow-out phase to land-based facilities and closed cages, or to more exposed locations.

1.2.2 Exposed sites

The interest in exposed sites has increased with the growth of the industry as the number of available sites dwindle (Holmer, 2010; Bjelland et al., 2015; Gentry et al., 2017). Exposed locations are expected to have more stable water flow conditions and higher water exchange rates which is beneficial with regards to waste dispersal and water quality (Johansson et al., 2007; Holmer, 2010; Bjelland et al., 2015). Moving to more exposed sites may also reduce contamination of lice and other pathogens between farms by increasing the distance between them (Svåsand et al., 2017), and will also reduce interaction with coastal flora and fauna (Holmer, 2010).

Despite the growing interest of moving to more exposed locations, there is no clear definition of an exposed site (Holmer, 2010). There is a general understanding that these sites are located more remotely off the coast, even offshore, and are associated with rougher weather conditions, periods of stronger and more persistent water flow, and high waves (Sandberg et al., 2012; Bjelland et al., 2015; Hvas et al., 2020). Strong current flow can however also be experienced at sheltered sites. For instance those placed within narrow straits where the tidal forces result in the water accelerating as it passes due to the incompressible nature of water.

To mitigate the many issues related to the expected harsher environment new cage designs have been developed such as the OceanFarm1 (Salmar AS, Fig. 1.7) and Havfarm (Nordlaks Oppdrett AS, Fig. 1.7). OceanFarm1 has a diameter of 110 m, and can be categorised as a semisubmersible as it has the ability to alter the depth of the cage, and potentially lift it all the way out of the water. Havfarm has the outline of a ship, but with open frame construction where six net cages can be deployed, and is anchored using a swivel design. The solid frames of these designs simplifies daily operations during bad weather. Both of these new structures can still be defined as open

Figure 1.7: Towing of Nordlaks' HavFarm and Salmar's OceanFarm1. (Photo: Nordlaks AS and Salmar AS, shared with permission.)

cages as they utilise nets. It is therefore necessary to evaluate how periods with stronger water currents and high waves impact not only the structure, but also the fish.

1.3 Fish welfare and optimal rearing conditions

Although the public's concern for animal welfare has grown the last decades, this concern is not necessarily extended to fish (Röcklinsberg, 2015). The industry and scientific community has however had an increased focus on fish welfare in Atlantic salmon farming. There is however no universal definition of the term welfare (Noble et al., 2018), and the term is used loosely (Broom, 2017). Broadly speaking there are three categories of welfare definitions. The first is nature-based and defines good welfare as the animal being able to lead a natural life and permitted to express natural behaviour (Turnbull and Huntingford, 2012; Noble et al., 2018). The second category consists of function-based definitions that state that good welfare is obtained when the animal can adapt and thrive in its current environment (Broom, 1986; Turnbull and Huntingford, 2012; Noble et al., 2018). The final category is feeling-based and defines welfare by the animal's subjective mental state, that is being free of negative experiences while experiencing positive ones (Turnbull and Huntingford, 2012; Stien et al., 2012; Noble et al., 2018). Often it is a combination of these that is applied, for instance in the definition by the European Parliament: "the welfare of an individual is its state as regards its attempts to cope with its environment. Welfare includes feelings and health and can be measured scientifically" (Broom, 2017).

Independent of the specific definition of welfare, the methods for assessing the welfare status of fish are important for food and aquaculture authorities to uphold animal protection laws. For instance, in Norway Atlantic salmon possess animal rights according to the Norwegian Animal Welfare Law as it is a vertebrate species (Norwegian Ministry of Agriculture and Food, 2009). According to this law the keeper of the animals must ensure that the animal is kept in an environment which ensures good welfare defined by its species-specific and individual needs (Norwegian Ministry of Agriculture and Food, 2009). This means that Atlantic salmon farms utilising cleaner fish must consider the welfare of both species.

One method for assessing the welfare is the use of animal welfare assessment protocols, such as the Salmon Welfare Index Model protocol (SWIM 1.0) (Stien et al., 2013). These protocols assess the welfare of the animal by assessing if the needs of the animal are met. The needs of salmon are divided into two main classes, physical and behavioural. The physical needs are respiration, osmotic balance, nutrition, health and thermal regulation, while the behavioural needs are behavioural control, feeding, safety, protection, social contact, exploration, kinesis, rest, sexual behaviour and body care (Stien et al., 2013).

Many of the salmon's needs are met through the environment. The physiologically influential factors are temperature, salinity, oxygen and water flow. The temperature and salinity inside the cages are not influenced by the fish themselves, but are a result of the conditions outside the cage. As fish are poikilothermic animals, their body temperature is similar to the environmental temperature and the temperature can influence metabolic processes such as food intake and growth (Oppedal et al., 2011; Stien et al., 2013). For the cold-water fish Atlantic salmon the optimal sea water temperature should be within their preferred range of 11 to 18 °C (Johansson et al., 2006; Oppedal et al., 2011; Stien et al., 2013). However, the Atlantic salmon is a versatile fish, and can survive at conditions outside this range, if there is sufficient dissolved oxygen and a gradual transition between the temperatures.

Unlike temperature and salinity, dissolved oxygen (DO) levels inside the cage are influenced by the presence of fish as they use the oxygen for energy production (Lekang, 2020). Oxygen enters the water either through the mixing of atmospheric oxygen across the water's surface or by photosynthesis of algae (Le Menn, 2012). In Atlantic salmon farming, physical transport of water through the cage is the main source for fresh oxygenated water (Wildish et al., 1993; Johansson et al., 2006). Colder and less saline

water contain more oxygen (Stien et al., 2013), and higher temperatures result in enhanced DO demand of Atlantic salmon (Remen et al., 2013, 2016). Low DO can result in reduced metabolic rates and growth, and if levels are sufficiently low increased mortality (Oppedal et al., 2011; Stien et al., 2013).

Dissolved oxygen is reported as either a concentration or the percentage saturation. The concentration gives the amount of gas dissolved in water, and depends on several factors such as water temperature, pressure, salinity and substances in the water. It is more common to report DO as percentage saturation as it gives a more intuitive understanding of the DO levels with regards to fish welfare. Percentage saturation describes the ratio of DO in the water to the amount the water could have held at the given temperature and salinity, that is it is the ratio between the measured concentration and the concentration at saturation (Le Menn, 2012).

A sufficient water flow through the cage is necessary to supply fresh oxygenated water, but also for the removal of waste and oxygen depleted water. Weak currents can result in low DO levels inside cages (Johansson et al., 2007). While too strong currents can exceed the swimming capacity of the fish, depriving the fish of its behavioural control and opportunity for rest, and in extreme cases force the fish into the net (Stien et al., 2013). With the increased interest for exposed sites current speed has become an important welfare indicator.

1.4 Current flow and fish farms

All cages related to the grow-out phase at sea must take into account how they interact with the ocean current and wave loads independently of design. Most fish farms in Norway are located in sheltered waters, either in fjords, near land or sheltered by nearby islands. They are therefore influenced by the two major current systems: the relatively fresh Norwegian Coastal Current and the more saline Norwegian Atlantic Current (Sætre, 2007). The main driving forces of the Norwegian Coastal Current are tides, wind conditions, Atlantic water, bottom topography and freshwater, with the Baltic outflow as the main source of freshwater followed by runoff from Norway along the coast (Sætre, 2007). How these driving forces influence the water mass at any specific fish farm is dependent on both the location of the fish farm, but also spatial and temporal variability in each driving force.

The current flow at a specific farm site is also influenced by the structures present such as the net. The nets can be constructed in several different ways and with different materials, which are either connected through knots

or sewn together (knotless) (Lekang, 2020). At the most fundamental level, when the current passes through a net panel it is decelerated (see for example: Løland 1993, Patursson 2008, Klebert et al. 2013). For a traditional gravity sea cage there will be a reduction in speed over the front of the cage, but also over the net at the opposite side of the cage. The reduction in speed is therefore clearly observed when measuring the current upstream and downstream of a cage, but also when measuring the current upstream and downstream of an entire farm (Klebert et al., 2013; Winthereig-Rasmussen et al., 2016; Klebert and Su, 2020).

How large the reduction is over a sea cage depends on several factors such as the orientation and organization of the farm (Rasmussen et al., 2015), flow conditions at the site, local topography (Klebert et al., 2013), biomass in cage (Chacon-Torres et al., 1988; Klebert et al., 2013; Gansel et al., 2014; Michelsen et al., 2019; Klebert and Su, 2020), cage structure (Klebert et al., 2015) and additional structures such as a lice shielding skirt (Frank et al., 2015). The current speed is further reduced by increased solidity of the net, which can occur when the cage deforms as the inclination angle between the incoming current and the cage increases (Fredheim, 2005; Lader et al., 2008; Bi et al., 2013; DeCew et al., 2013; Lien et al., 2014; Klebert et al., 2015; Zhao et al., 2015), or by biofouling on the net (Bi et al., 2013; Gansel et al., 2015).

Sea cages alter the three-dimensional flow field downstream of the cage, but also the intensity and distribution of the turbulence levels (Klebert and Su, 2020). The sedimentation near the cage is greatly affected by the combination of turbulence downstream which keeps some particles suspended, and the flow reduction which reduces transportation away from the farms (Klebert and Su, 2020). The local current flow field thereby influences many of the described challenges in Chap. 1.2, both transportation of particles away from the farm, and the influx of oxygenated water into the farm.

The current flow through fish cages and farm can be studied by use of full-scale experiments and mathematical and physical modelling. Extensive work has been done on the interaction between water flow and cage structure using model-scale experiments and simulations (see for instance: Løland 1993, Fredheim 2005, Patursson 2008, Gansel et al. 2013, Klebert et al. 2013), creating a solid foundation for the understanding of the many factors which influence the current flow. The study of far-field effects of fish farms is usually permed by use of numerical ocean models such as the SINMOD (SINtef MODel) (Slagstad and McClimans, 2005). The spatial resolution of numerical ocean models range from >10 km down to 30 m. Finer mod-

elling is required to include the effects of sea cages into these models. This was recently done in a study by Broch et al. (2020). Parameters obtained through near-field computational fluid dynamics (CFD) simulations of cages were implemented in the SINMOD model which improved the comparison between the simulated flow field and the measured flow field.

Correctly scaled model-experiments and accurate simulations of cages allow for the controlled study of sea cage's impact on current flow, however, full-scale measurements are necessary for two reasons. Firstly, as of 2020, model-scale experiments and simulations lack the ability to fully integrate the effect the fish may have on the current as scaling the influence of fish is not fully understood (Xu and Qin, 2020). The three-dimensional flow is altered by the presence of fish with swimming activity increasing water exchange across the net (Chacon-Torres et al., 1988), high fish densities deflecting the ambient current (Gansel et al., 2014) and biomass presence increasing the reduction in current speed through a cage (Klebert and Su, 2020). It is also suggested that the specific swimming pattern will influence how the water current is attenuated and redirected (Chacon-Torres et al., 1988; Johansson et al., 2007).

It should be noted that there have been some experimental attempts such as He et al. (2018) using 814 fish of 16 cm length in one trial, and nine rigid model fish in another trial, to determine the mooring loads with fish. However, the scaling of fish is not straight forward, and as pointed out in Juell and Westerberg (1993), conclusions drawn from laboratory experiments with few fish are not necessarily representative for commercial farming situations as the behaviour of fish is influenced by both other individuals and environmental factors. Simulations of the influence of fish on the current flow resulted in different current flow patterns based on swimming behaviour (Tang et al., 2017). The results from these simulations could be improved by including the behavioural response of Atlantic salmon to several environmental cues, such as the behavioural Lagrangian model developed by Føre et al. (2009). However, to establish the correct environmental cues, data from the real world are still necessary.

Secondly, full-scale measurements are necessary for validation. For example, in the study by Broch et al. (2020) the model results were compared with full-scale data gathered from nearby current meters. Independently of type of simulation, validation is essential. Given the many factors which influence the current, full-scale data can also reveal new aspects which should be implemented in the models of the near-field effects of farming sites.

1.5 Thesis outline and contributions

This thesis is a contribution to the marine aquaculture field. The findings in contribute to the knowledge of current flow conditions at full-scale Atlantic salmon farm sites. The focus of this thesis is the local current conditions on sites. Specifically how to evaluate these with fish welfare in mind and how lice shielding skirts interact with the current and impact the internal environment of the cage.

The thesis is organized into five chapters. Chapter 1 gives an introduction to aquaculture in Norway and developments within the industry. Chapter 2 presents the instrumentation used at fish farms and in this thesis. Chapter 3 and 4 contain in-depth presentations of the contributions of this thesis. Chapter 3 focuses on on-site current conditions and fish welfare, presenting a more extensive discussion about conditions at exposed sites, and how species specific swimming capacities can be utilised for site evaluation. Chapter 4 revolves around the use of lice shielding skirts, and therefore includes a detailed description of this technology and how the skirts influence current conditions and the environment inside the fish cage. Lastly, Chapter 5 attempts to draw a conclusion and discuss potential further work. The following list summarizes the main academic contributions presented in Chapter 3 and 4:

Chapter 3: On-site current conditions and site evaluation

- A new classifying method for current data from site surveys taking into account the swimming capabilities of Atlantic salmon was presented. This novel method was applied to data from five farming sites along the Norwegian coastline and the sites were evaluated with regards to both Atlantic salmon and lumpfish. Of the five sites only one was suitable for lumpfish, while only one was not suitable for small post-smolts.
- Publications related to this chapter: A

Chapter 4: Current flow and shielding skirts

- Current conditions were measured inside the same stocked fish cage with the shielding skirt deployed and without. When the skirt was deployed there was a weak vertical upwelling in the centre of the cage and the reduction in current speed from upstream to inside the cage was higher than when the skirt was removed. The skirt had no visible impact on the vertical swimming behaviour of the salmon. However, the skirt did accentuate the drop in DO causing unfavourable levels. The

DO levels reached similar levels to those outside the cage 30 minutes after the skirt was removed (Paper C).

- The characteristic current flow pattern around a conical cage with a permeable skirt was established and compared with previous studies of the flow pattern around cylindrical cages. The current speed inside and downstream of the cage was significantly reduced compared to the upstream current, and the weakest recorded current speed was inside the cage at 6 m depth. Unlike the current flow field downstream of cylindrical cages, the reduction in current speed downstream of the conical cage became little to non-existing at 22 m depth, probably due to the tapered form of the cage. This may have implications for the benthic impact of the farm (Paper D).
- DO data was presented from two hydrographically different sites demonstrating how different hydrographical conditions interact with shielding skirts. The more homogeneous site had better DO levels inside the cage than the more stratified site, which aligns with previous studies. At the stratified site DO conditions inside the cage appeared to change together with the stratification in the water column outside, indicating a complicated relation between shielding skirt, hydrography, DO and current conditions (Paper B).
- Publications related to this chapter: B, C, D.

1.6 List of publications

1.6.1 Journal papers

Paper A:

- Jónsdóttir, K. E., Hvas, M., Alfredsen, J. A., Føre, M., Alver, M. O., Bjelland, H. V., Oppedal, F., 2019. Fish welfare based classification method of ocean current speeds at aquaculture sites. Aquaculture Environment Interactions, 11, 249-261

Paper B:

- Jónsdóttir, K. E., Volent, Z., Alfredsen, J.A., 2020. Dynamics of dissolved oxygen inside salmon sea-cages with lice shielding skirts at two hydrographically different sites. Aquaculture Environment Interactions, 12, 559-570

Paper C

- Jónsdóttir, K. E., Volent, Z., Alfredsen, J.A., 2021. Current flow and dissolved oxygen in a full-scale stocked fish-cage with and without lice shielding skirts. Applied Ocean Research, 108, 102509

Paper D:

- Jónsdóttir, K. E., Klebert, P., Volent, Z., Alfredsen, J. A., 2021. Characteristic current flow through a stocked conical sea-cage with permeable lice shielding skirt. Ocean Engineering, 223, 108639

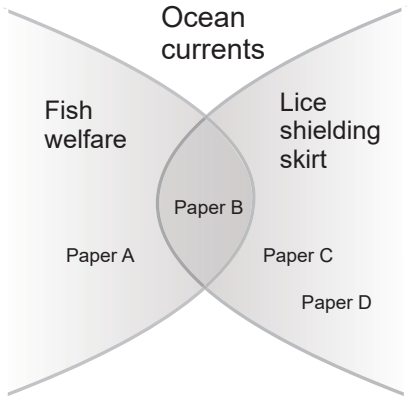

Figure 1.8: Thematic framework of papers.

1.6.2 Related work not included in this thesis

- Volent Z, Jónsdóttir KE, 2019. Luseskjørt: Målinger av strøm rett utenfor og rett innenfor luseskjørtet. SINTEF Ocean Report 2019:01435

- Jónsdóttir KE, Volent ZE, Klebert P, Mathisen R, Andorsen S, Sæternes R, Sunde LM, 2020. Påvirker tetthetsgradienten strømmen og oksygennivået i en fiskemerd med luseskjørt? Norsk Fiskeoppdrett 1, pp. 62 – 66.

- Misund A, Volent Z, Jónsdóttir KE, Sunde LM, 2020. Hvordan forholder oppdrettere seg til skjermingsteknologi mot lakselus? Norsk Fiskeoppdrett 9, pp. 52-57

- Volent Z, Jónsdóttir KE, Misund A, Steinhoveden KB, Chauton MS, Sunde LM, 2020 Sluttrapport: Luseskjørt som ikke-medikamentell metode for forebygging og kontroll av lakselus – Utvikling av kunnskap om miljøforhold for økt effect og redusert risiko (SKJERMTEK). Sinte Ocean Report 302003409

- Volent Z, Jónsdóttir KE, Misund A, Sunde LM, 2020. Luseskjørt kompendium: Kunnskapssammenstilling om bruk av skjørt mot lakselus. SINTEF Ocean

Chapter 2

Instrumentation in fish farming

2.1 Ocean processes and measurements

Instrumentation in sea cages is not new, and the greatest potentials were early identified to be environmental monitoring and control, and fish stock inventory assessment (Zahradnik, 1987). The continuous development of new instrumentation has resulted in an increase of available and affordable sensors for the harsh ocean environment. This has opened the possibilities for precision fish farming (PFF). PFF aims to apply control-engineering principles to fish production by monitoring, controlling and documenting the biological processes to facilitate informed decision making and optimise production results (Føre et al., 2018). Despite this growing interest in instrumentation in sea cages the parameters monitored daily at fish farms remain low (Misund et al., 2020).

The most relevant oceanic parameters for environmental monitoring are temperature, salinity, dissolved oxygen (DO), turbidity, chlorophyll, ocean currents, waves, wind and turbulence. These properties change with time and space, and monitoring requires different instrumentation and measurement techniques with correct sampling procedures. The use of instrumentation in the marine aquaculture industry today can roughly be divided into two: site selection and daily rearing operations. Which oceanic parameters are monitored varies for these two tasks.

In Norway the NYTEK regulations dictate that before any facilities can be installed, a site survey must be carried out in accord with the technical standard NS-9415:2009 (Standards Norway, 2009). The site survey is executed to establish design parameters for the future installation, and must therefore document the topography, current, wind and wave conditions at

the site. The current is estimated to be the largest environmental load on the farm, hence it must be well documented to ensure proper design (Fredheim and Langan, 2009). The survey must also establish what are the main contributors to the current, that is, tidal current, wind-generated surface current, outbreaks from the coastal current or spring flood due to snow and ice melting (Standards Norway, 2009). Despite these requirements, NS-9415 only require one month of monitoring.

After installation of a site in Norway the "Regulations on the operation of aquaculture facilities" require monitoring to ensure that the water quality and current strength are sufficient to ensure good living conditions. Specifically, dissolved oxygen, temperature and other water parameters which have significant influence on welfare must be measured (Norwegian Ministry of Trade and Industry, 2017).

Monitoring of daily rearing operations has traditionally been a manual activity. This has changed due to the rapid increase in available and reliable instrumentation for automation and monitoring in aquaculture (Lekang, 2020). There are still uncertainties regarding which variables are crucial to monitor, and where in the cage they should be sampled. Dissolved oxygen and temperature are mentioned specifically in Norwegian Ministry of Trade and Industry (2017), but "other water parameters" is not defined, and neither are the sampling procedures. It is therefore up to the farmers to decide what, where and when to sample. In a recent in-depth interview of 13 informants from sites along the Norwegian coastline it was revealed that apart from DO and temperature, the variables that were monitored varied, and also the measurement procedures (Misund et al., 2020).

Although it is often the variables that vary through a production cycle that interest the farmers, the slow varying changes of the ocean also have a direct impact on the industry. Monitoring these slow-varying changes of the ocean requires considerable scientific cooperation and is there most often studied through global research programs. For instance, to study the long-term fluctuations and impact of climate change large areas are monitored for long periods of time. One method for monitoring large areas is using non-contact or remote sensing instruments such as satellites equipped with radars and hyperspectral cameras. These instruments collect quantitative and qualitative information regarding Chlorophyll a, total suspended matter, water transparency, coloured dissolved organic matter and the sea surface temperature by use of the ocean colour (Johnsen et al., 2009).

These large scales studies are relevant for the aquaculture industry as the rise in temperatures will influence the ocean currents (Sætre, 2007) which

Figure 2.1: A stack of instrumentation used during the experimental work done for this thesis. The sensors were attached to the orange buoys using rope at different depths. To the right of the box on the pallet is one acoustic Doppler current profiler from Nortek and one from Aanderraa (ADCP/DCP). Ontop of the box is a Nortek Vector (ADV) with a "wing" attached to make it turn towards the current. Behind it is an Opotode with it's sensing head protected by bubble-wrap.

can have detrimental effects given the optimal rearing temperature of Atlantic salmon. More commonly in marine aquaculture research it is specific sites and variations through shorter periods or entire production cycles which are of interest. This chapter presents the most common instrumentation used in this setting and during the field experiments executed as part of this thesis. Specifically the instrumentation used for monitoring the water environment, fish development and current conditions.

2.2 Monitoring the water environment

Optimal water quality depends both on the species and its life stage. Based on the interviews performed by Misund et al. (2020) the most common water environment variables that were monitored, in addition to temperature and DO, were salinity and turbidity. How often and where in the farms these variables were monitored differed, with some sampling continuously, and

others sampling only once a day.

As the upper water column temperature is influenced by solar radiation, it has both temporal and spatial variations with a strong seasonal characteristics (Parra et al., 2018). Temperature is a slow varying variable and is the easiest ocean property to measure accurately. The three most common approaches to measure temperature in oceanography has been the expansion of a liquid or metal, change in electrical resistance or infrared radiation from the sea surface (Thomson and Emery, 2014).

Infrared radiation from the sea surface is the only non-contact method of these three utilised by for instance satellites, while the other two sensors are contact sensors. The most common non-electrical temperature sensor is the mercury- or alcohol-in-glass thermometers where the temperature is determined visually by the liquids expansion. In oceanography however, the electrical temperature sensor is most common due to their fast response and accuracy, and they can be divided into two main groups: Resistance and voltage instruments. Thermocouple is a voltage instrument where the temperature is determined from the voltage difference over two different elements (The Seebeck-effect). The resistance instruments, resistance-temperature detectors (RTD) and thermistors, are more commonly used. These contain a material which changes resistance as a function of temperature and the physical properties of the material.

Temperature measurements are necessary both to monitor if temperatures are within the optimal range for salmon, but also to determine other variables such as salinity and density. Historically, salinity was measured using a variation of titration methods, but electrical conductivity quickly became the main approach as the conductivity of a water mass depends on the ion content in the sample, which is proportional to the salinity. Conductivity can be measured using either conductive or inductive methods, with conductive methods being the most used as it has greater accuracy and faster response (Thomson and Emery, 2014). The conductive methods consists of two or more electrodes with a voltage applied across them. The electric current which occurs between the electrodes is proportional to the ion concentration in the water (Lekang, 2020).

Temperature measurements are necessary for salinity measurements as conductivity varies with temperature, and both of these variables can vary both horizontally and vertically inside the cage. The position of the measurement must therefore also be documented. The vertical position, or depth is most commonly measured indirectly through measurements of pressure using strain gauges (Thomson and Emery, 2014). These three variables are

all interlinked, and are often measured simultaneously using a conductivity-temperature-depth (CTD) sensor usually consisting of a resistance thermometer, a conductive conductivity sensor and a strain-gauge pressure sensor. The CTD is lowered (downcast) and lifted (upcast) through the water column to create profiles of the water column and determine the water density which cannot be measured directly, but is determined from the salinity and temperature measurements. Density does not have a direct impact on fish welfare, but the information can be used to establishing if there are any stratifications in the water column, and to identify different water masses and their motions.

Seawater density increases with higher temperature and salinity, while it decreases with colder and less saline water. Temperature gradients can occur when the upper layers of the water are heated or cooled by the ambient temperature, or by the influx of water with different temperature, such as from a river. Salinity gradients can occur due to the influx from freshwater, for instance a river, melting snow or precipitation, or from the influx of saline water from the Atlantic current (Sætre, 2007). Stratification in the water column will therefore vary throughout the season, with weather conditions and local variations.

The stratification may not have a direct impact on the water quality at a site, but stratification can have a direct influence on the current flow. When a vertical stratification is present in the water column, it will inhibit vertical mixing between the layers (Imberger, 2013). The lower density water will position itself above the higher density water, and these two layers can now operate independently of one another and even have opposite facing current flows outside of the boundary layer. Stratification at sites has also been shown to have a direct link to DO levels at sites, with stratified sites showing lower DO levels than homogeneous sites (Johansson et al., 2006).

For measuring dissolved oxygen there are two main methods: chemically and optically. The wet-chemical Winkler titration technique (1888) is still to this day the standard reference method (Bittig et al., 2018), but is impractical for in situ measurements as it requires the addition of reagents to the water bottle sample and titration. The two electronic options are the use of a membrane covered polarographic “Clark” cell, and the fluorescence quenching technology. The polarographic cell’s membrane needs to be routinely replaced as it ages, and is susceptible to biofouling (Lekang, 2020). Another option is then to use optodes.

Optodes utilise the principle of quenching or dynamic extinction of fluorescence (Le Menn, 2012). The optode consists of a film with several layers.

The oxygen molecules in the ambient environment diffuse through to a sensing foil. This sensing foil has the characteristic that when exposed to blue light fluoresces it is excited, and relaxes to its ground state by light emission of a red light (Le Menn, 2012). When the sensing foil is in contact with oxygen molecules a non-radiative transition takes place. This reduces the intensity of the returned light signal and a faster decay (Bittig et al., 2018).

Some of the farmers interviewed in Misund et al. (2020) measured turbidity at their sites, which is related to suspended sediments in the water column, either due to inert particles or by living particles, such as plankton. Abrupt changes in turbidity is not normal and can be caused by high phytoplankton blooms (Parra et al., 2018). The simplest and oldest method for measuring turbidity is the use of a Secchi disk. The disk is manually lowered until it is no longer visible, the depth is noted, and then the disk is lifted, and the depth it becomes visible at is noted. Instruments that don't require manual labour however apply either optical or acoustic methods. The optical methods either measure the absorption of transmitted light in the medium or the percentage scattered light (Le Menn, 2012). The acoustic method can be done using an acoustic Doppler velocimeter (ADVs), which is mainly used to measure the current speed, and is discussed in more detail in subsequent chapters.

In addition to providing information on the specific variables, the described variables can be applied to study the dynamics of the water mass. Temperature, salinity, DO and nutrients are all conventional tracers which can be used to track the diffusive and advective processes. Salinity is a conservative tracer, which is only affected by mixing and diffusive processes, while DO is a non-conservative tracer which is also modified by chemical and biological processes (Thomson and Emery, 2014), for instance fish feeding activities. However, these variables are mostly measured to investigate whether environmental conditions meet acceptable levels at farm sites.

2.3 Monitoring fish development and behaviour

The growth and development of the fish is one of the most important factors for the success of a fish farm (Balchen, 1987). The counting of stock and monitoring of growth rates are necessary to plan and execute precise feeding strategies (Zion, 2012), while behavioural changes such as sudden lethargic or erratic swimming are key indicators of unfavourable conditions, stress, distress or pathogenic conditions (Conte, 2004).

Both growth rates and fish behaviour can be monitored through visual

inspection (Ruff et al., 1995), with submerged cameras being one of the most common tools found on fish farms (Føre et al., 2018). The use of automatic image analysis for remote monitoring of fish was early identified as a potential improvement of the aquaculture process (Balchen, 1987). Following the introduction of visual inspection through use of cameras, stereo image analysis was presented for observing and measuring fish in three dimensions to estimate mass (Ruff et al., 1995). In recent years, computer vision technologies and improved image-processing algorithms present exciting possibilities in both improved mass estimation and welfare monitoring (Zion, 2012), but also identifying and counting sea lice (Horntvedt, 2020).

Hydroacoustic devices are the most common research tool used for fish monitoring (Føre et al., 2018). The salmon can either be monitored as a group using echosounder and sonar, or individually using acoustic fish telemetry. Individual tracking can be done by equipping the fish with electronic transmitters containing sensors measuring different properties, such as heart beat rate or swimming activity (Føre et al., 2017; Svendsen et al., 2020). However, all of these require handling of the fish, and often surgery (Føre et al., 2018), it is therefore often more convenient to monitor the group dynamics.

To monitor the welfare of the group, behavioural swimming patterns and responses are considered good operational welfare indexes (McKenzie et al., 2020). Echosounders are the most common tool used in aquaculture research for the study of group behaviour in cages (Føre et al., 2018). They can monitor the vertical distribution of the fish by either being mounted on the sea bottom, or from floating buoys. The vertical positioning of the fish is strongly affected by environmental factors such as temperature, light and feeding (Oppedal et al., 2011), hence deviant behaviour can be discovered through monitoring the vertical behaviour.

There are many different types of echosounders, the simplest one being the single-beam echosounder. The echosounders converts electronic vibrations into mechanical vibrations, typically by using piezoelectric ceramic disks to emit a soundwave. The acoustic wave is reflected when it meets an object with different acoustic impedance than the medium the sound is travelling through. For Atlantic salmon, the reflection is caused by the swim bladder which contains air. The time it takes from the signal was emitted until the echo is received is proportional to distance travelled (Thomson and Emery, 2014). Information regarding the position and type of obstacle is thereby found from the time between emitted sound and received echo, and the strength of that echo.

As the single-beam echosounder provide little information about the quantity of the targets, it is more common to use the split-beam echosounder which was developed to record the target strength directly. The split-beam emits a range of frequencies and its transducer consists of a series of elements divided into quadrants that emit and receive the echo. By determining the difference in phase shift between these four quadrants it is possible to extract information regarding swimming speed, location and direction of travel (Simmonds and MacLennan, 2005). The 3D distribution and movement of fish can also be tracked using the multibeam sonar system (Simmonds and MacLennan, 2005). However, when the density of fish is high within the beam, it can no longer isolate the echo of individual fish. Echosounders in aquaculture settings are therefore mainly used to determine how the fish shoal is behaving.

There are several complexities involved in any form of underwater acoustic propagation. The soundwave radiates spherically from the transmitter, and how fast it travels depends on the elasticity and density of the material it travels through. As the density of seawater changes with temperature, salinity and pressure, an assumption must be made regarding the propagation of the soundwave. Another issue with the use of soundwaves is that a portion of the acoustic wave is lost due to absorption, scattering and geometrical spreading. The absorption is mainly caused by the conversion of soundwave into heat, while the scattering can be caused by suspended material in the water column. Bubbles in the upper 25 m of the water column are also major scatterers (Thomson and Emery, 2014). These air bubbles are introduced and pulled down into the water column when waves break, and are a major problem when using upwards looking echosounders at wave exposed sites.

A new approach which is currently being investigated is using the sound emitted by the fish itself to monitor its wellbeing (OWITOOLS, FHF project nr: 901594). Here sound recordings are used to interpret the state of the fish, for instance if they are hungry or stressed. The future development and improvement of tags for individual monitoring, combined with use of sound to monitor group behaviour, presents interesting possibilities for the study of behaviour and welfare of fish.

2.4 Monitoring current conditions

Sufficient water transport is necessary to ensure good environmental conditions within the cage, but very few farms measure and monitor current

speed and direction routinely as part of their daily operation. There are a documented cases of farms using current measurements to aid in decision making regarding feasibility of operations such as delousing with tarpaulin (Sandberg et al., 2012), but more commonly currents are monitored prior to site installation or in research settings.

There are several different principles which can be utilised when measuring water flow, but not all of these are applicable for measurements in the open ocean. Several of the available sensors, such as the turbine flowmeter, are limited by their ability to only measure flow at one discrete point. The preferable method for measuring current speed is the use of acoustic Doppler current profilers (ADCPs) which measure the current speed at several depths.

The ADCP, like the echosounder, uses acoustics to gather information, and thereby suffers the same limitations. Unlike the echosounder however, the ADCP contains a minimum of three transducers as separate beams are required for the measurement of each current velocity component. The beams are installed with a fixed orientation from the vertical plane, often 20°, 25°or 30°. ADCPs emit a pulse at a known frequency in each beam which is scattered by suspended particles such as zooplankton in the water column. The echo that is reflected back to the transmitter is Doppler shifted and it is this information that is used to determine the current speed. The key assumption for all ADCPs is that the water is loaded with suspended particles that drift with the current and that these have a radial component towards or away from the emitted soundwave (Le Menn, 2012).

The Doppler frequency shift that occurs in the signal is based on the radial motion of the suspended particles with respect to the transducer. The frequency is reduced when the scatterers move away from the beam and increased when moving towards the beam, proportional to the relative velocity between the ADCP and scatterers. Hence the radial velocity component in each beam is determined from the Doppler frequency shift. Some Doppler sonars measure the frequency shift directly, while others use the time dilation by measuring the change in arrival time from successive pulses. This is broadly speaking the main difference between using a narrowband or broadband approach. The broadband emits a pulse pair with a lag, where the phase shift between the pulses is used to find the current speed. Narrowband instead emits a long pulse with known frequency, and the along-beam velocity is determined by comparing the difference in sent and received frequency. The main limitations of the two approaches is the poorer depth resolution of narrowband, while broadband allows range ambiguity and may

struggle if the current is too high (Le Menn, 2012).

The current profile is created by range gating. The results of each beam is grouped into depth cells, which are uniformly spaced, by dividing the received signal into successive segments based on the travel distance of the signal. A second assumption when using ADCP is that the flow is homogeneous within each depth cell and between each beam, that is the current must be horizontally homogeneous (Gordon and Instruments, 1996).

Due to the nature of the data gathered using acoustic sensors, a certain amount of processing is necessary. The instantaneous current flow is quite complex due to its temporal variability, and it is therefore often the averaged velocity field which is of interest. The profilers average over the entire depth of each cell to reduce the effects of spatial aliasing, that is the effect where high frequency signals appear like low frequency signals. The averages over each depth cell is typically not uniform, rather the cell is most sensitive to the velocities at the centre of the defined cell (Gordon and Instruments, 1996).

Temporal averaging is also necessary as the velocity errors in a single-ping are often large. This averaging is also why the assumption of horizontal homogeneity is necessary. The short-term uncertainty, or random error, is usually removed in the averaging process. Short-term errors are usually caused by internal factors such as profiler frequency, depth cell size, number of pings averaged together and beam geometry, or by external factors such as turbulence, internal waves and motion of the profiler.

Averaging does however not remove biases, or long-term errors, however these are often of a much smaller magnitude. The size of the bias depends on several factors such as temperature, mean current speed, signal/noise ratio, beam geometry and more (Gordon and Instruments, 1996). In addition, the ADCP uses an estimation of speed of sound based on a temperature measurement done at the ADCPs position. If the temperature were to change drastically with depth, this would alter the speed of sound and could cause large issues for the measurement of the vertical velocity component.

The underlying assumption that the particles in the water column float and on average move at the same velocity as the water is the main reason why ADCPs can not be used inside stocked fish cages. The echo from a volume with a moving fish would not measure the ambient current speed, but rather the swimming speed of the fish. To measure current speeds inside a stocked fish cage the same principle can be applied, but instead of taking the average over a depth cell one only measures the current at one discrete point in

space. As with the ADCP, the Acoustic Doppler Velocimeters (ADVs) have a minimum of three transducers, but these are all focused on a small volume roughly 15 cm away from the sensor. The different between profilers and the single-point velocimeters is usually the precision and accuracy of each measurement. ADVs can be applied to measure turbulence due to their high resolution.

One of the main complications of using ADVs is the Doppler noise floor and ADV spikes caused by aliasing. Spike detection is therefore an important step when using ADV data. And even more so when used inside a stocked fish cage, as the fish can cause additional spikes in the sample volume and obstruct one or more of the acoustic beams. Studies done on water containing air bubbles have concluded that noise filtering methods using low correlation and signal-to-noise ratio as thresholds are not adequate (Mori et al., 2007), while the phase-space filter by Goring and Nikora (2002) significantly removed spike noise. A hybrid method suggested by Birjandi and Bibeau (2011) has also shown promising results in bubbly flows. The hybrid method first removes the high amplitude spikes to reduce the standard deviation of the data set before filtering using the phase-space filter. In this thesis the hybrid method has been applied to all ADV data.

There are several ways to install and use these sensors. Installing the ADCPs on the sea-bottom looking upwards would create more reliable measurements of the vertical component, but this is an expensive and complicated operation compared to simply mounting them from buoys. Mounting them from buoys however allows for larger range of motion of the sensor with waves and wind, which can disrupt the vertical velocity data. ADCPs can also be installed on moving platforms, and through use of statistical space-time methods, such as Kriging, create estimates for the flow field behind fish farms (see for instance Winthereig-Rasmussen et al. 2016 and Klebert and Su 2020).

Chapter 3

On-site current conditions and site selection

3.1 Exposed sites and current conditions

Exposed sites are expected to experience periods of strong water currents. This is potentially an advantage for the production environment as higher water exchange rates increases the nutrient assimilation capacity and supply of fresh dissolved oxygen (Marra, 2005; Johansson et al., 2007; Holmer, 2010; Klebert et al., 2013; Gentry et al., 2017). Stronger water currents can however also cause large net deformations, excessive loads on farm structures and complicate farming operations (Lader et al., 2008; Kristiansen and Faltinsen, 2012; Bjelland et al., 2015; Klebert et al., 2015; Gansel et al., 2018). Particularly operations that require handling of equipment under water are challenging at sites exposed to strong currents (Sandberg et al., 2012). Exposed sites are also expected to have periods of higher waves, which is a challenge when using lifting equipment from working boats and carrying out operations on the floating collar (Sandberg et al., 2012).

Stronger currents and higher wave conditions have also raised concern for the welfare of the fish. The primary concern regarding current flow is how the magnitude, duration and frequency of strong current events will affect behaviour, growth, stress and mortality rates (Johansson et al., 2014; Solstorm et al., 2015; Remen et al., 2016; Hvas and Oppedal, 2017; Hvas et al., 2020). A constant current speed of 1.5 body lengths per second over 6 weeks caused a significant reduction in growth (Solstorm et al., 2015), while the group behaviour of Atlantic salmon is observed to change as a function of current speed both in commercial farms and experimental setups (Johansson

et al., 2014; Hvas et al., 2017b).

At low current speeds salmon are observed to swim in a circular schooling pattern. This behaviour is believed to be a density-dependent adaption to the cage environment (Juell, 1995) and a result of the fish avoiding the wall (Føre et al., 2009). Swimming speeds are voluntary and independent of the ambient environment when currents are weak, while stronger currents may force the fish to swim at speeds dictated by the environment (Johansson et al., 2014; Hvas et al., 2017b). In general, stronger water currents up to a threshold lead to more organised swimming behaviour (Johansson et al., 2014; Solstorm et al., 2016; Hvas et al., 2017b) and a reduction in agonistic behaviour (Solstorm et al., 2016). As the current speed increases, the salmon stop swimming in a circular pattern, and instead stand on the current remaining stationary while swimming against the current (Johansson et al., 2014; Hvas et al., 2017b). In extreme current conditions fish can experience physiological fatigue, severe stress, injury and even death as the fatigued fish loses locomotive control and gets stuck on the downstream net pen wall (Oppedal et al., 2011; Remen et al., 2016).

There are claims that providing the salmon with an active current to swim against may promote growth. In a report describing experiences and analysis of five sites regarded as exposed it was concluded that there was little evidence of reduced fish welfare, and that it instead appeared to be improved (Sandberg et al., 2012). However a recent review on the subject of utilising current speeds to exercise the fish concluded that more research is still required to understand the potential advantages of swimming exercise and how this can be applied to improve production (McKenzie et al., 2020).

The impact of waves on fish behaviour is not well documented. Little research exists on the impact of waves on fish behaviour, mostly due to the practical limitations of how to study the behaviour in waves (Hvas et al., 2020). The studies that exist indicate that the impact of waves on fish behaviour depends on the wave's period (Johannesen et al., 2020). Shorter choppy waves may prevent the salmon from avoiding collisions with each other and the net, but its influence in the water column decreases with depth hence the fish may in theory avoid the waves by swimming deeper (Johannesen et al., 2020). This is not the case with long period swells. In general, the few studies carried out indicate a complex interaction between waves with different periods, current speed and cage deformation (Johannesen et al., 2020). Further research is needed to determine the consequences of waves on Atlantic salmon.

The uncertainty regarding how waves and currents affect fish welfare

raises the question of how to chose optimal exposed sites. To ensure fish welfare at future sites it is necessary to establish an assessment tool for the local environment with regards to both Atlantic salmon and any potential cleaner fish species. One potential method for evaluation sites with regards to current speed is to utilise the swimming performance of the relevant species (Plaut, 2001).

3.2 Species specific swimming capacity

According to Norwegian law the lumpfish as a vertebrate species has the same animal rights as Atlantic salmon (Norwegian Ministry of Agriculture and Food, 2009). However, as they are mainly used to combat the lice issue, the species needs are often not prioritized. This may have led to unsuitable environmental conditions for the lumpfish (Overton et al., 2020). The optimal environment for the two cohabiting species differ in several ways. For instance, their response to strong currents vary significantly due to different swimming capacities.

There are three main categories of swimming to describe a fish's swimming capacity: sustained, prolonged and burst swimming (Beamish, 1978). Sustained swimming is defined as speeds that can be maintained by the fish for extended periods of time (>200 minutes) without exhaustion (Brett, 1964; Beamish, 1978). Prolonged and burst swimming on the other hand both end in fatigue, where burst swimming can only be maintained for short periods (<20 seconds) while prolonged can be maintained for up to 200 minutes (Beamish, 1978).

The main methods for evaluating swimming performance focus on gait transition speed (Drucker, 1996), endurance (Beamish, 1978) and critical swimming speed (Brett, 1964). The critical swimming speed (U_{crit}) of fish is a standardized method of assessing the upper current velocities fish can handle on an acute timescale (Brett, 1964). U_{crit} values are determined in swim tunnels, where fish are exposed to a flow of constant velocity in systematic increments. Typically this is done by increasing the current speed by a specific amount at every 15-30 min until the fish is fatigued. In that sense it is an evaluation of prolonged swimming, but of a shorter period than suggested by Beamish (1978). The U_{crit} value is determined for individual fish as a function of the current speed of the last completed current velocity U_f, time spent in the current velocity where fatigue was reached t_f, time spent at each velocity increment t_i and the magnitude of the velocity increments U_i (Brett, 1964):

$$U_{crit} = U_f + \frac{t_f U_i}{t_i}$$

This incremental increase in current and stable flow is a situation rarely experienced in nature (Plaut, 2001). Hence when evaluating the current at a potential site, sustained swimming speed should also be considered because sustained swimming assesses the maximum swimming speed that can be maintained without resulting in fatigue (Beamish, 1978). Atlantic salmon can sustain at least 80% of their U_{crit} for up to 4 hr (Hvas and Oppedal, 2017).

As swimming at U_{crit} or higher speeds can result in fatigue, which is detrimental for the fish, it is a good proxy for the maximum acceptable current speed at a site. Using U_{crit} as a limit when evaluating site data is complicated by the fact that U_{crit} varies with environmental and biological factors such as water temperature, fish size, individual variations and diseases (Brett, 1964; Beamish, 1978; Remen et al., 2016; Hvas et al., 2017a,b). However, the use of swimming capacity for evaluating current data from different sites opens up the opportunity to evaluate if the site is suitable for all species present in the cage including cleanerfish.

The U_{crit} of lumpfish is considerably lower than for Atlantic salmon. This is due to the lumpfish' smaller size and it's morphology being unfit for fast swimming (Hvas et al., 2018). Vaccinated lumpfish are usually deployed when they are near 30 g (Sigstadstø, 2017). They are most efficient at eating lice before they reach sexual maturation, which occurs roughly around 400 – 500 g or after 16-18 months (Imsland et al., 2014, 2016). In that same period the Atlantic salmon post-smolt will have grown from 80 g to 4.5 - 5 kg.

Fig. 3.1 visualises the difference in swimming performance of the two species taking into account the effect of temperature. The temperature dependent critical swimming was derived by polynomial regression. A 2nd degree polynomial was fitted to the data for Atlantic salmon of ∼450 g acclimated to five different temperatures (Hvas et al., 2017a). The derived function for the salmon of 450 g was scaled to fit the critical swimming speed of the smaller and larger salmon. For the smaller smolt of 80 g and the adult salmon of 1750 g, the data from Remen et al. (2016) was used. The same approach was applied for the lumpfish with data for lumpfish of ∼300 g (Hvas et al., 2018), which was then scaled down to lumpfish of ∼75 g. It should be noted that there are individual differences within each species, for instance can the U_{crit} of larger salmon be as high as 125 cm/s

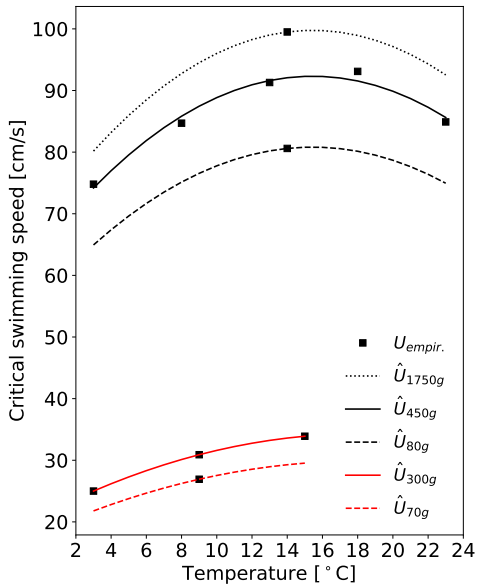

Figure 3.1: Temperature-dependent critical swimming speed ($\hat{U}_{crit}$) for Atlantic salmon (black lines) and lumpfish (red lines) of different sizes. The empirical critical swimming speed data (U_{empir}) for Atlantic salmon are from Hvas et al. (2017a) and Remen et al. (2016), and for lumpfish from Hvas et al. (2018)

(Hvas et al., 2017b). If however the individual is exposed to either disease of parasites, the U_{crit} can be reduced (Hvas et al., 2017c). This also holds true for lumpfish.

A similar graph could be made for other potential species at the farm site, for instance the much used cleanerfish ballan wrasse. However, the U_{crit} for ballan wrasse could not be established for fish acclimated at temperatures lower than 25 °C as they could not be stimulated to swim for prolonged periods. At 25 °C their critical swimming speed was 27.3 cm/s (Yuen et al., 2019).

Although the lumpfish has a low critical swimming speed they can sustain strong currents for a short period using their ability to adhere to surfaces. The lumpfish can remain attached to a surfaces for 1 min when exposed to currents of 110 cm/s (Hvas et al., 2018). Independently of current speed however the lumpfish could not adhere to a surface for more than 20 min (Hvas et al., 2018). As exposed sites may experience strong currents

for longer periods, the difference in critical swimming speed between salmon and lumpfish, and the short duration it can adhere to surfaces, suggests that lumpfish are at greater risk of experiencing poor welfare at exposed sites. A comprehensive evaluation of a site should therefore also include an evaluation of which species are acceptable to use.

3.3 Site evaluation using fish welfare parameters

In Paper A an outline was drawn for how to evaluate current data from sites with regards to fish welfare. The main concept of Paper A was that the current data gathered during a site survey could be examined and classified applying knowledge of the Atlantic salmon's swimming performance. Specifically, a new class system for the current strength in the likes of NS-9415 was presented (Table 3.1 and 3.2), but the classes were defined based on behavioural patterns (Gansel et al., 2014; Johansson et al., 2014) and critical swimming speed (Remen et al., 2016; Hvas et al., 2017a,b).

The 'Very weak' and 'Weak' classes in Table 3.2 have the same swimming behaviour, but were separated to isolate events of low dissolved oxygen (DO) levels inside the cages, which may occur during periods of low current flow. 'Moderate', 'Substantial' and 'Strong' were all defined applying the noted swimming behaviour. The 'Very strong' was defined using conservative estimates of critical swimming speed. U_{crit} was defined as the lowest value found in the polynomial regression for the smallest post-smolt (80 g) at 3 °C, that is 64.5 cm/s (Fig. 3.1). To account for individual differences, the limit was set to 60 cm/s. This is a very conservative estimate as there is a substantial reduction in current speed through the cage net of roughly 21.5% (Klebert et al., 2015). The reason for using such a conservative esti-

Current class	$V_c(m/s)$	Exposure designation
A	0.0-0.3	Little
B	0.3-0.5	Moderate
C	0.5-1.0	Substantial
D	1.0-1.5	High
E	>1.5	Extreme

Table 3.1: Classification of aquaculture sites in Standard NS-9415 (Standards Norway, 2009) based on the 10 yr return period of the current velocity (V_c).

mate was to determine a limit which would ensure that the wellbeing of all fish including those that might suffer some ailment would be preserved.

The NS-9415 determines the current class at a site by multiplying the maximum current recorded at 5 m depth and 15 m depth by a given factor (Table 3.1). The idea behind the new classification scheme was that by classifying each measurement at each depth, and finding the percentage of time the current was defined as each class, would provide more insight into the environment experienced by the fish. The new classification scheme was applied on current data gathered by use of ADCPs at five different sites for a minimum of 5 months (Fig. 3.2). The NS-9415 classes of each site were also determined and are summarised in Table 3.3.

The location Froya2 was the most exposed site and was classified as 'Extreme exposure' using NS-9415 (Table 3.3). This site was the least shielded and was fully exposed to the current coming in from the open sea. Using the NS-9415 classification Aafj, Fr1 and Fr3 were all classified as having 'High exposure', but when inspecting the maximum current speed in the top 10 cells of each locations these sites appear quite different (Fig. 3.3). Furthermore, applying the classification presented in Table 3.2 the current at Aafj appeared to be generally weak (Fig. 3.4). The NS-9415 classification of Aafj was based on the short period of strong currents in June 2015 (Fig. 3.3). As the NS-9415 only requires one months of measurements Aafj would have been classified differently based on when the site survey had been carried out. This demonstrates some of the critique which NS-9415 has received in recent years regarding the calculation of extreme limits and why there is currently a suggestion to change how locations are classified (Eidnes et al., 2018).

Current		Swimming behaviour
Speed (cm/s)	Class	
0-10	Very weak	Freely
10-20	Weak	Freely
20-40	Moderate	Circular pattern is disrupted; some fish standing on current
40-50	Strong	All fish standing on current
>60	Very strong	Exceeds U_{crit}

Table 3.2: Definition of current classes based on established limits related to the onset of behavioural changes and critical swimming speed (U_{crit}) of Atlantic salmon

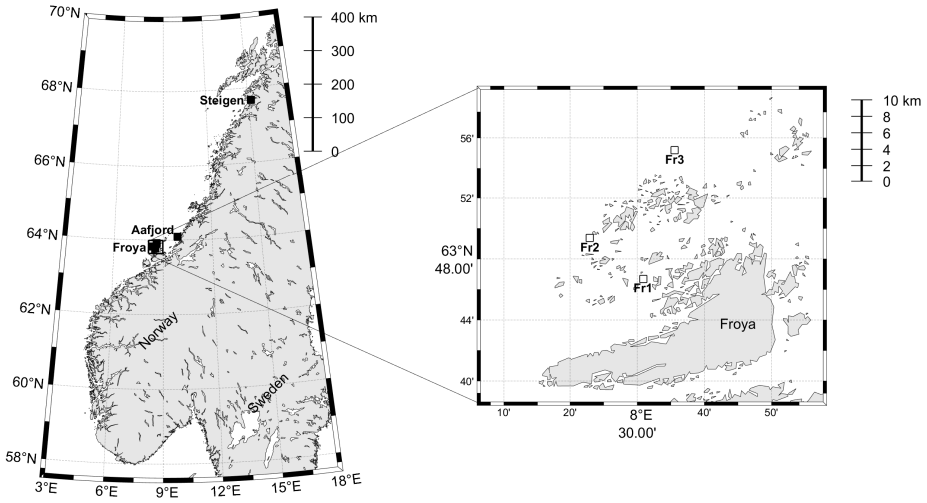

Figure 3.2: Locations of the acoustic Doppler current profilers (ADCPs) at Åfjord (Aafj), Steigen (Ste), and the Frøya archipelago (Fr1, Fr2 and Fr3)

Site	Current								NS
	Mean	Medi.	Mode	Max	SD	Sign. max	Sign. min	10 yr. return	9415 class
Aafj	8.8	7	3.5	62.1	6.9	16	3.5	102.5	D
Fr1	12.6	11.7	7	57.4	8.1	21.6	5.2	104.4	D
Fr2	17.6	15.2	9.4	112.5	11.8	30.5	6.9	176	E
Fr3	13.9	12.9	5.9	71.5	8.2	22.2	6.4	110.2	D
Ste	7.2	6.2	3.2	36	4.6	11.3	3.8	56.6	C

Table 3.3: Descriptive statistics for all locations displaying mean, maximum, SD, and significant maximum and minimum current speeds. The 10 yr return period calculated in accordance with Standard NS-9415 (Standards Norway, 2009) and the corresponding current classification are also listed.

To get a better understanding of the currents at the five locations the duration of each class was determined (Fig. 3.5). The 'Very weak' current class at Aafj could persist for over 125 consecutive hours for the top 20 m of the water column. This further clarified the distinction between Aafj, Fr1 and Fr3. The long duration of the 'Very weak' currents could indicate that Aafj is susceptible to periods of low water exchange through the cage, which could result in low DO levels. DO was however not recorded during the same period and could not be verified.

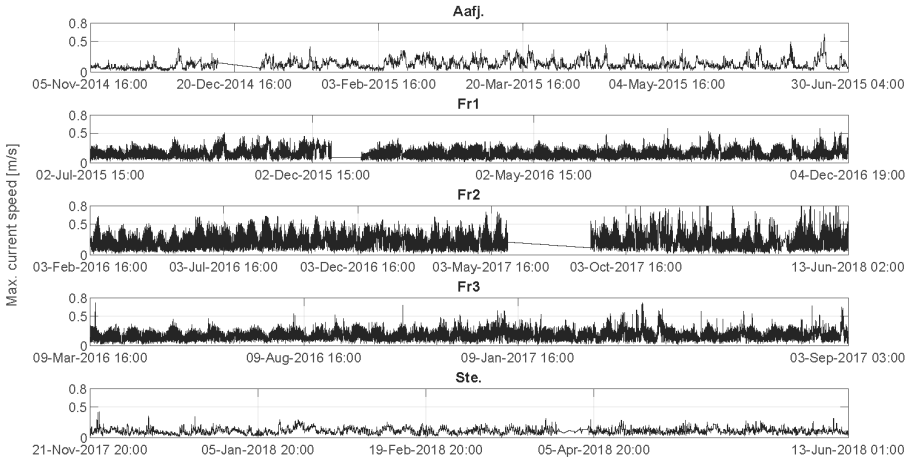

Figure 3.3: Maximum current speed in the top 10 cells of each location, also showing the periods were data was collected.

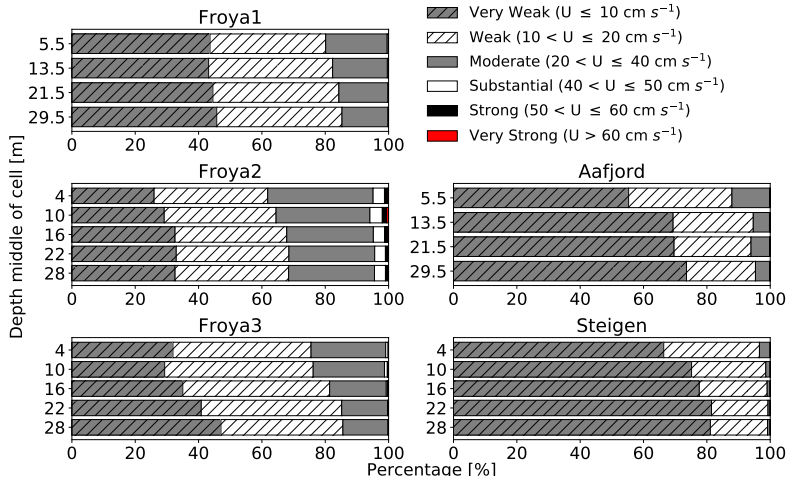

Figure 3.4: Total distribution of current classes over the entire duration of deployment for selected depths at each location. U: current speed.

To evaluate how suitable each site was for Atlantic salmon post-smolt of 80 g and for lumpfish, the measured current was evaluated using the temperature dependent critical swimming function displayed in Fig. 3.1. Using the temperature sensor on the ADCP, the recorded current speed was transformed into a percentage of the critical swimming speed at that given temperature. Instead of using the classes defined above the current speed

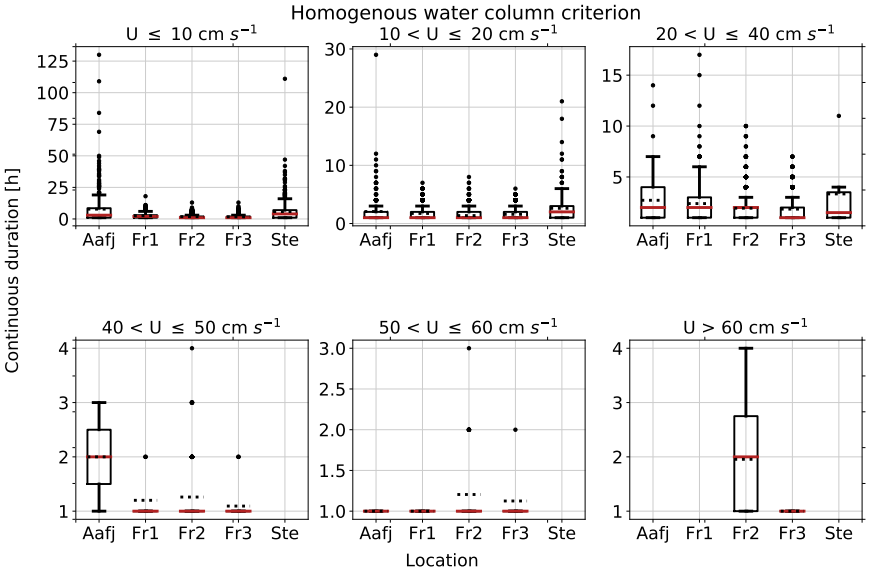

Figure 3.5: Number of consecutive hours in each current class using the homogeneous criterion for the water column. Red line: median; horizontal dotted line: mean. Lower whisker extends to first quartile (Q1) minus 1.5 times the interquartile range (IQR). Upper whisker to Q3 + 1.5 × IQR. Data outside of the whiskers are represented as dots and are valid data points. Dots do not necessarily represent a single occurrence. U: current speed.

was categorized as either between 0.6 U_{crit} and 0.8 U_{crit}, between 0.8 and U_{crit}, and exceeding U_{crit} values for both Atlantic salmon and lumpfish (Fig. 3.6).

Fr2 was the only site considered unsuitable for salmon post-smolt of 80 g. Anecdotally, the farm operators at the farm closest to Fr2 reported that they used large post-smolt and their main struggle was carrying out day-to-day operations, not fish welfare. With regards to fish welfare Fr2 might be a better site than for instance Aafj and Ste as Fr2 had shorter periods with weak currents. This is however not the case for lumpfish. Evaluating the current speeds using the critical swimming speed of lumpfish it would appear that only Steigen was a suitable site for lumpfish. In general this supports the notion that special care must be taken when utilising lumpfish together with Atlantic salmon (Hvas et al., 2020; Overton et al., 2020).

Applying all three methods of evaluating the current speed as presented in Paper A is redundant. The approaches in the paper demonstrate how

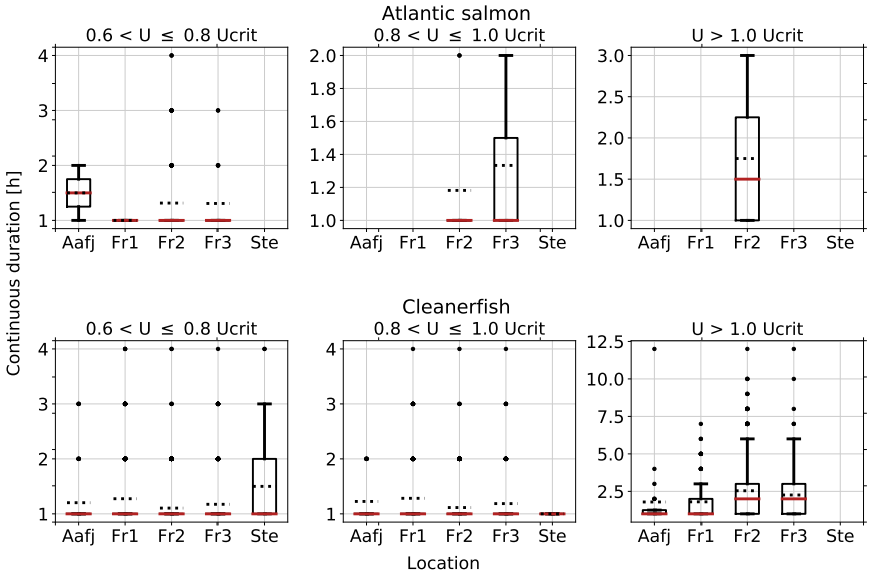

Figure 3.6: Number of consecutive hours where the currents were within given ranges of the critical swimming speed (U_{crit}) for Atlantic salmon and lumpfish using the homogeneous criterion and the temperature dependant assessment of the critical swimming speed limit.

inspecting the current speeds over the entire deployment period, instead of just extracting the maximum value, can give insight into potential issues experienced at the site. The data also exemplifies the harsh conditions the lumpfish may face in a cage considered suitable for Atlantic salmon rearing.

The suggested approach for evaluating a site would be to first inspect the ADCP data using the classification scheme (Table 3.2) to determine what issues might arise at the site. If currents are in the 'Very Strong' class, the current speed should be evaluated using the temperature dependent critical swimming speed for all potential species at that site. If the U_{crit} is exceeded, the site may still be suitable and there are several remedies. The simplest one is to use larger post-smolt, as this would increase the U_{crit} value. Given the temperature dependency of the critical swimming, the necessary size of post-smolt could vary between spring and autumn deployment, hence temperature measurements are also necessary for informed decision making about optimal size of post-smolt. An increase in size will however not help the lumpfish, as their swimming capacity increase little with size, and their lice grazing is reduced if they reach a size of 350-500 g and sexual maturation.

The novelty of Paper A is not the exact limits suggested, but rather the method and concept of evaluating the current speed from site surveys with regard to the sites suitability for different species. Paper A also exemplifies the large variability between sites regarding currents.

Chapter 4

Current flow and shielding skirts

4.1 Salmon lice and lice shielding skirts

Of the many preventative-focused methods for handling sea lice, barrier technology shows great potential (Barrett et al., 2020). Barrier technology utilises the behavioural traits of the louse to keep them out of the cage. Salmon lice's position in the water column is determined by its response to several environmental cues and aims to maximise host interaction. Salmon lice copepodids follow a diurnal vertical migration pattern by rising towards the surface during the day and sinking at night, which is the opposite of salmon, hence maximizing interaction opportunities as they cross each other in the water column (Huse and Holm, 1993; Heuch et al., 1995). In addition to the diurnal vertical migration, the different life stages of the louse show a clear preference for certain temperatures and salinity levels. The nauplii stages avoid salinities below 30 ppt (Crosbie et al., 2019) and prefer colder water temperatures (Crosbie et al., 2020), while the copepodids are found in water with salinities as low as 16 ppt (Crosbie et al., 2019) and show no preference for temperature (Crosbie et al., 2020). Due to its preferred environment and diurnal pattern, there is a higher prevalence of salmon lice in the upper layers of the water column (Huse and Holm, 1993; Heuch et al., 1995; Hevrøy et al., 2003; Oppedal et al., 2017; Geitung et al., 2019; Barrett et al., 2020). This information has led to the development of barrier technology.

The common goal of barrier technology is to prevent lice-salmon interaction. One such technology is the lice shielding skirt, which is extensively

used along the Norwegian coastline. There are currently several different forms of lice shielding skirts used in the industry. The most common one is the tarpaulin skirt, but there are also variations such as the permeable skirt which is made of a fine-masked fabric letting some of the water pass. Both of these are available in different lengths. What type of skirt and when they are deployed, cleaned and removed vary from site to site (Misund et al., 2020).

The use of skirts is not without problems. Firstly, the efficiency of lice shielding skirts on preventing lice infestations are varied with some sites experiencing reduction in lice infestations (Næs et al., 2014; Grøntvedt et al., 2018; Stien et al., 2018; Bui et al., 2020b), while others find little to no effect when using skirts (Grøntvedt and Kristoffersen, 2015; Lien et al., 2015; Grøntvedt et al., 2018). These differences could be caused by local current conditions and hydrography, but they could also be caused by different lice families responding differently to hydrostatic pressure (Coates et al., 2020).

Secondly, as the skirts disrupt the normal current flow pattern through the cage, the usage of lice shielding skirts can have an adverse impact on the environment within the cage. Some farms experience low dissolved oxygen (DO) levels when using skirts (Stien et al., 2012; Misund et al., 2020), and some report issues with gill diseases (Misund et al., 2020). These issues are not encountered on all sites, hence the difference in lice shielding efficiency and impact on internal environment could be caused by local current and hydrographical conditions.

4.2 Lice shielding skirts and current flow

For an empty non-shielded cage a reduction in current speed is expected as the current travels through the cage. Klebert et al. (2015) measured the current speed upstream, downstream and inside a non-shielded cage, and documented the gradual reduction in current speed through the cage with a reduction of 21.5% from upstream to inside the cage. A higher reduction is expected when using lice shielding skirts.

Lice shielding skirts disrupt the natural current flow by increasing turbulence levels and reducing current speed (Frank et al., 2015; Klebert and Su, 2020), but also by altering the current flow pattern inside the cage. Computational Fluid Dynamics (CFD) simulations of a laminar current flow around a cage with a rigid shielding skirt show that the ocean currents are pressed around, but also underneath the skirt and into the cage (Lien and Høy, 2011; Lien et al., 2015). This rerouting of the current into the fish cage

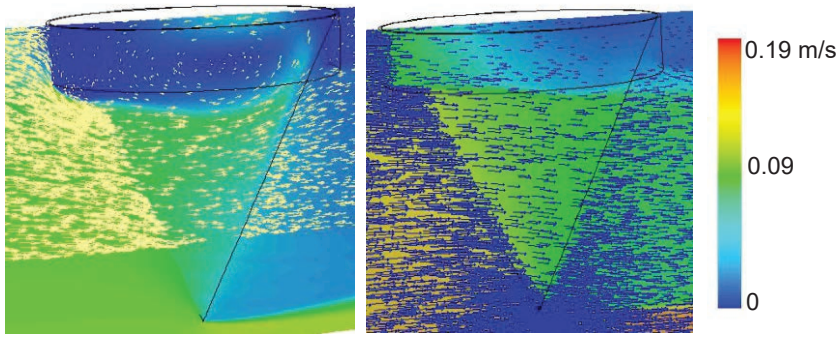

Figure 4.1: CFD simulation of conical cage with non-permeable (left) and permeable (right) skirt. The color of the incoming arrows are just to make the recirculation pattern with the non-permeable skirt clearer, the colour in the background gives the current speed. (Simulation from P.Klebert SINTEF Ocean, shared with permission.)

is also observed in full-scale dye experiments where dye was released outside of the skirt, but managed to pass underneath and into the cage (Frank et al., 2015). CFD simulations show that once inside the cage the current flow traverses the cage and makes contact with the skirt downstream and is pushed upwards, before moving in towards the centre of the cage again. Fig. 4.1 illustrates this recirculation patter. This pattern is also observed in model-scale experiments (Lien et al., 2014) and full-scale measurements when the shielded cage was empty, but not when stocked (Klebert and Su, 2020). It is uncertain if this recirculation pattern is apparent when using permeable skirts. Simulations in Fig. 4.1 show the recirculation pattern when the skirt is non-permeable, but not when modelling the skirt as a permeable surface.

In the dye experiment by Frank et al. (2015) two trials were executed and the amount of dye entering the cage varied. As the current conditions were similar during the two trials, it was suggested that the variation was either due to different hydrographical conditions during the trials, or the fish's swimming pattern. It is theorized that when the fish swim in a torus shape, they push the water outwards at depths of high biomass, resulting in an area of low pressure drawing in water from the depths above and below (Gansel et al., 2014; Frank et al., 2015). Simulations of this behaviour support this theory (Tang et al., 2017), however, no such theorized upwelling was observed in a full-scale stocked shielded cage (Klebert and Su, 2020). This may indicate that different hydrographic conditions during the two

trials in Frank et al. (2015) caused the varying amount of dye that entered the cage.

With the widespread use of skirts, and the large variance in both efficiency and encountered issues, there were two overarching themes that were investigated as part of this thesis. The first was how the current behaves when skirts are deployed, both with permeable and non-permeable skirts, and the second how the skirts influence the internal environment of the cage.

4.3 Current flow with and without lice shielding skirts

Several studies have investigated the current flow around cylindrical gravity cages, both with and without skirts. Comparing results from different studies is however complicated due to variable cage geometry, topography, hydrography and different stocking densities. Full-scale measurements were therefore performed at the same cage at Hosnaøyan with and without the skirt deployed (Paper C).

Hosnaøyan was a 28 m deep cylindrical cage with a diameter of 50 m equipped with a 6.7 m long non-permeable tarpaulin skirt (Fig. 4.2 and 4.3). Vertical positioning of the fish was documented using an echosounder, DO sensors were used both inside and outside the cage and current measurements were performed at three depths inside the cage using an ADV and

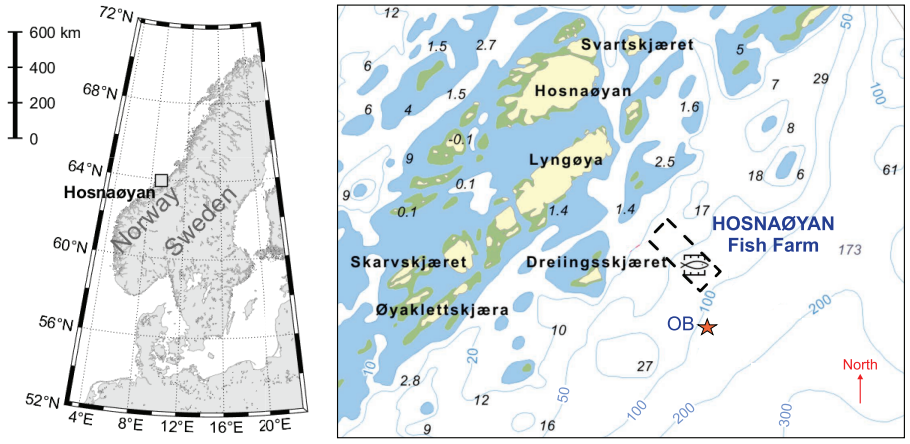

Figure 4.2: Location of the fish farm at Hosnaøyan, where the measurement campaign was carried out in November 2018.

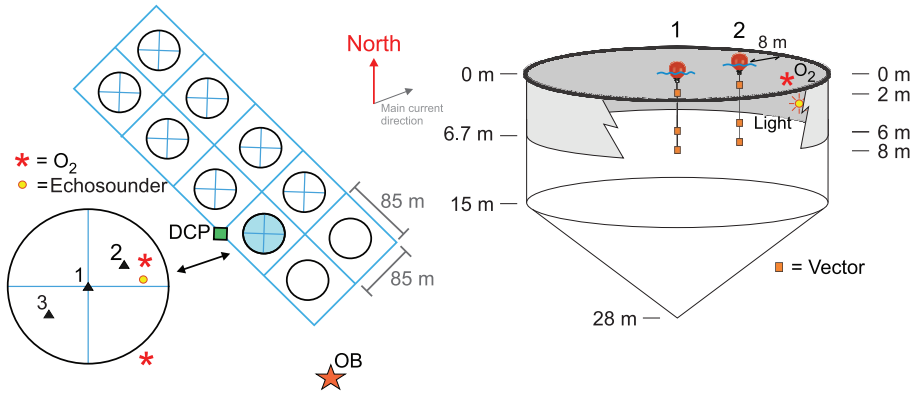

Figure 4.3: Instrument placement at Hosnaøyan. The shaded blue cage was used as the experimental cage. The Aanderaa current profiler (DCP) was placed at the square marked DCP. The vector current meters (ADV) were moved between the two positions 1 and 2. Three ADVs were used, positioned at 2, 6 and 8 m depth suspended from a floater held in place with ropes attached to the cage ring. Two dissolved oxygen (DO) sensors were deployed, one on the inside also suspended from a floater 3 m from the cage ring, and one outside of the cage suspended from the cage ring (marked with *), both at 3 m depth. A light source was mounted at 5 m depth inside the cage. The position of the oceanographic buoy (OB) is marked with a star. The main current direction during Case 1 and 2 (see Fig. 4.4 for relevant periods) is also marked just beneath the North sign.

with an ADCP profiler outside. DO, current and waves were also recorded at a nearby oceanic buoy, but with a much lower temporal resolution than the other sensors due to its long-term deployment.

The DO level inside the cage was clearly influenced by the presence of the skirt (Fig. 4.4). The skirt was mounted on the cage the 4^{th} of November, one day prior to the study taking place and removed on the 6^{th} of November 09:48 local time due to a steep fall in DO. As the skirt was removed the DO improved immediately, and after ∼30 the DO reached similar levels as at the oceanic buoy. When the skirt was removed both DO inside and just outside the cage improved. The increase in DO just outside was probably due to a non-optimal positioning of the sensor in the wake of the cage, evident by the near constant DO observed at the oceanic buoy.

Initially the DO levels inside the cage were similar to those recorded just outside and on the oceanic buoy. During the night on both the 6^{th} and

the 7th there was a drop in DO with a steeper drop on the 6th. These drops in DO were most likely caused by a weak turning current as seen in the DCP and an increase in swimming and feeding activity during the morning seen in the echosounder (Fig. 4.4). With the skirt deployed the lowest recorded DO was 59% (∼6.9 mg/L), while the lowest value was 69% (∼7.9 mg/L) without the skirt. The drop in DO is most likely an unavoidable occurrence when the current turns at this location, but the severity of the drop was intensified by the presence of the skirt. Due to the short duration of the study it is unclear whether DO inside the cage would have improved without intervention and if low DO was a prevalent issue at this location. Anecdotally it should be noted that the operators did not have the skirt deployed prior to this study due to concerns regarding low DO levels.

The fish followed a diurnal pattern with the fish migrating toward the surface at night, and swimming deeper during the day. During the steep drop in DO the salmon spread out more vertically, it is uncertain if this increase in activity was caused by the drop in DO, or if it contributed to the drop, as a similar spread in vertical positioning occurred on the 7th of November in the morning (Fig. 4.4).

This diurnal vertical swimming pattern is in accord with previous studies of vertical behaviour (Oppedal et al., 2011), but in contrast to the results found in Gentry et al. (2020) where the schooling fish were observed to avoid the skirt volume. It is possible that the difference in behaviour was due to the type of skirt, or length of deployment. In Gentry et al. (2020) a permeable 6 m long skirt was used, and the study spanned 49 days, while this study was only two days long and used a dense skirt. It is uncertain if the fish would have avoided the skirt to a larger extent if it had been deployed for a longer period.

Unsurprisingly, the skirt had a direct influence on the current flow. The current at Hosnaøyan was mainly coastal driven and appeared to be stratified with currents moving in different directions at different depths during the study. This was apparent both at the oceanic buoy and the DCP. It should be noted that the DCP had an obstruction in its line of sight at roughly 8 m depth, most likely the frame mooring (Fig. 4.4). This obstruction was considered non-problematic due to the conical shape of the sound signal, but the depth layers spanning 7 – 9 m were not included in further analyses.

To study the impact the skirt had on the current flow two periods, Case 1 and Case 2, were selected based on criteria set for the current direction and speed summarised in Table 4.1. The criteria were that the current had

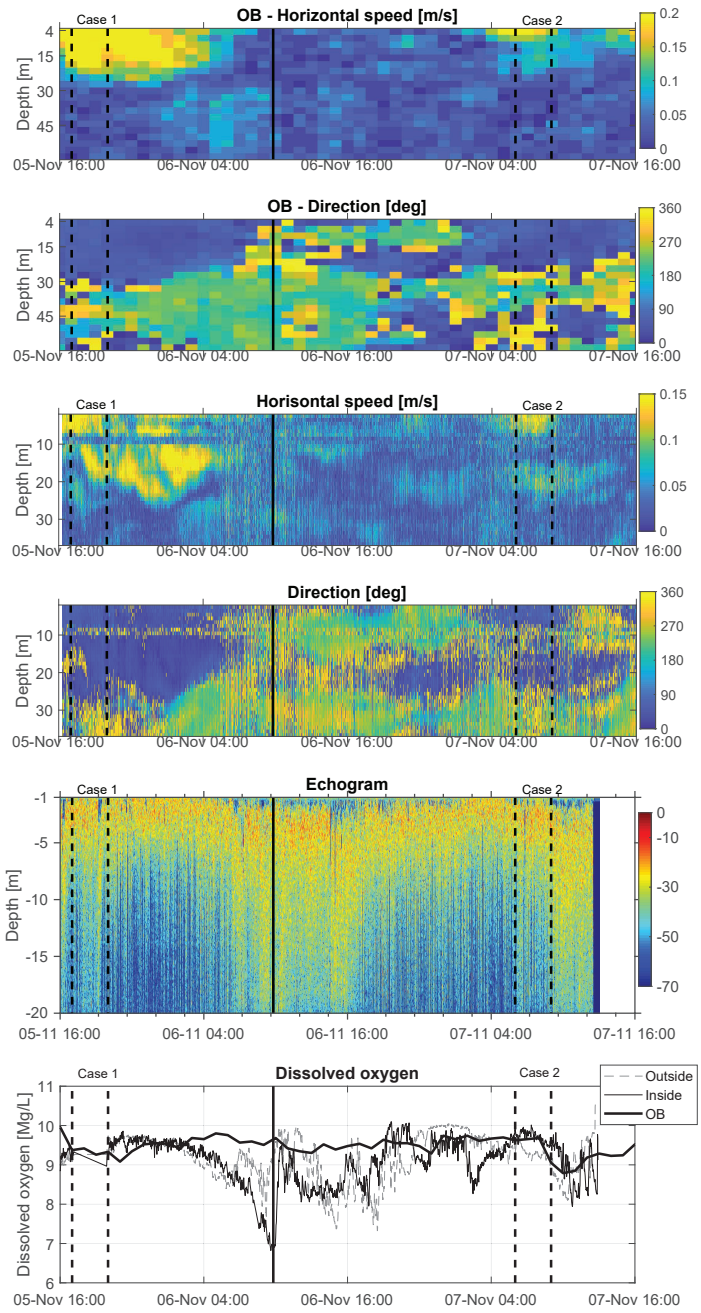

Figure 4.4: Current speed and direction at the OB and DCP. Echogram showing acoustic backscattering strength (S_v) [dB]. DO in Mg/L recorded inside and outside of the cage, and at the OB. Case 1 and Case 2 are marked with dotted lines, while the solid line marks when the lifting of the skirt was initiated.

to move along the depth isobaths (see Fig. 4.2) and had to be reasonably stable and unobstructed by surrounding farm structures. Only data where the average hourly current direction was aligned with the depth isobaths towards 45-90° (North-East to East) were included. As an additional requirement the hourly current direction at the DCP had to deviate less than ± 25° from the current direction measured at the oceanographic buoy in the same period.

Case	ADV Position	Skirt condition	Date	Time interval
1	1	Down	5.11.2018	17:00 - 20:00
2	2	Lifted	7.11.2018	06:00 - 09:00

Table 4.1: Description of cases including ADV position and time intervals.

The average reduction from the DCP outside to the ADVs inside showed a clear increase in reduction when the skirt was deployed (Table 4.2). Interestingly, the reduction at 6 m depth was less when the skirt was deployed. This is probably due to an interaction between the current and the depth of the skirt. As the current is pressed underneath the skirt, it is accelerated, and it is possible that it is this effect that is observed.

During Case 2 when the skirt had been removed the ADVs were unfortunately placed further downstream in Position 2. The reduction of 32% was higher than expected, as similar studies have found a reduction closer to 21.5% when no skirt is deployed (Klebert et al., 2015). However, in a study by DeCew et al. (2013) the average reduction through a stocked experimental cage with a diameter of 4.57 m was 31% at 2 m depth, where DeCew et al. (2013) theorized that this higher reduction was due to biofouling. This is not a sufficient explanation at Hosnaøyan as the nets were cleaned just four days prior to the study taking place. It is more likely that the high

	Mean reduction [%] (± STD)	
Depth	Case 1 (with skirt)	Case 2 (without skirt)
2m	56.9 (± 21.4)	32.0 (± 12.3)
6m	10.4 (± 15.1)	17.9 (± 19.5)
8m	18.6 (± 16.0)	14.6 (± 18.0)

Table 4.2: Mean reduction through cage for each depth for the two cases with and without skirt. Readers should note that the ADV in Case 1 is located in position 1, while it is position 2 in Case 2

reduction at 2 m was due to the high biomass at this depth (Fig. 4.4) as biomass can increase the reduction in current speed (Klebert and Su, 2020). The echosounders beamwidth is only 26°, hence the volume that it observes is small compared with the volume of the cage. But given the diurnal swimming pattern of the fish, it seems reasonable to assume that the recording is representative for the cage.

A positive upwelling was seen in the centre of the cage when the cage was shielded similar to that in Klebert and Su (2020) and in the simulations in Tang et al. (2017), but was not present when the cage was unshielded. It should be noted that this component was small, but given the results of Klebert and Su (2020) it would indicate that the upwelling appears to be a consequence of the shielding, and not the biomass.

To summarise, the results of Paper C indicate that the presence of a tarpaulin skirt has a direct influence on the current flow by reducing the current speed inside the cage and causing a weak upwelling in the centre of the cage. The skirt also accentuated the drop in DO and caused unfavourable levels.

4.4 The flow field around a conical cage with permeable skirt

The characteristic current flow field at a farm dictates how nutrients, waste and food pellets are transported through the cage and downstream of the cage. The reduction in current speed that occurs as the current passes through the net can increase sedimentation near the cage, while the increase in turbulence downstream can keep certain particles suspended for longer periods (Klebert and Su, 2020). There have been several full-scale studies of the current flow around and downstream of a cylindrical cage, but none around conical cages. The current flow field around a conical cage is expected to be different from the cylindrical cage as the inclination angle is higher for conical cages, increasing the reduction through the net (Bi et al., 2013; Zhao et al., 2015). The objective of Paper D was therefore to determine the characteristic flow pattern around a conical cage equipped with a permeable skirt.

The study was carried out on Fornes between the 2nd to the 5th of July 2019 (Paper B and D). Measurements were taken around and inside a 55 m deep conical cage with 50 m diameter equipped with a 10 m deep permeable skirt (Fig. 4.5). To establish the characteristic current flow field, the current outside the cage was required to have a relatively stable direction through a

30-minute period and the water column had to be near homogeneous. Due to a density gradient the first two days, only the last two days of the study could be used to determine the characteristic current flow. The hydrographic conditions and influence on DO inside the cage was studied in Paper B and are discussed in Chap. 4.5.

The periods that passes the requirements are summarised in Table 4.3. Based on the direction of the incoming current the data was classified as either heading Northwards or Southwards. To ensure that there were no topographic effects or other effects dependent on the direction of the current, the two groups Northwards and Southwards were preserved when determining the characteristic current flow. A more detailed description of data scrubbing can be found in Paper D.

Comparing the results for the shielded conical cage with that of a non-shielded cylindrical cage in Klebert et al. (2015) revealed several distinctions. The first was that the reduction in current speed downstream of the conical cage faded at roughly 22 m depth probably due to the tapered shape and smaller diameter of the cage at that depth, which was only 28 m (Fig. 4.6). Beneath this point there was no clear reduction in current speed. At the shallow site investigated in (Klebert et al., 2015) the current flow accelerated beneath the cage which may influence the sedimentation process and possibly result in better transportation of the waste away from the cage.

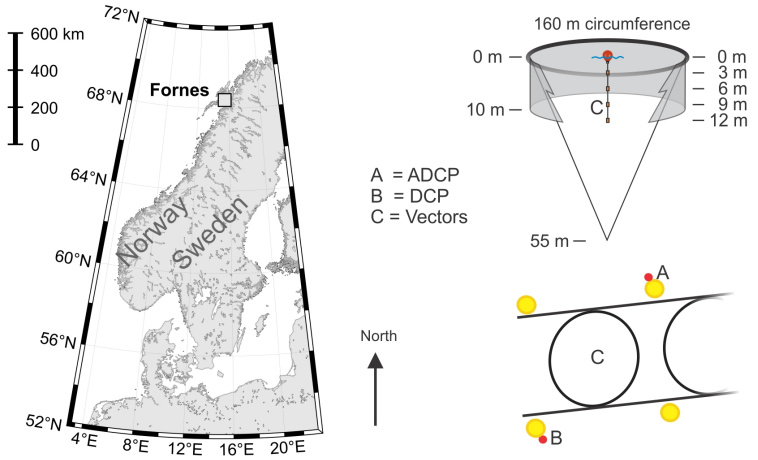

Figure 4.5: Left: Location of the fish farm at Fornes were the measurements were carried out. Right: Shape and dimensions of the cage and shielding skirt studied, and the location of sensors.

Northward		Southward	
Name	Date and Time	Name	Date and Time
N1	04-07-19 19:30–20:00	S1	05-07-19 02:15–02:45
N2	04-07-19 20:00-20:30	S2	05-07-19 02:45–03:15
N3	04-07-19 20:30–21:00	S3	05-07-19 03:15–03:45
N4	04-07-19 21:00–21:30	S4	05-07-19 03:45–04:15
N5	05-07-19 06:30–07:00		
N6	05-07-19 07:00–07:30		
N7	05-07-19 07:30–08:00		

Table 4.3: Periods where the upstream current passed the requirements. See Paper D for more details.

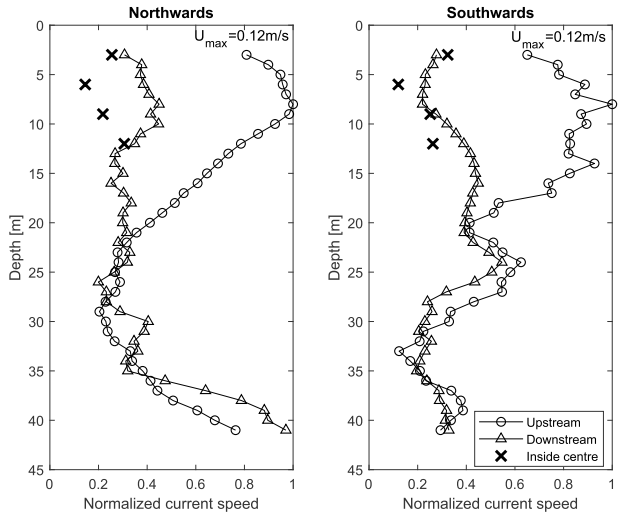

Figure 4.6: Average normalized horizontal current speed recorded at each depth in sensors upstream, downstream and inside the cage. The maximum average current speed was 0.12 m/s independent of direction.

This acceleration was also apparent in simulations (Bi et al., 2013). Secondly, the current speed through the non-shielded cylindrical cage had a near linear decrease in speed, while no such pattern was observed for the shielded conical cage (Fig. 4.6).

Downstream of the cage the reduction diminished beneath 9 m, most evident when the current was heading southwards (Fig. 4.6). This could be

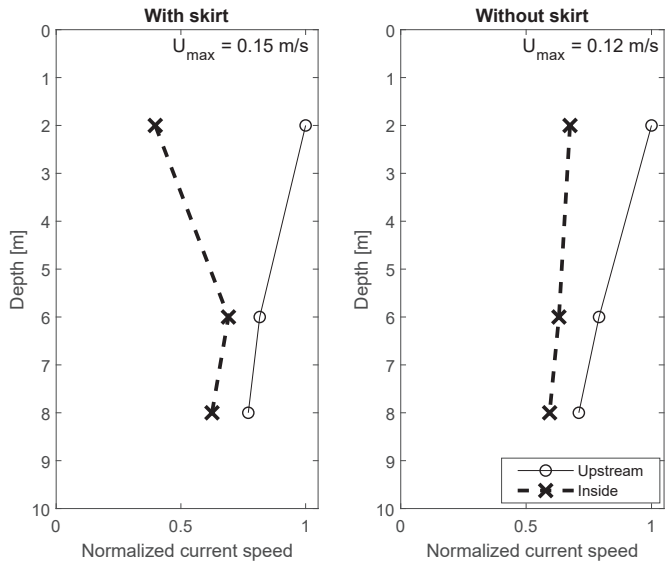

Figure 4.7: Normalized current speed upstream and inside the cage at Hosnaøyan. Note for the case without the skirt deployed, the ADVs were placed roughly 15m downstream of center. The skirt was 6.7 m long.

due to deformations of the skirt. Both impermeable and permeable skirts can experience large deformations when exposed to strong currents (Lien et al., 2015). When the current speed is sufficiently high the upstream section of the skirt can creep upwards as it is pushed into the cage, while the downstream section will lift and stand out like a sail (Lien et al., 2014). How the skirt deforms is influenced by how it is installed. At Fornes the skirt was installed as one piece of fabric with a 10 m overlap at the south side of the cage. At the overlap the skirt was at times observed to balloon out up to several meters (Fig. 4.8). The ballooning in Fig. 4.8 was probably due to a shorter period of currents close to 20 cm/s roughly an hour prior to the picture being taken (Fig. 4.12). A preliminary study at the same site in 2018 observed skirt deformations by use of pressure sensors along the bottom of the skirt and registered greater vertical deformation of the skirt downstream than upstream when currents exceeded roughly 13 cm/s (Volent et al., 2020). It should be noted that the horizontal speed inside and downstream of the cage were very low during the selected periods for determining the characteristic current flow, so it's uncertain if the skirt was deforming at all during the selected periods.

The reduction inside the cage varied with depth, similarly to that at

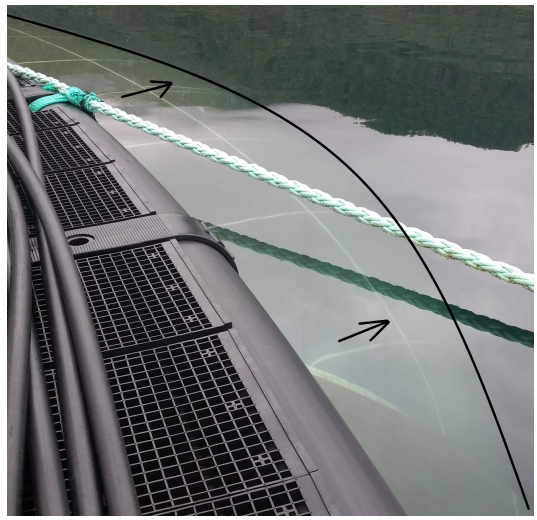

Figure 4.8: Black line marks the visible edge of the skirt being lifted due to the current. Black arrows indicate the main current direction. Overlap is visible just beneath the bottom arrow.

Hosnaøyan, but the reduction inside the cage was much stronger, with a maximum reduction of 86% recorded at 6 m depth (Fig. 4.7 and 4.6). It is theorized that the main cause for the high reduction at 6 m was the biomass as the presence of fish in a shielded cage increases the reduction in speed through the cage (Klebert and Su, 2020). The stocking density at Fornes was 20 kg/m^3, while it was 21 kg/m^3 at Hosnaøyan. Salmon rarely distribute themselves evenly throughout the cage, and have a tendency to swim deeper during daylight (Oppedal et al., 2011), as observed at Hosnaøyan. There was continuous daylight throughout the study at Fornes, so it is uncertain if the fish followed the normal pattern. It is also possible that the effective stocking density at Fornes was higher than at Hosnaøyan. It is unlikely that the salmon were spread evenly throughout the depth of the cage as the environmental drivers will often result in a preferred depth layer for the salmon (Oppedal et al., 2011). Another potential explanation for the high reduction inside the cage at Fornes was biofouling of the skirt. The permeable skirt was deployed 10 days prior to the study, and given that this was in July, it is likely that some biofouling took place however this was not verified during the study.

The reduction in current speed downstream of net panels have usually been studied in model cages or numerically (reviewed in Klebert et al. 2013),

with only a few studies performed at full scale in commercial cages with fish (Johansson et al., 2007; Klebert et al., 2015; Klebert and Su, 2020). All of the full-scale experiments have been carried out on cylindrical cages. These have compared relatively well with the analytical expressions developed by Løland (1993), but it was uncertain if that would be the case for the current study due to the conical shape of the cage and the permeable skirt. The reduction in current speed through the cage was therefore compared with the expected reduction in current speed determined by the analytical expressions developed by Løland (1993) and Føre et al. (2020) (Fig. 4.9).

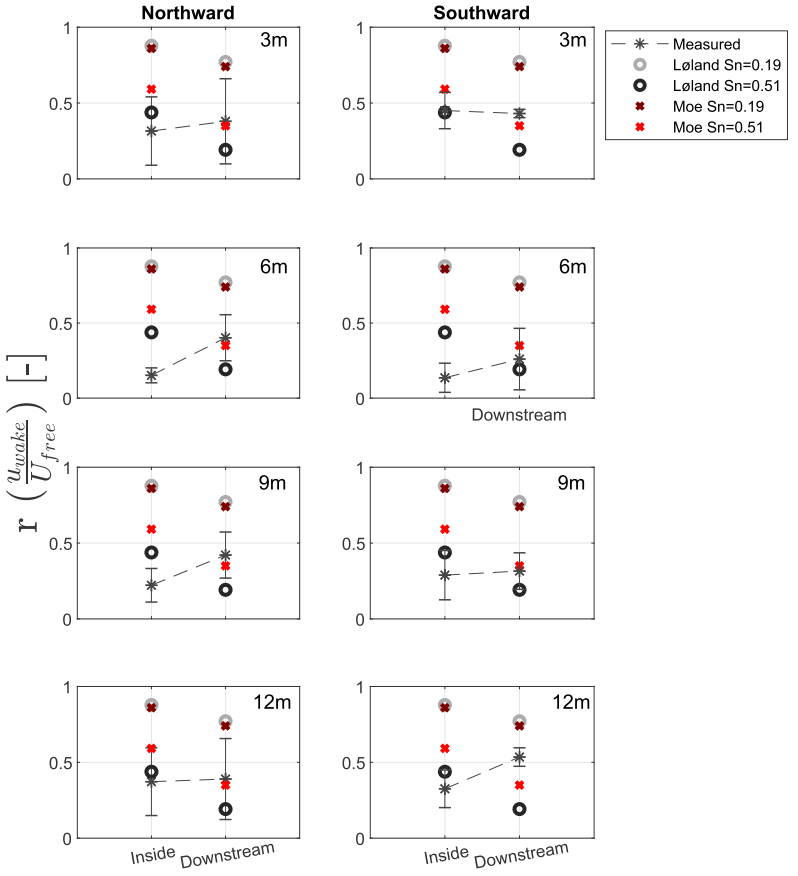

Figure 4.9: Average reduction ratio (r) between current speed inside and upstream, and downstream and upstream, measured in this study. Expected reduction ratio behind one net panel and two net panels using Løland (1993) and Føre et al. (2020) are also marked using S_n=0.19 and S_n=0.51.

Løland (1993) proposed a theoretical expression for the non-dimensional velocity reduction factor r behind a net panel based on the solidity (S_n) of the nets: $r = u_w/U_0$ where u_w is the flow velocity in the wake of the cage and U_0 is the free-stream velocity. The velocity reduction factor r is defined as $r = 1 - 0.46C_d$, where C_d is the drag of the netpanel calculated from the Sn with the following expression $C_d = 0.04 + (-0.04 + 0.33S_n + 6.54S_n^2 - 4.88S_n^3)$. With a twine thickness (d) of 2.7 mm and a mesh size (s) of 29 mm, the calculated net solidity ($S_n = 2d/s$) of the cage at Fornes was 0.19, while the solidity of the skirt was $S_n = 0.51$. The results were also compared with the expression by Føre et al. (2020) $r = 1.02 - 0.84S_n$, which was determined by performing measurements with net panels with S_n ranging from 0.15 to 0.32.

The expression by Føre et al. (2020) was better at estimating the current reduction downstream of the skirt (S_n=0.51) than Løland (1993) (Fig. 4.9). However, none of the estimates were particularly good inside or downstream of the non-shielded part. The reduction from upstream to inside the cage was higher than expected compared with both expressions. This could be due to the low current speed in this study as the lowest incoming current speed utilised in Føre et al. (2020) was 0.25 m/s, compared to 0.05 m/s in this study. Furthermore, both Løland (1993) and Føre et al. (2020) utilised stretched out plane nets. The conical cage in this study had an inclination angle and could deform, and there was potentially biofouling on both net and skirt, which would have increased the reduction. Comparing the results with these analytical expressions might therefore not be optimal.

To summarise, this study gives an indication of how the current flow differs around a conical cage compared to a cylindrical one, and shows how the current is reduced through a stocked conical sea-cage with permeable skirts. This information can be applied and implemented in future simulations of the far-field environment to increase the understanding of how different nets can influence far-field dispersal of particles.

4.5 Dynamics of dissolved oxygen levels at two hydrographically different sites

The DO level inside unshielded fish cages has proven to vary in time and space, both vertically and horizontally within the cage (Solstorm et al., 2018). By altering the current flow the use of skirts can reduce the water quality inside the cage as physical transport of water through the cage is the main source for fresh oxygenated water (Wildish et al., 1993; Johansson

et al., 2006). Some sites experience unfavourable environments inside the cage with low DO when using skirts (Stien et al., 2012), while others measure sufficient DO inside the cages (Næs et al., 2014; Stien et al., 2018).

As discussed in Chap. 2 many farms monitor the DO levels inside shielded cages as low DO and hypoxia can reduce feed intake and specific growth rates (Remen et al., 2014; Misund et al., 2020). Even moderate levels of hypoxia can reduce aerobic capacity and swimming performance (Oldham et al., 2019). The DO demand of Atlantic salmon also increases with higher temperatures (Remen et al., 2013, 2016), making monitoring during the summer extra important.

Low DO levels can be caused by weak currents (Johansson et al., 2007), but another cause is the local hydrography and stratification in the water column. Stratified sites show lower DO levels than homogeneous sites (Jo-

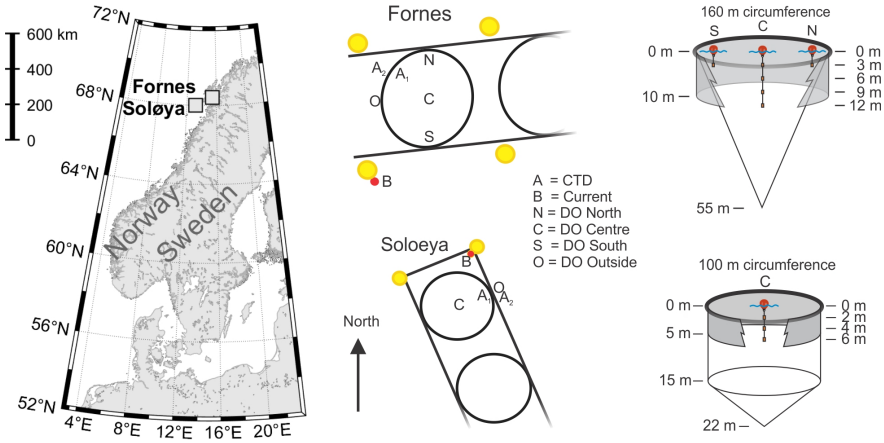

Figure 4.10: Locations of sites where measurement campaigns were carried out, Soløya in May 2019, and Fornes in July 2019. Figures in the second column show the measurement positions of dissolved oxygen (DO), conductivity, temperature and depth (CTD) profiles and current profiles at Fornes and Soløya. DO was measured in position O outside the cage at 3 m depth and inside the cage in position C at 3, 6, 9 and 12 m at Fornes and at 2, 4 and 6 m at Soløya. At Fornes DO was also measured at 3 m depth in position N and S 4 m from the floating collar. The CTD profiles were measured manually inside and outside the cage at position A_1 and A_2, respectively. Current speed and direction profiles were measured at position B.

hansson et al., 2006, 2007) and salinity gradients are reported to influence the deflection of the ambient current around empty fish cages (Gansel et al., 2014). Stratifications influence the DO level by altering how the current moves. When a vertical stratification is present in the water column it will inhibit vertical mixing between the layers (Imberger, 2013). The lower density water will position itself above the higher density water and these two layers can to a certain degree operate independently of one another. The two layers can even have opposite facing current flows outside of the boundary layer. Vertical stratification thereby creates a vertical barrier which allows for more complex current patterns. By altering the current flow stratification can also influence how the current interacts with the lice shielding skirt as noted by Stien et al. (2012) who suggested that the combination of relative low salinity and high temperature around the skirt depth was the reason for the low DO levels inside the fish cage.

Given the different flow pattern around a conical and a cylindrical cage, and when using a permeable and impermeable skirt, it was initially expected that comparing DO levels within a conical cage with a permeable skirt and a cylindrical cage with impermeable skirt would further exemplify how the current flow varied. The DO was therefore measured inside at Fornes and at a third location Soløya in Paper B (Fig. 4.10). The internal environment inside the cages exemplified how DO levels vary at two hydrographically different sites.

DO gradients in unshielded cages are reported to increase with depth at some sites (Johansson et al., 2007; Solstorm et al., 2018), while others see a decrease with depth (Johansson et al., 2007; Oldham et al., 2018). The DO at Soløya was lower inside the cage than outside and had a gradual improvement with depth, with an almost linear relation (Fig. 4.11). The DO at Fornes also improved with depth, although without a linear trend with depth (Fig. 4.12). Improved DO with depth are observed in studies using both non-permeable skirts (Stien et al., 2012) and permeable skirts (Stien et al., 2018), similar to those used in this study. It's therefore likely that the increase with depth when using shielding skirts is due to the shielding skirt itself, rather than any hydrographical effect.

The water column at Soløya was non-stratified with near identical characteristics inside and outside the cage (Fig. 4.11). The lack of stratification meant that there was no inhibition of vertical mixing at Soløya, and the good DO conditions could be a result of vertical mixing. If that was the case, it is uncertain if the skirt would actually be effective in preventing lice from entering the cage. Anecdotally the operators at the farm reported of a

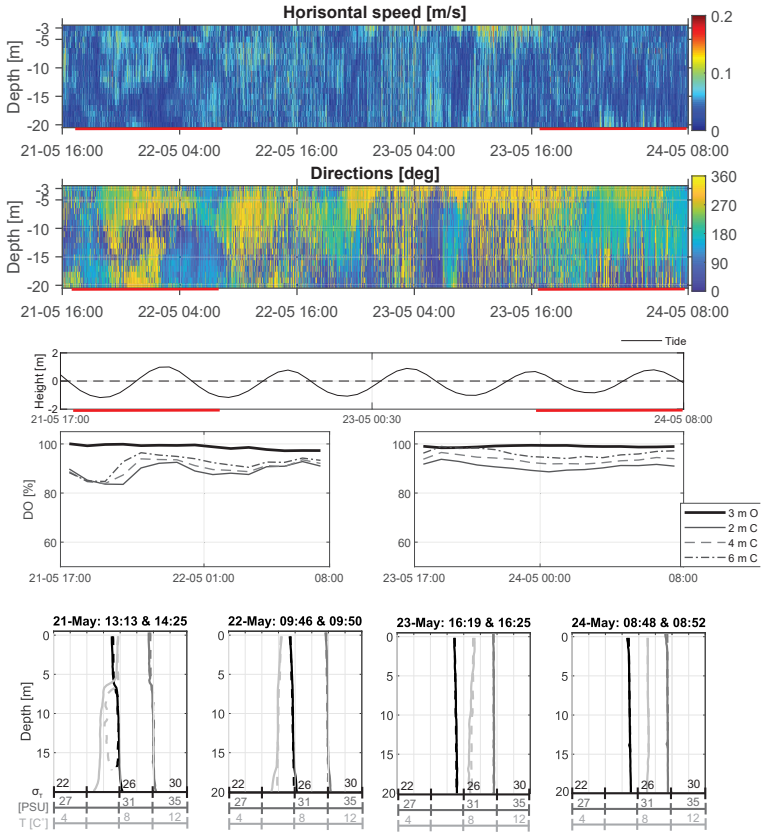

Figure 4.11: Current speed and direction at Soløya in the top 20 meters of the water column, measured by the Doppler current profiler (DCP) in position B, for the entire period from 21.05.19 to 24.05.19. The red horisontal line along the X-axis indicates the periods where DO measurements were taken. The figure beneath the DCP data shows the expected tidal height (thin black line). The figures on the fourth row show hourly median dissolved oxygen (DO) for all sensors during the periods marked with red above. Bottom row shows water density (σ_t), salinity (PSU) and temperature (°C) measured by the CTD outside the fish cage in position A_2 (solid line), and inside at position A_1 (dashed line). The timestamps above each figure represent the time the measurement was started outside and inside for each date, respectively.

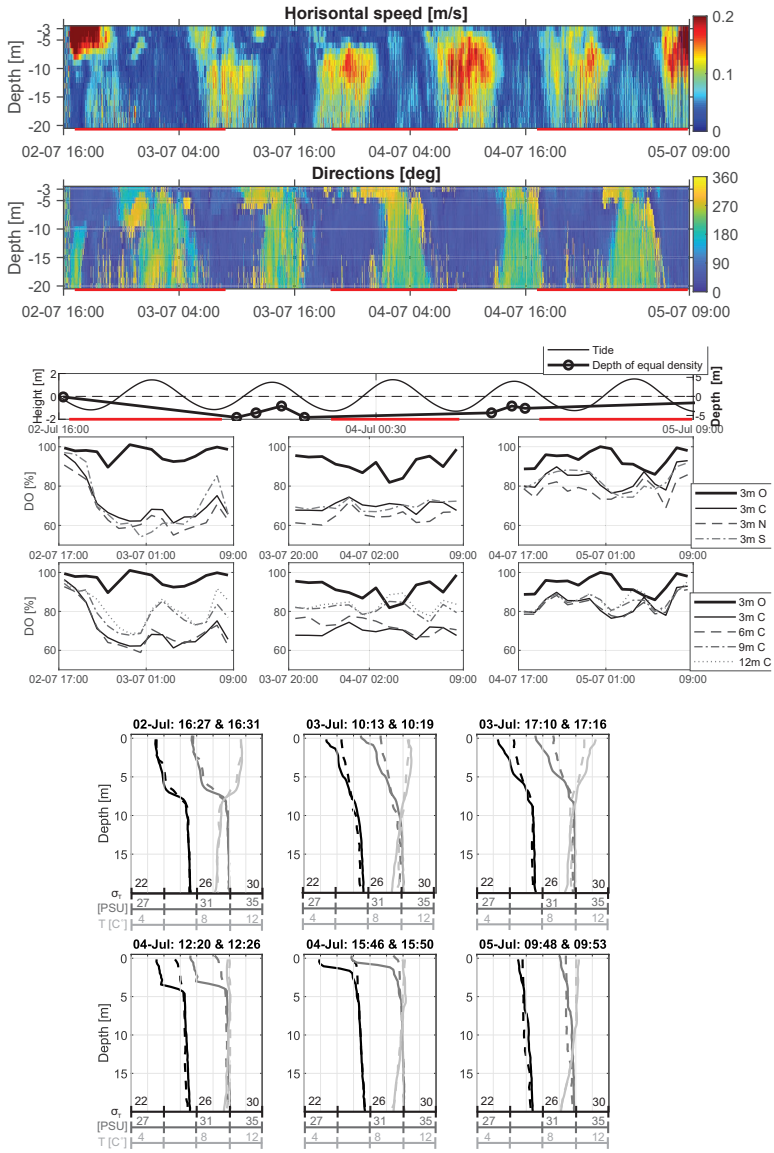

Figure 4.12: Current speed and direction at Fornes in Pos. B. Note potential noise at 02.07 16:00 between 3 and 10 m due to nearby boat. Red horisontal line indicate when DO was measured. Expected tidal height and depth where density inside and outside the cage were equal are marked in the figure below. Fourth row show hourly median DO for sensors at 3 m depth, both outside and inside the cage, fifth row shows DO for sensors in the center and outside the cage. Bottom row shows CTD measurements taken outside in Pos. A_2 (solid line) and inside at A_1 (dashed line). Timestamps of when measurement started outside and inside, respectively.

previous trial to determine the efficiency of lice shielding skirts, and claimed that they had seen no improvement at Soløya when using skirts.

During the three days the study spanned, the DO at Fornes had a higher variability, and this variability appeared to co-occur with alterations in stratification. DO at Fornes was initially good, and there was a clear pycnocline present at roughly 8 m depth (Fig. 4.12). During the first night a sudden drop occurred similar to that observed at Hosnaøyan. The specific reason for the drop the first night cannot be interpreted from the data, but potential causes are high stocking density and a weak turning current. A drop in DO was also observed on the final day of the study at 02:00 on the 5^{th} of July outside the cage, yet it did not result in low DO levels inside the cage. It was therefore concluded that the current alone could not explain the varying DO levels inside the cage.

The stocking density and fish activity combined with the 10 m long skirt could explain some of the variability, but in a similar study by Stien et al. (2018) the DO levels inside a conical cage of 37 m with a 10 m permeable skirt never dropped beneath 70% during a 3-month period. The lowest DO recorded inside the cage in Paper B was 52%. The higher stocking density at Fornes and the larger cage size could possible explain this discrepancy (Oldham et al., 2018), but they do not explain the variability. It was therefore theorized that the stratification at Fornes could be the cause for the variation in DO levels.

The variability at Fornes indicates that the vertical stratification obstructed the current flow and water exchange within the skirt volume. There were two ways fresh oxygenated water could enter the cage at Fornes. The first was by the water being pressed through the permeable skirt. The second was by the water being pressed underneath the skirt and into the cage (Lien et al., 2015; Klebert and Su, 2020). Both of these could have been influenced by the pycnocline. When a pycnocline is positioned above the skirt depth, it could prevent the water above the pycnocline from moving down along the skirt and into the fish cage, thereby reducing the amount of water being pressed underneath the skirt and into the cage. The pycnocline in this study also caused a difference in density of the water inside the cage compared to the water outside. This could have influenced the permeability of the skirt. The higher density observed inside the cage could have forced a larger portion of the water around the cage as more energy would be required to force the water mass through the permeable skirt than if the densities had been equal.

It is uncertain whether the low DO levels at Fornes had any negative

effect on the fish. Moderate hypoxia of 50% DO in water of 16 °C significantly reduces aerobic capacity and swimming performance of Atlantic salmon (Oldham et al., 2019), but the temperature at Fornes never exceeded 11°C and the DO never dropped below 52%. Furthermore, the observations were made over a relatively short period and DO was higher at other locations in the cage (Fig. 4.12). The fish therefore had the opportunity to avoid the areas with low DO, although evidence indicate that DO is not a primary driver of behaviour as as avoidance behaviour is documented for DO <35%, but not for sub-optimal waters with DO <60% (Burt et al., 2011; Oldham et al., 2017; Stehfest et al., 2017).

The different DO environments at Fornes and Soløya exemplify the complex interaction between current, hydrography, shielding skirt and biomass. It is possible that the higher density water inside the cage created a blocking effect, where the high density water forced more of the low density water around the cage, that would otherwise have passed through it. If it is indeed the stratification that causes the water current to behave differently, then information about local and seasonal variability in stratification can enhance decision making regarding operational use of skirts.

Chapter 5

Conclusion and further work

In this thesis the current flow field was studied through long-term data collected at five sites along the Norwegian coastline and through executing three full-scale experiments. The current flow at the five sites were evaluated with regards to fish welfare (Paper A), while the three full-scale experiments were carried out to investigate the impact of lice shielding skirts on the local flow conditions. The impact of a non-permeable tarpaulin skirt on the current flow field inside the cage was studied in Paper C and the characteristic current flow field around a conical sea cage equipped with a permeable skirt was established in Paper D. The reduction in current speed through the was also measured in both of these papers. Lastly Paper B investigated the dynamics of dissolved oxygen levels inside cages at two hydrographically different sites.

The vast difference in flow conditions at the five sites in Paper A and the increasing interest for moving farms to more exposed sites underline the importance of evaluating each site with regard to all relevant species. By evaluating the current flow using the swimming capacities of Atlantic salmon and lumpfish the results indicated that only one of the five sites in Paper A was fit for lumpfish, while only one was potentially unfit for small post-smolts.

The critical swimming speed limit used to evaluate the sites may have been overly conservative as current speed at a site is reduced as it passes through the cage net. This effect was observed both in Paper C and D. The reduction in current speed is enhanced when using skirts, both non-permeable tarpaulin (Paper C) and permeable skirts (Paper D). This reduction in current speed can cause low levels of dissolved oxygen, however the interaction between skirt, current speed and dissolved oxygen is complex as

illustrated by the two farms, Soløya and Fornes, studied in Paper B.

The interaction between hydrography and skirts should be studied in more detail, particularly the situations where density inside and outside the cage differ similar to that at Fornes in Paper B, but also the opposite situation with lower density inside the cage. Some farmers report of issues with the skirt being sucked in all around the cage at a certain depth taking on an hourglass like shape (Misund et al., 2020). It is possible that this is caused by lower density inside the cage than outside. This effect has not been documented scientifically, and it would be interesting to investigate how and when this occurs, and if it has an effect on the dissolved oxygen levels inside the cage.

The use of acoustic Doppler instrumentation inside fish cages has its limitations. ADCPs can not be used inside the cages if fish is present, and ADVs can only measure the current at one position in the cage. It may therefore be advantageous for future studies of current flow in cages, both with and without skirts, to utilise tracers rather than acoustic Doppler sensors. Tracers, either in the form of neutral buoyant sensors or chemicals such as fluorescein dye, could provide new insight into how the current flow travels through the cage. Tracers can also enlighten the complex interaction between current flow and fish, and may be a better method than using ADVs for assessing if the fish create an upwelling in the centre of the cage.

If the marine aquaculture industry is to provide food and nutrition for future generations it has to be sustainable, both economically and ecologically. Improved understanding of how the current flow travels through a stocked cage can give new insight into how to optimise production and which challenges are to be expected regarding fish welfare as future sites move to more exposed locations.

Publications

Paper A

Fish welfare based classification method of ocean current speeds at aquaculture sites

Jónsdóttir, K. E., Hvas, M., Alfredsen, J. A., Føre, M., Alver, M. O., Bjelland, H. V., Oppedal, F., 2019. Fish welfare based classification method of ocean current speeds at aquaculture sites. Aquaculture Environment Interactions, 11, 249-261

Vol. 11: 249–261, 2019
https://doi.org/10.3354/aei00310

AQUACULTURE ENVIRONMENT INTERACTIONS
Aquacult Environ Interact

Published June 6

Fish welfare based classification method of ocean current speeds at aquaculture sites

Kristbjörg Edda Jónsdóttir[1,*], Malthe Hvas[2], Jo Arve Alfredsen[1], Martin Føre[1,3], Morten Omholt Alver[1,3], Hans Vanhauwaert Bjelland[3], Frode Oppedal[2]

[1]Department of Engineering Cybernetics, Norwegian University of Science and Technology, 7491 Trondheim, Norway
[2]Research Group of Animal Welfare, Institute of Marine Research, 5984 Matredal, Norway
[3]SINTEF Ocean, 7465 Trondheim, Norway

ABSTRACT: A major trend in marine aquaculture is to move production to more exposed sites with occasionally rough ocean current events. However, it is unclear whether fish will thrive in these extreme environments, since thorough descriptions of ambient current conditions with regards to fish welfare is lacking. In the present study, ocean current data were collected using acoustic Doppler current profilers at 5 exposed sites along the Norwegian coast over minimum periods of 5 mo. To evaluate welfare risks, current data was compared to known limits of swimming capabilities, such as onset of behavioural changes and critical swimming speeds (U_{crit}), of Atlantic salmon *Salmo salar* and lumpfish *Cyclopterus lumpus*. Specifically, at each site, current speeds were classified into 6 categories based on expected impact on swimming behaviours of Atlantic salmon, and duration of currents within each category were inspected using a homogeneous and non-homogeneous criterion for the water column. Current speeds were then compared with projected U_{crit} at relevant temperatures and fish sizes of Atlantic salmon and lumpfish. Furthermore, a detailed characterization of extreme events at the most exposed site was performed. Of the 5 locations, only 1 exceeded the U_{crit} of Atlantic salmon, while all sites featured currents above U_{crit} of lumpfish for up to 33 h at a time. These results suggest that responsible Atlantic salmon farming is possible at sites considered exposed, while lumpfish should be restricted to more sheltered environments. The presented method can be applied for other aquaculture fish species if adequate data are available.

KEY WORDS: Atlantic salmon · Lumpfish · U_{crit} · Exposed farming · Ocean current speed · Swimming behaviour · Sea cage environment

1. INTRODUCTION

With the continuing expansion of the marine aquaculture industry and a decrease in available sites in nearshore areas due to spatial conflicts and competing claims, there is a growing interest in moving new production sites to more exposed coastal and offshore locations (e.g. Holmer 2010, Bjelland et al. 2015, Gentry et al. 2017). These sites are exposed to harsher wind, wave and current conditions (Holmer 2010, Bjelland et al. 2015). The stronger water currents may be advantageous, as higher water exchange rates result in larger nutrient assimilation capacity, higher levels of dissolved oxygen and generally better water quality (Johansson et al. 2007, Holmer 2010, Klebert et al. 2013, Gentry et al. 2017). However, stronger water currents may induce excessive loads on the farm structure and large net deformations, resulting in challenging conditions for farming operations (Lader et al. 2008, Kristiansen & Faltinsen 2012, Bjelland et al. 2015, Klebert et al. 2015, Gansel et al. 2018). The currents may also be evaluated from a fish-welfare perspective, the primary concern being how the magnitude, duration

*Corresponding author: kristbjorg.jonsdottir@ntnu.no

Publisher: Inter-Research · www.int-res.com

and frequency of strong current events affect behaviour, growth, stress and risks of mortality (Johansson et al. 2014, Solstorm et al. 2015, Remen et al. 2016, Hvas & Oppedal 2017).

The response of farmed fish to ocean currents may be expressed as behavioural changes. Specifically, the group structure of Atlantic salmon *Salmo salar* in commercial farms and experimental setups is observed to change from circular schooling to 'standing' on the current, i.e. remaining stationary while swimming against the current as the current speed increases (Johansson et al. 2014, Hvas et al. 2017b). At low current velocities, swimming speeds are therefore voluntary and independent of the ambient environment, while stronger currents may force the fish to swim at speeds dictated by the environment (Johansson et al. 2014, Hvas et al. 2017b). Preventing fish from swimming at their preferred cruising speed for prolonged periods is a legitimate welfare concern (Hvas et al. 2017b), and the excess energy expenditure required for faster swimming will also, to some extent, affect production performance (Solstorm et al. 2015).

In more extreme current conditions, the maximum swimming capacity of farmed fish may be exceeded, resulting in physiological fatigue, severe stress, injury and even death as the fish gets stuck on the downstream net pen wall (Oppedal et al. 2011, Remen et al. 2016). Experimental measurement of the critical swimming speed (U_{crit}) of fish (e.g. Remen et al. 2016, Hvas & Oppedal 2017) is a standardized method to assess the upper current velocities farmed fish are able to handle on acute timescales. U_{crit} is a measure of prolonged swimming capacity originally defined by Brett (1964). Since swimming at U_{crit} or higher speeds leads to fatigue, farmed fish should never be exposed to current conditions of such magnitudes in sea cages. Furthermore, U_{crit} and swimming behaviour are affected by environmental and biological factors such as water temperature, fish size, individual variations and diseases (Brett 1964, Beamish 1978, Remen et al. 2016, Hvas et al. 2017a,b), which complicate welfare risk assessments at exposed locations. Weak currents may also become problematic, especially when combined with high temperatures, owing to increased risks of hypoxia inside salmon cages, which reduces feed intake and growth (Johansson et al. 2007, Remen et al. 2014, Solstorm et al. 2018).

The primary focus concerning the welfare of Atlantic salmon farmed in exposed environments is on the evaluation of their swimming behaviour and their ability to cope with the prevailing environmental conditions. However, in recent years, there has been a drastic increase in the use of cleaner fish in sea cages for delousing, where the lumpfish *Cyclopterus lumpus* is the most widely used species (Imsland et al. 2014, Powell et al. 2017). In Norway alone, the use of lumpfish has increased from 15.8 million lumpfish in 2016 to 27 million in 2017 (Fiskeridirektoratet 2018). As a vertebrate species, lumpfish possess the same animal rights as Atlantic salmon according to Norwegian laws (Dyrevelferdsloven 2009), thus the same concern regarding welfare in an exposed setting applies to lumpfish. The U_{crit} of lumpfish is considerably lower than in Atlantic salmon owing to smaller sizes and a morphology less suited for fast swimming (Hvas et al. 2018). This suggests that lumpfish are more likely to experience poor welfare at sites with rough current conditions.

In accordance with Norwegian law, all planned aquaculture sites must be surveyed to classify the prevailing environmental conditions. All fish farm systems must be certified according to the rules in Standard NS-9415 (NAS 2009) which ensure the structural integrity of the farm and prevent escapes. NS-9415 defines 5 current classes based on speed, ranging from 'little exposure' to 'extreme exposure' (Table 1). This system for classifying locations does not consider fish welfare, a cause for concern when considering the documented swimming capabilities of Atlantic salmon. For example, the middle category of NS-9415, termed 'substantial exposure', corresponds to an interval of current magnitudes similar to the U_{crit} of Atlantic salmon post-smolts ranging from 80 to 800 g (Remen et al. 2016, Hvas & Oppedal 2017).

Since exposed salmon farming is a new concept, thorough environmental descriptions of sites are currently lacking, and their suitability for responsible fish production has not yet been clarified. Hence, the purpose of this study was to characterize current conditions at exposed locations and assess whether fish welfare is at risk by comparing the ambient environment with known swimming capabilities of Atlantic

Table 1. Classification of aquaculture sites in Standard NS-9415 (NAS 2009) based on the 10 yr return period of the current velocity (V_c)

Current class	V_c (m s^{-1})	Designation
A	0.0–0.3	Little exposure
B	0.3–0.5	Moderate exposure
C	0.5–1.0	Substantial exposure
D	1.0–1.5	High exposure
E	>1.5	Extreme exposure

salmon and lumpfish. To achieve this, a new method was presented and evaluated based on data from site surveys. This method consisted of 2 parts. First, a new scheme for classifying water currents based on known swimming behaviours and capacities of Atlantic salmon was derived as a supplement to NS-9415. To identify potential low oxygen events (i.e. when currents are weak) and to determine if the swimming capacities of the fish are exceeded, the number of continuous hours the measured currents occurred within each current class was determined. Secondly, the suitability of specific sites was inspected using current and temperature data and known U_{crit} limits for Atlantic salmon and lumpfish. The method was applied to data from 5 sites along the Norwegian coast, most of them representative of the present trend of moving Atlantic salmon farms to more exposed locations. For the most exposed site, a characterization of extreme events was also established.

2. MATERIALS AND METHODS

2.1. Data collection and locations

Ocean current data were collected using acoustic Doppler current profilers (ADCP; Aquadopp 400 kHz, Nortek) at 5 selected locations along the Norwegian coast between November 2014 and July 2018. Each ADCP was deployed on a multi-sensor SEAWATCH buoy (Fugro Oceanor) equipped with a conductivity and temperature sensor (Aanderaa 3919A, Aanderaa Data Intruments).

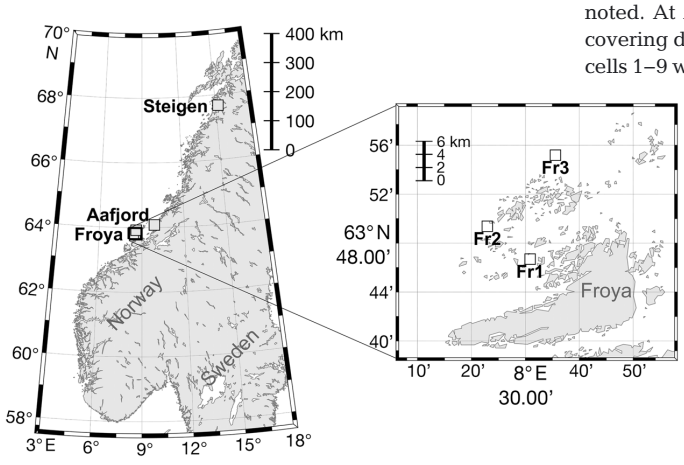

Fig. 1. Locations of the acoustic Doppler current profilers (ADCPs) at Åfjord (Aafj), Steigen (Ste), and the Frøya archipelago (Fr1, Fr2 and Fr3)

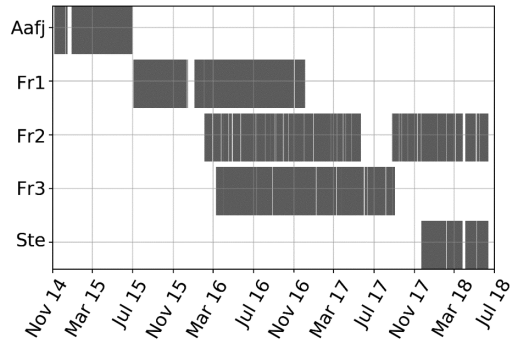

Fig. 2. Deployment and active periods for the ADCPs from 2014 to 2018. From deployment to recovery, the temporal coverage was 94% at Aafj (with hours sampled, n = 5332), 96% at Fr1 (n = 11969), 86% at Fr2 (n = 17675), 99% at Fr3 (n = 13019) and 95% at Ste (n = 4612). See Fig. 1 for site locations

Three of the ADCPs were located in the Frøya archipelago (Fr1, Fr2 and Fr3), and the other 2 in Åfjord (Aafj) and Steigen (Ste) municipality, respectively (Fig. 1). Fig. 2 shows when the ADCPs were deployed and active at the different locations. The minimum deployment span for each ADCP was 5 mo, and all units were active during at least 1 winter season from November to February. The velocity profile measured by the ADCP is divided into uniform segments called depth cells. The size of the depth cells varied between locations. At 2 of the locations, Aafj and Fr1, the cell size was set to 4 m, while the remaining ADCPs operated with a cell size of 3 m. Because of varying depths at the different locations, only the data from the first 30 m in each dataset were studied unless otherwise noted. At Aafj and Fr1, this corresponds to cells 1–7 covering depths 3.5–31.5 m, while at Fr2, Fr3 and Ste, cells 1–9 were applied, covering 2.5–29.5 m.

All ADCPs were installed facing downward and configured to perform measurements over the last 10 min of each hour and produce averaged values of these data series. This sampling procedure is sufficient to resolve the tidal fluctuations, as the semidiurnal tidal constituents dominate along the Norwegian coastline (Sætre 2007), as well as strong currents in the upper water column due to interaction between tides and strong winds. Averaging over 10 min will smooth out turbulent motion and measurement error, but may also to some degree remove information on the exact size of current

peaks. This is not considered an issue, as it is the generalized characteristics of the sites that are of interest here rather than short-term fluctuations.

2.2. Initial processing of data

Unrealistic data points were removed in accordance with recommended procedures for quality control of buoy-mounted ADCPs (SeaDataNet 2010). For each dataset, the mean, SD and maximum and minimum current speed were calculated. The significant maximum and minimum, defined as the mean of the 1/3 largest and 1/3 smallest current speeds, were also determined.

The 10 yr return current describes the current speed which is exceeded on average once every 10 yr. This value is used officially for site classification in Norway, was calculated at depths of 7 and 9.5 m, depending on location. The current was determined following the method described in Standard NS-9415 (NAS 2009) for 1 mo site surveys using the maximum current speed measured during the entire deployment.

2.3. Defining current classes

A proposed classification scheme for ambient current conditions based on previous studies of swimming behaviours and U_{crit} of Atlantic salmon *Salmo salar* is summarized in our Table 2 (Gansel et al. 2014, Johansson et al. 2014, Remen et al. 2016, Hvas et al. 2017a,b). The classes representing the weakest currents, 'very weak' (0–10 cm s^{-1}) and 'weak' (10–20 cm s^{-1}), define the interval of current speeds where large Atlantic salmon are known to swim freely and unaffected. The 'very weak' class was included to isolate events of low oxygen levels that may occur in stagnant water. The third class, 'moderate' (20–40 cm s^{-1}), covers the speeds where large Atlantic salmon start showing signs of breaking up their circular swimming pattern and some of the fish begin to stand on the current. Previous studies have observed that in sea cages, all fish stand on the current when current speeds exceeded roughly 45 cm s^{-1} (Johansson et al. 2014, Hvas et al. 2017b). The 'substantial' class (40–50 cm s^{-1}) therefore covers the transition from a non-homogeneous swimming pattern to a polarized school where most fish stand on current, while the 'strong' (50–60 cm s^{-1}) class contains only the latter behaviour. Finally, the 'very strong' class was based on conservative estimates of the U_{crit} where low temperatures and smaller fish sizes are considered and reflects current conditions where fish are at risk of reaching physiological fatigue. This was done using the U_{crit} value of 80.6 cm s^{-1} for small post-smolts of 80 g swimming in groups at 14°C (Remen et al. 2016) and assuming a 20% decrease in swimming performance when reducing the temperature to 3°C (Hvas et al. 2017a), resulting in a U_{crit} value of 64.5 cm s^{-1}. To also account for individual differences, the 'very strong' limit was set to 60 cm s^{-1}.

Table 2. Definition of current classes based on established limits related to the onset of behavioural changes and critical swimming speed (U_{crit}) of Atlantic salmon

Current		Swimming behaviour
Speed (cm s^{-1})	Class	
0–10	Very weak	Swimming freely
10–20	Weak	Swimming freely
20–40	Moderate	Circular pattern is disrupted; some fish standing on current
40–50	Substantial	Most fish standing on current
50–60	Strong	All fish standing on current
>60	Very strong	Exceeds U_{crit}

2.4. Identification and duration of classes

Current conditions theoretically experienced by the fish were studied by classifying the mean current speeds at each location for each time sample and depth layer using the defined classes in Table 2. The distribution of classes within each depth layer over the entire deployment was determined by sorting all mean values collected for each individual cell.

To assess the impact of current speed on swimming capacity of Atlantic salmon, the number of successive hours the water column stayed within a given current class was determined. As it remains uncertain whether fish will actively seek to avoid depth layers with adverse currents (Oppedal et al. 2011), 2 different criteria were used to define the class of the water column, homogeneous and non-homogeneous. The homogeneous criterion requires that all depth layers in the water column share a single class. If 1 or more depth layers differ from the others, the sample is considered mixed. When using the homogeneous criterion, 2 samples are considered consecutive only if all depth layers in both samples have the same class. The non-homogeneous criterion is less stringent in only requiring 1 depth layer in the water column to be of a given class. This means that a single time sample will be classified according to all classes

present in the water column. Two samples are then considered consecutive if at least 1 cell in each sample shares classification.

The most relevant depth layers for assessing fish welfare are those containing the largest biomass. Due to observed preferred swimming depth and diurnal swimming pattern (Oppedal et al. 2011), it was assumed that the top 20 m of the water column would contain most of the biomass. Hence, only the top 20 m were included when determining the duration of events where the water column was defined within specific current classes. These were cells 2–5 at Fr2, Fr3 and Ste and cells 2–4 at Fr1 and Aafj, corresponding to depth intervals of 5.5–17.5 and 7.5–19.5 m, respectively. The first depth cell at each site was excluded, as buoy-mounted ADCPs can experience a bias in near-surface observations (Mayer et al. 2007).

In addition, the duration of periods where current speeds continuously exceeded 30 cm s^{-1} were extracted, since it has been shown that chronic exposure above this magnitude may compromise growth performance in post-smolts (Solstorm et al. 2015).

2.5. Evaluation of current data using U_{crit} and water temperature

To account for thermal effects on U_{crit}, the measured horizontal current speeds were normalized using a temperature-dependent function, $\hat{U}_{crit}(T)$. Normalized current speeds ($\tilde{U}$) >1 then represent current speeds higher than measured U_{crit} values at the given temperature.

$\hat{U}_{crit}(T)$ was created by polynomial regression, fitting a 2nd-degree polynomial function to data for Atlantic salmon of ~450 g acclimated to 5 different temperatures (Hvas et al. 2017a) (Fig. 3). Furthermore, this function was scaled down to represent a smaller post-smolt of 80 g with a scaling factor k, using the measured maximum U_{crit} = 80.6 cm s^{-1} for fish of that size at 14°C (Remen et al. 2016):

$$k = 0.806\ (\text{m/s}) / \hat{U}_{crit}(14°\text{C}) \quad (1)$$

A scaling factor was also created for adult salmon of 1750 g using data from Remen et al. (2016), and the $\hat{U}_{crit}(T)$ for this group is also presented in Fig. 3.

A similar approach was used for lumpfish *Cyclopterus lumpus* of ~300 g, acclimated to different temperatures (Hvas et al. 2018) using a 2nd-degree polynomial (Fig. 3). The polynomial function was also scaled down to represent lumpfish of ~75 g (Hvas et al. 2018) using a scaling factor with U_{crit} = 26.9 cm s^{-1} at 9°C. Due to the small difference in $\hat{U}_{crit}(T)$, the polynomial function for larger lumpfish was applied when evaluating the current data. Second-degree polynomials were considered adequate for both salmon and lumpfish as they accounted for over 95% of the variability in the data for both species (r^2 = 0.98 for salmon, r^2 = 1.0 for lumpfish).

Eq. (2) expresses the normalized horizontal current speed $\tilde{U}_i^t$, where U_i^t is the current speed observed at time t in cell i, k is the scale parameter, $\hat{U}_{crit}$ is the temperature-dependent function, and T^t the measured temperature at time t.

$$\tilde{U}_i^t = U_i^t / [\hat{U}_{crit}(T^t) \cdot k] \quad (2)$$

Temperature measurements were gathered at 1 m depth and assumed constant throughout the water column, which is an oversimplification that may have an impact on the results. Specifically, when inspecting temperature variations within sea cages in surface waters, temperature profiles will typically correlate positively with depth during winter and negatively with depth during summer (Johansson et al. 2006, Oppedal et al. 2011). This means that using temperature measured at 1 m depth will be a conservative approach when determining $\hat{U}_{crit}$ during winter, while too high temperatures will be applied for $\hat{U}_{crit}$ during summer.

For all locations, linear interpolation was applied to fill in missing temperature values. The buoy at Fr3 encountered technical problems and ceased logging temperature 1 mo after deployment. Temperature measurements from Fr2 nearby were used to normal-

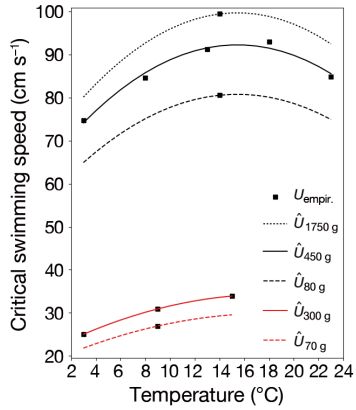

Fig. 3. Temperature-dependent critical swimming speed ($\hat{U}_{crit}$) for Atlantic salmon (black lines) and lumpfish (red lines) of different sizes. The empirical critical swimming speed data ($U_{empir.}$) for Atlantic salmon are from Hvas et al. (2017a) and Remen et al. (2016), and for lumpfish from Hvas et al. (2018)

ize the current at Fr3, and linear interpolation was carried out when Fr2 was not operative in June and July 2017. This is unlikely to have a notable impact on the results, since the sea temperature changes slowly during the summer, and because the strongest currents occurred during the winter months.

2.6. Duration and frequency of extreme events

For the most exposed location, a study was done to determine the duration and frequency of events with current speeds in the 'very strong' class (i.e. exceeding 60 cm s^{-1}) and the number of successive events exceeding the limit. The non-homogeneous criterion for the water column was applied as the homogeneous criterion was deemed too strict when identifying extreme events.

Ocean currents along the Norwegian coast are influenced by several factors, such as tides, freshwater runoff, Atlantic water inflow, bottom topography, wind and weather conditions (Sætre 2007). For the tides, the principal lunar and solar semidiurnal tidal constituents are dominant, with periods of 12.42 and 12 h, respectively (Sætre 2007). Strong currents can occur with both falling and rising tides. From the perspective of the fish, this means that extreme current speed events may arise twice in a 12 h period. Hence, the number of successive events where the speed was classified as 'very strong' and where there were >5 and <13 h between events were identified.

3. RESULTS

3.1. Overview and classification of locations

The current speeds observed at each site are summarized in Table 3. The highest current speed measured was 112.5 cm s^{-1} at Fr2, while Ste had the calmest conditions overall with a maximum current speed of 36.0 cm s^{-1}. The classification for each location using Standard NS-9415 shows the same trend, with Fr2 categorized as 'extreme exposure' and Ste as 'substantial exposure'. Aafj, Fr1 and Fr3 were all classified as having 'high exposure'.

3.2. Distribution and duration of current classes

The distribution of the different current classes for selected depths is shown in Fig. 4. Observations from Ste and Aafj were predominantly within the 'weak' and 'very weak' classes, with nearly 99% of all current speeds measured at Ste and 93% at Aafj in 1 of these 2 classes. All sites in Frøya had a higher percentage of currents in the stronger classes. The data series from Fr2 and Fr3 contained several incidents of currents in the 'very strong' class, while Aafj only had a single occurrence. The recorded 'very strong' currents cover 0.31% and 0.03% of the entire deployment time at Fr2 and Fr3, respectively.

The continuous duration of events within each class using the homogeneous and non-homogeneous criterion for the water column are shown as boxplots in Figs. 5 & 6, respectively. Non-homogeneous water columns were experienced close to twice as often as homogeneous water columns at all locations. Independent of criteria used to inspect the depth layers, Aafj and Ste had the longest durations of 'very weak' currents, and Fr2 had the longest duration of 'very strong' currents. The total number of hours with current speeds over 30 cm s^{-1} based on both the homogeneous and non-homogeneous water column criterion is presented in Fig. 7. The longest durations were 33 and 32 h at Fr3 and Fr2, respectively, when applying the non-homogeneous water column.

Table 3. Descriptive statistics for all locations displaying mean, maximum, SD, and significant (see Section 2.2) maximum and minimum current speeds. The 10 yr return period calculated in accordance with Standard NS-9415 (NAS 2009) and the corresponding current classification are also listed. See Fig. 1 for site locations

Site	Current speed (cm s^{-1})								NS-9415 class.
	Mean	Median	Mode	Max.	SD	Signif. max.	Signif. min.	10 yr return	
Aafj	8.8	7	3.5	62.1	6.9	16	3.5	102.5	D
Fr1	12.6	11.7	7	57.4	8.1	21.6	5.2	104.4	D
Fr2	17.6	15.2	9.4	112.5	11.8	30.5	6.9	176	E
Fr3	13.9	12.9	5.9	71.5	8.2	22.2	6.4	110.2	D
Ste	7.2	6.2	3.2	36	4.6	11.3	3.8	56.6	C

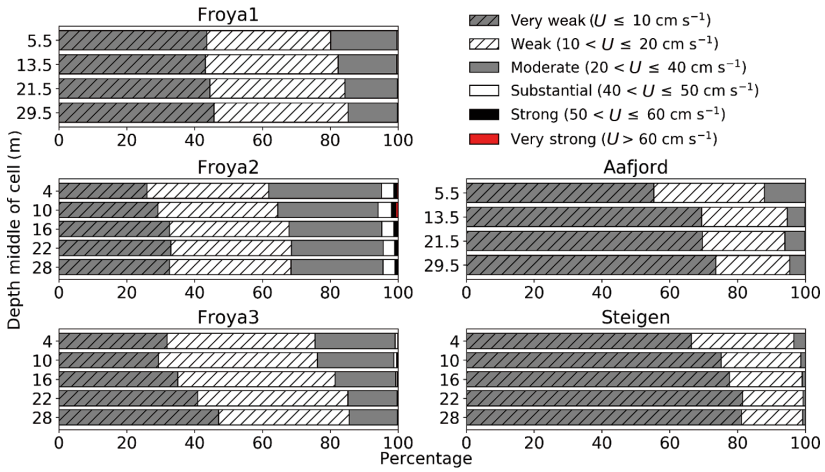

Fig. 4. Total distribution of current classes over the entire duration of deployment for selected depths at each location. *U*: current speed. See Fig. 1 for site locations

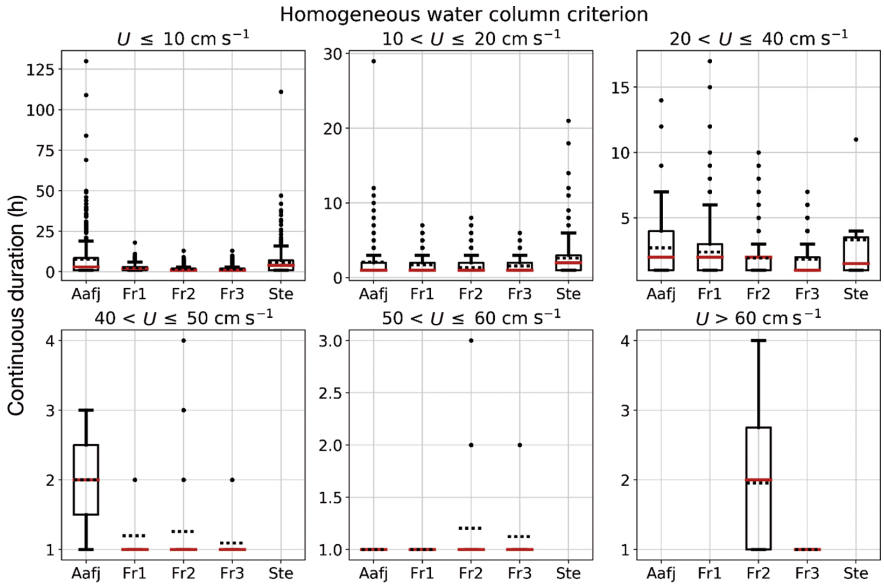

Fig. 5. Number of consecutive hours in each current class using the homogeneous criterion for the water column. Red line: median; horizontal dotted line: mean. Lower whisker extends to first quartile (Q1) minus 1.5 times the interquartile range (IQR). Upper whisker extends to the third quartile (Q3) plus 1.5 × IQR. Data outside of the whiskers are events that exceed Q3 + 1.5 × IQR. These are represented as dots and are considered valid data points. Dots may overlap; hence dots do not necessarily represent a single occurrence. Note the different *y*-axes. *U*: current speed. See Fig. 1 for site locations

3.3. Evaluating current data using U_{crit} and water temperature

Fig. 8 shows the number of consecutive hours where the currents were within given ranges of U_{crit} for Atlantic salmon *Salmo salar* using both the homogeneous and non-homogeneous criterion. Only Fr2 exceeded the U_{crit} of Atlantic salmon, independent of which criterion was used, for up to 4 h at a time. The results for lumpfish *Cyclopterus lumpus* are presented in Fig. 9 and show that U_{crit} was exceeded at all sites when using the non-homogeneous criterion, and at all sites except Ste when using the homogeneous criterion. These conditions could persist for up to 33 h.

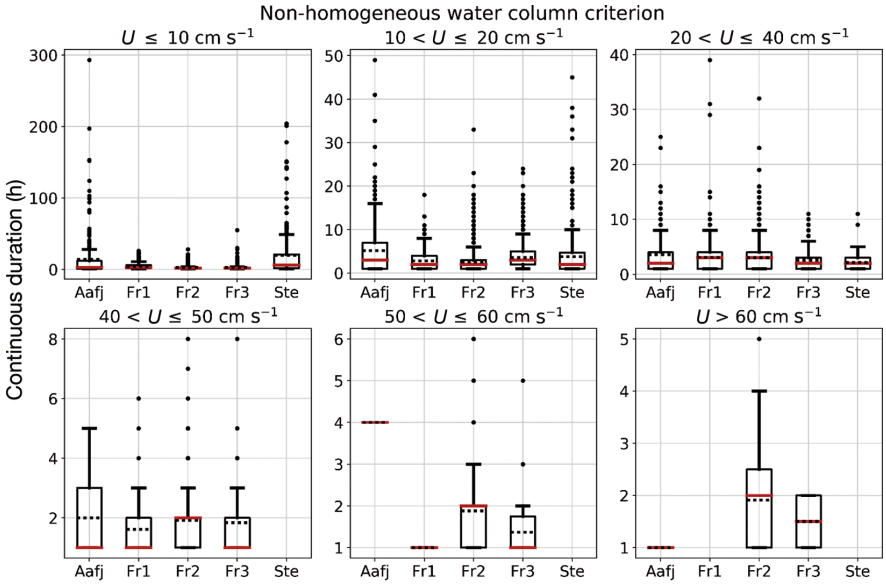

Fig. 6. Number of consecutive hours in each current class using the non-homogeneous criterion for the water column. Other details are the same as for Fig. 5

3.4. Extreme events at Fr2

Site Fr2 was selected for the study of extreme events, as it had the most frequent occurrence of current measurements above 60 cm s^{-1}. Dates containing more than 3 consecutive tidal cycles are presented in Table 4, and the total hours of each event was found as the time span from the first to the last measured current measurement classified as 'very strong'. The longest duration observed was 51 h in January 2018, while the maximum recorded current speed and largest mean value were 112.5 and 42.3 cm s^{-1}, respectively.

4. DISCUSSION

4.1. Current class definitions based on fish behaviour

The classification obtained by using Standard NS-9415 gives little insight into the actual conditions experienced by the fish, and its usefulness as a descriptive tool should be questioned. For instance, the NS-9415 classification of both Aafj and Fr3 as 'high exposure' sites does not reflect the fact that Aafj, unlike Fr3, has long periods of low currents. The method presented in the present study attempts to resolve this issue by employing observed limits related to behavioural changes and swimming capacities when evaluating the current data. However, certain aspects of the classification should be considered when interpreting the results.

U_{crit} values are determined in swim tunnels, where fish are exposed to a continuous flow of constant velocity in systematic increments, a situation rarely experienced in nature (Plaut 2001). In addition, current speeds inside and outside of a sea cage are not necessarily alike, as a significant reduction of speed may occur over the net of sea cages and over the entire farm installation (Klebert et al. 2013,

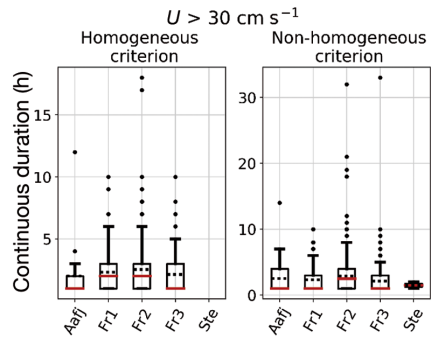

Fig. 7. Number of consecutive hours with current speeds exceeding 30 cm s^{-1} based on both the homogeneous and non-homogeneous water column criterion. Other details are the same as for Fig. 5

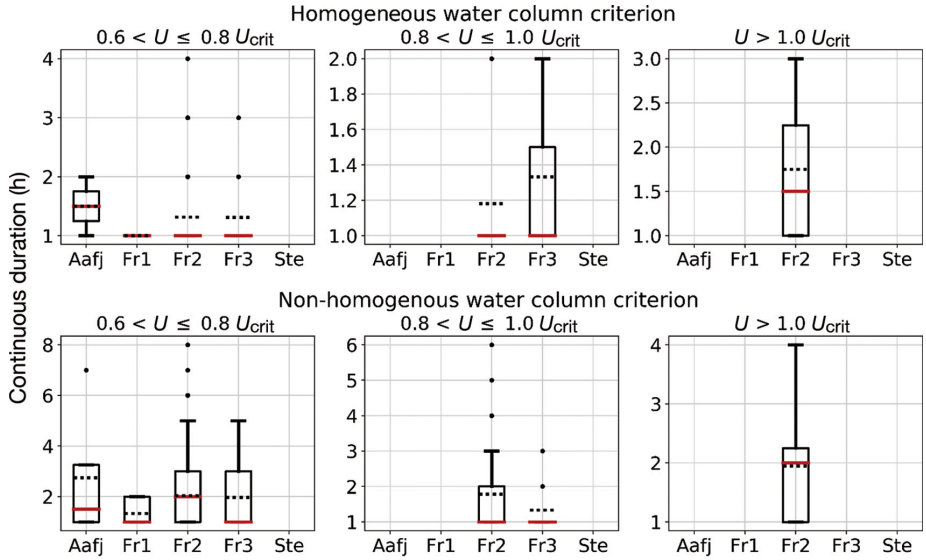

Fig. 8. Number of consecutive hours where the currents were within given ranges of the critical swimming speed (U_{crit}) for Atlantic salmon *Salmo salar* using both the homogeneous and non-homogeneous criterion. Other details are the same as for Fig. 5

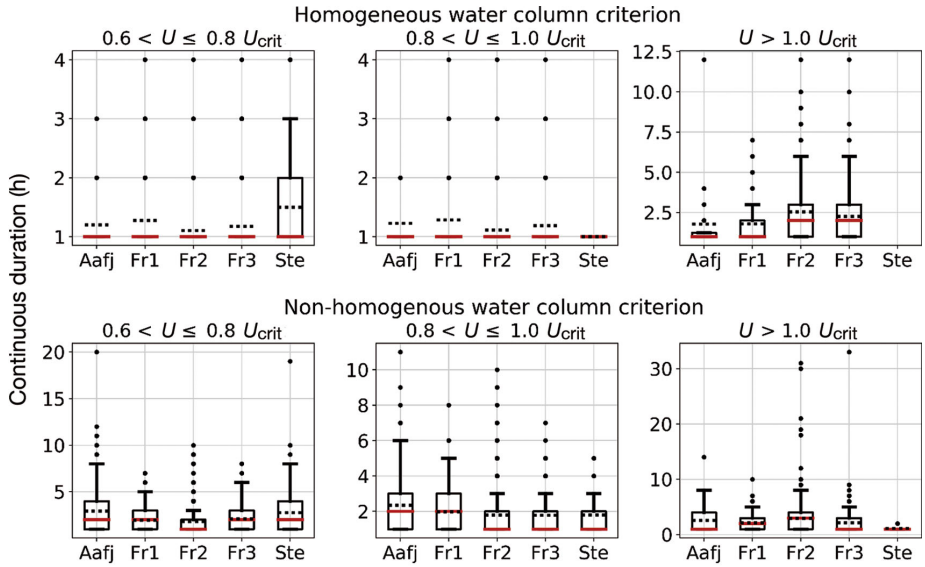

Fig. 9. Number of consecutive hours where the currents were within given ranges of the critical swimming speed (U_{crit}) for lumpfish *Cyclopterus lumpus* using both the homogeneous and non-homogeneous criterion. Other details are the same as for Fig. 5

Winthereig-Rasmussen et al. 2015). Several factors influence this reduction in speed, such as net dimensions, biofouling, presence of fish and potentially the deformation of the sea cages (Klebert et al. 2013, Gansel et al. 2014, Winthereig-Rasmussen et al. 2016). Klebert et al. (2015) report a reduction of 21.5% in current speed from a reference point outside to inside a fish pen, which compares well with the reduction of 20% found applying the empirical method of Løland (1991). Higher reductions have

Table 4. Statistics for periods containing consecutive cycles with currents in the 'very strong' class. Total hours: duration from the first recorded to the last recorded 'very strong' current that has >5 and <13 h between them

Year/ date	No. of tidal cycles	Total time (h)	Current speed (cm s^{-1}) Max.	Mean	Min.
2017					
3–4 Nov	3	18	70.3	35.5	1.2
3–4 Dec	3	26	77.3	33.3	7.0
2018					
3–5 Jan	5	51	96.1	33.6	1.2
1–3 Feb	4	39	80.9	29.6	0.0
24–25 Apr	3	27	72.7	42.3	8.2
30 Apr–1 May	3	27	112.5	40.0	0.0

however been reported when the sensors are located such that fish may influence the measurements (Johansson et al. 2014).

The measurements used in this study were collected in open water outside and apart from farm structures, and it is reasonable to assume that the current speed could be reduced by 20% within a sea cage. This has implications for the defined current classes, and it can be argued that the 'very strong' class limit of 60 cm s^{-1} is somewhat low and should be increased to account for the reduction over the net. In addition, U_{crit} of larger Atlantic salmon *Salmo salar* have been reported as high as 125 cm s^{-1} (Hvas et al. 2017b), while the 'very strong' class is based on results for small post-smolts swimming at 3°C, which represent the conditions of poorest swimming capacity. Furthermore, the presence of diseases or parasites may lead to a further reduction of U_{crit} (Hvas et al. 2017c). Ideally, the 'very strong' class should reflect the specific species in question, body size and ambient temperature and account for inherent variation in swimming capacities in the population so that weaker individuals are protected. The 'very strong' class could thus be used to give an indication whether current speed should be considered more carefully at a prospective site or not.

4.2. Choice of criteria and implications for results

The duration of the 'very weak' and 'weak' classes vary with choice of criteria for the water column. For instance, the maximum continuous duration of 'very weak' currents were 130 and 293 h at Aafj, and 111 and 204 h at Ste, using the homogeneous and non-homogeneous criterion, respectively. This variation between choice of criterion was higher than that observed for the 'strong' and 'very strong' classes. For example, the maximum duration of the 'very strong' class at Fr2 only increased by 1 h with the non-homogeneous criterion.

Current speed generally tends to decrease with depth in the upper water column, a trend seen in Fig. 4. If the non-homogeneous criterion is applied, the possible variation in current speed with depth gives fish the theoretical option to avoid strong currents by changing their depth. Atlantic salmon are rarely distributed evenly inside a sea cage, and often display circadian rhythms with respect to swimming depth, where they descend and swim relatively deep during the day and closer to the surface at night (Johansson et al. 2006, 2007, Oppedal et al. 2011). However, there are currently no studies that have shown that salmon actively avoid depth layers with high current speeds (Johansson et al. 2007, Oppedal et al. 2011), suggesting that the non-homogeneous criterion should be preferred when evaluating the effect of strong currents on fish welfare.

When investigating the probability of low oxygen levels because of slow currents, the homogeneous water column criterion is more suitable, as low oxygen levels are expected only when the current speeds are low in all relevant layers. Earlier work has indicated that salmon may avoid areas of slightly lowered oxygen levels (Oldham et al. 2017) and extreme hypoxia (Dempster et al. 2016, Stehfest et al. 2017), but this may be overruled by their preferred temperature at the depth of hypoxia (Stien et al. 2012). The homogeneous criterion is therefore more suitable when considering the risk of hypoxia in weak currents.

4.3. Classification and site suitability

Applying the suggested method to ocean current data from the 5 sites can reveal crucial information about the environment as experienced by the fish. The long durations of the 'very weak' currents recorded at Aafj and Ste could have implications for hypoxia events. Long durations of 'very weak' currents, or at high frequencies, especially during late summer and autumn when temperatures are elevated or stocking densities are high, are associated with environmental hypoxia, which can be detrimental to fish growth and health (Burt et al. 2012, Remen et al. 2013, 2014).

Current speeds over 30 cm s^{-1} were measured at all locations, with durations up to 33 h with the non-homogeneous criterion. Post-smolts kept at currents around 30 cm s^{-1} for 6 wk display reduced growth

(Solstorm et al. 2015). Slack current conditions of 4 cm s^{-1}, on the other hand, resulted in higher lipid content in the muscle compared to post-smolt kept at moderate currents of 18 cm s^{-1} (Solstorm et al. 2015). Nevertheless, this may not be relevant for salmon in commercial cages where salmon frequently display daytime schooling with swimming speeds of >0.5 fish length s^{-1} (Oppedal et al. 2011, Hansen et al. 2017).

Atlantic salmon have been observed to sustain 80% of U_{crit} for at least 4 h (Hvas & Oppedal 2017). Fr2 was the only location to exceed this, with current speeds between 80 and 100% of U_{crit} persisting up to 6 consecutive hours when employing the non-homogeneous criterion. This location was also the only one to exceed the U_{crit} of small post-smolts and had up to 5 consecutive events with current speeds in the 'very high' class (Table 4). Depending on fish size and the reduction of current through the cage walls, the maximum current of 92 cm s^{-1}, measured during this extreme period in January 2018, could have a detrimental effect on the fish. The minimum velocity during this period was 1 cm s^{-1} (Table 4), meaning that restitution between the 'very strong' current speeds could be possible with a maximum period between 2 extreme events set to 13 h. Should the fish withstand the strong currents during the peaks, this may provide sufficient time for recovery. However, it is uncertain how the cumulative impact of 5 cycles of strong currents will affect the welfare of Atlantic salmon, and the welfare of the much smaller lumpfish *Cyclopterus lumpus*.

Unlike salmon, lumpfish has the option to adhere to surfaces such as rocks and seaweed by use of a ventral suction disc and can thereby withstand currents much higher than their U_{crit} (Hvas et al. 2018). For instance, lumpfish can remain attached to a surface for 1 min when exposed to currents of 110 cm s^{-1} (Hvas et al. 2018). For this reason, exceeding U_{crit} may not have the same short-term consequences as for salmon. However, lumpfish in swimming tunnels did not adhere to a surface for more than 20 min, independent of current speed (Hvas et al. 2018). The long duration of currents exceeding U_{crit} at all of the studied locations could therefore be a serious challenge for their wellbeing.

The suitability of the 5 locations for both species can be summarized by saying that all sites except Fr2 could be suitable for post-smolts as small as 80 g, while none of the locations appear suitable for lumpfish as they all exceed their U_{crit} for as long as 33 h at a time.

Despite each ADCP having similar configurations, direct comparisons between locations are complicated by the different cell sizes, deployment dates and duration of deployment. For instance, Fr2 had the longest deployment time, increasing the probability of recording strong current speeds. Further work should focus on expanding the method presented in this paper to classify existing and prospective farm sites using model data from ocean models such as SINMOD (SINTEF) or Norkyst800 (Havforskningsinstituttet). Combining these classifications with wind-wave exposure classification using the fetch analysis in Lader et al. (2017) would establish a good foundation for defining an exposed location and fish welfare at such a site. The effect of strong waves on fish welfare should also be studied in more detail, such that a greater understanding of welfare at exposed sites can be obtained.

5. CONCLUSION

Standard NS-9415 aims to prevent escapes and focuses on assessing the environment with regard to structural loads. However, if fish farmers only commission providers of site surveys to comply with Standard NS-9415, important information about the environment as experienced by the fish is lost. In this study, a new method for classification of aquaculture sites with respect to current conditions and their implications for fish welfare was proposed and applied to 5 different locations along the Norwegian coast.

The steps of the method can be summarized as follows. For a specific site, define the 'very strong' class on the U_{crit} of the relevant species and classify current data in accordance with the scheme. To evaluate if hypoxia may become an issue, the duration of 'very weak' currents should be inspected with a homogeneous water column criterion. If 'very strong' current speeds are registered, the duration of the strong currents should be inspected with the non-homogeneous water column criterion. The current speeds should also be evaluated using a temperature-dependent function, $\hat{U}_{crit}(T)$, for all relevant species, if temperature data is available. Of the 5 sites included in this study, only Fr2 had current speeds that exceeded U_{crit} of small post-smolt *Salmo salar*, while all sites surpassed the U_{crit} of lumpfish *Cyclopterus lumpus*. The use of lumpfish at these sites may therefore be problematic with regards to their welfare.

The presented method should be adapted and offered as part of the site surveys for fish farmers to assess prospective sites and to plan production and

stocking of fish. The method is easily adapted to different species if their U_{crit} is known. By analyzing the prevalence and persistence of different current speed classes and comparing this with known limits of a specific species' U_{crit}, prospective production sites can be assessed with respect to fish performance and welfare.

Acknowledgements. This study was funded by SINTEF OCEAN and the Research Council of Norway, EXPOSED Aquaculture Research Centre, grant number 237790. We are thankful for access to measurement data provided by SINTEF ACE and the fish farmers participating in EXPOSED.

LITERATURE CITED

Beamish FWH (1978) Swimming capacity. Fish Physiol 7: 101–187

Bjelland HV, Føre M, Lader P, Kristiansen D and others (2015) Exposed aquaculture in Norway. In: Conf Proc OCEANS 2015. Institute of Electrical and Electronics Engineers (IEEE) and Marine Technology Society (MTS), Washington, DC, p 1–10

Brett JR (1964) The respiratory metabolism and swimming performance of young sockeye salmon. J Fish Res Board Can 21:1183–1226

Burt K, Hamoutene D, Mabrouk G, Lang C and others (2012) Environmental conditions and occurrence of hypoxia within production cages of Atlantic salmon on the south coast of Newfoundland. Aquacult Res 43:607–620

Dempster T, Wright D, Oppedal F (2016) Identifying the nature, extent and duration of critical production periods for Atlantic salmon in Macquarie Harbour, Tasmania, during summer. Fisheries Research and Development Corporation (FRDC) Rep no. 2016-229-DLD. FRDC, Deakin

Dyrevelferdsloven (2009) Lov om dyrevelferd (LOV-2009-06-19-97). https://lovdata.no (accessed 7 Nov 2018)

Fiskeridirektoratet (2018) Utsett av rensefisk 1998-2017. https://www.fiskeridir.no (accessed 10 Sep 2018)

Gansel LC, Rackebrandt S, Oppedal F, McClimans TA (2014) Flow fields inside stocked fish cages and the near environment. J Offshore Mech Arctic Eng 136:031201

Gansel LC, Oppedal F, Birkevold J, Tuene S (2018) Drag forces and deformation of aquaculture cages—full-scale towing tests in the field. Aquacult Eng 81:46–56

Gentry RR, Froehlich HE, Grimm D, Kareiva P and others (2017) Mapping the global potential for marine aquaculture. Nat Ecol Evol 1:1317–1324

Hansen TJ, Fjelldal PG, Folkedal O, Vågseth T, Oppedal F (2017) Effects of light source and intensity on sexual maturation, growth and swimming behaviour of Atlantic salmon in sea cages. Aquacult Environ Interact 9: 193–204

Holmer M (2010) Environmental issues of fish farming in offshore waters: perspectives, concerns and research needs. Aquacult Environ Interact 1:57–70

Hvas M, Oppedal F (2017) Sustained swimming capacity of Atlantic salmon. Aquacult Environ Interact 9:361–369

Hvas M, Folkedal O, Imsland A, Oppedal F (2017a) The effect of thermal acclimation on aerobic scope and critical swimming speed in Atlantic salmon, *Salmo salar*. J Exp Biol 220:2757–2764

Hvas M, Folkedal O, Solstorm D, Vågseth T, Fosse JO, Gansel LC, Oppedal F (2017b) Assessing swimming capacity and schooling behaviour in farmed Atlantic salmon *Salmo salar* with experimental push-cages. Aquaculture 473:423–429

Hvas M, Karlsbakk E, Mæhle S, Wright DW, Oppedal F (2017c) The gill parasite *Paramoeba perurans* compromises aerobic scope, swimming capacity and ion balance in Atlantic salmon. Conserv Physiol 5:cox066

Hvas M, Folkedal O, Imsland A, Oppedal F (2018) Metabolic rates, swimming capabilities, thermal niche and stress response of the lumpfish, *Cyclopterus lumpus*. Biol Open 7:bio036079

Imsland AK, Reynolds P, Eliassen G, Hangstad TA, Foss A, Vikingstad E, Elvegård TA (2014) The use of lumpfish (*Cyclopterus lumpus* L.) to control sea lice (*Lepeophtheirus salmonis* Krøyer) infestations in intensively farmed Atlantic salmon (*Salmo salar* L.). Aquaculture 424-425:18–23

Johansson D, Ruohonen K, Kiessling A, Oppedal F, Stiansen JE, Kelly M, Juell JE (2006) Effect of environmental factors on swimming depth preferences of Atlantic salmon (*Salmo salar* L.) and temporal and spatial variations in oxygen levels in sea cages at a fjord site. Aquaculture 254:594–605

Johansson D, Juell JE, Oppedal F, Stiansen JE, Ruohonen K (2007) The influence of the pycnocline and cage resistance on current flow, oxygen flux and swimming behaviour of Atlantic salmon (*Salmo salar* L.) in production cages. Aquaculture 265:271–287

Johansson D, Laursen F, Fernö A, Fosseidengen JE and others (2014) The interaction between water currents and salmon swimming behaviour in sea cages. PLOS ONE 9: e97635

Klebert P, Lader L, Gansel LC, Oppedal F (2013) Hydrodynamic interactions on net panel and aquaculture fish cages: a review. Ocean Eng 58:260–274

Klebert P, Patursson Ø, Endresen PC, Rundtop P, Birkevold J, Rasmussen HW (2015) Three-dimensional deformation of a large circular flexible sea cage in high currents: field experiment and modeling. Ocean Eng 104:511–520

Kristiansen T, Faltinsen OM (2012) Modelling of current loads on aquaculture net cages. J Fluids Structures 34: 218–235

Lader P, Dempster T, Fredheim A, Jensen Ø (2008) Current induced net deformations in full-scale sea-cages for Atlantic salmon (*Salmo salar*). Aquacult Eng 38:52–65

Lader P, Kristiansen D, Alver M, Bjelland HV, Myrhaug D (2017) Classification of aquaculture locations in Norway with respect to wind wave exposure. Paper no. OMAE 2017-61659. In: Proc ASME 2017, 36th Int Conf Ocean, Offshore and Arctic Engineering, Trondheim. Vol 6: ocean space utilization. American Society of Mechanical Engineers (ASME), New York, NY, p V006T05A005

Løland G (1991) Current forces on and flow through fish farms. PhD dissertation, Norwegian University of Science and Technology, Trondheim

Mayer DA, Virmani JI, Weisberg RH (2007) Velocity comparisons from upward and downward acoustic Doppler current profilers on the West Florida Shelf. J Atmos Ocean Technol 24:1950–1960

NAS (Norsk Allmennstandardisering) (2009) NS-9415 Marine fish farms—requirements for site survey, risk analy-

ses, design, dimensioning, production, installation and operation. ICS 65.150;67.260. Standards Norway, Oslo. www.standard.no (accessed 16 May 2018)
Oldham T, Dempster T, Fosse JO, Oppedal F (2017) Oxygen gradients affect behaviour of caged Atlantic salmon *Salmo salar*. Aquacult Environ Interact 9:145–153
Oppedal F, Dempster T, Stien LH (2011) Environmental drivers of Atlantic salmon behaviour in sea-cages: a review. Aquaculture 311:1–18
Plaut I (2001) Critical swimming speed: its ecological relevance. Comp Biochem Physiol A 131:41–50
Powell A, Treasurer JW, Pooley CL, Keay AJ, Lloyd R, Imsland AK, Garcia de Leaniz C (2017) Use of lumpfish for sea lice control in salmon farming: challenges and opportunities. Rev Aquacult 10:683–702
Remen M, Oppedal F, Imsland AK, Olsen RE, Torgersen T (2013) Hypoxia tolerance thresholds for post-smolt Atlantic salmon: dependency of temperature and hypoxia acclimation. Aquaculture 416–417:41–47
Remen M, Aas TS, Vågseth T, Torgersen T, Olsen RE, Imsland A, Oppedal F (2014) Production performance of Atlantic salmon (*Salmo salar* L.) postsmolts in cyclic hypoxia, and following compensatory growth. Aquacult Res 45:1355–1366
Remen M, Solstorm F, Bui S, Klebert P and others (2016) Critical swimming speed in groups of Atlantic salmon *Salmo salar*. Aquacult Environ Interact 8:659–664
Sætre R (ed) (2007) The Norwegian coastal current: oceanography and climate. Tapir Academic Press, Institute of Marine Research, Trondheim
SeaDataNet (2010) Data quality control procedures, version 2.0. www.seadatanet.org (accessed 28 May 2018)
Solstorm F, Solstorm D, Oppedal F, Fernö A, Fraser TWK, Olsen RE (2015) Fast water currents reduce production performance of post-smolt Atlantic salmon *Salmo salar*. Aquacult Environ Interact 7:125–134
Solstorm D, Oldham T, Solstorm F, Klebert P, Stien LH, Vågseth T, Oppedal F (2018) Dissolved oxygen variability in a commercial sea-cage exposes farmed Atlantic salmon to growth limiting conditions. Aquaculture 486: 122–129
Stehfest KM, Carter CG, McAllister JD, Ross JD, Semmens JM (2017) Response of Atlantic salmon *Salmo salar* to temperature and dissolved oxygen extremes established using animal-borne environmental sensors. Sci Rep 7:4545
Stien LH, Nilsson J, Hevrøy EM, Oppedal F, Kristiansen TS, Lien AM, Folkedal O (2012) Skirt around a salmon sea cage to reduce infestation of salmon lice resulted in low oxygen levels. Aquacult Eng 51:21–25
Winthereig-Rasmussen H, Patursson Ø, Simonsen K (2015) Visualisation of the wake behind fish farming sea cages. Aquacult Eng 64:25–31
Winthereig-Rasmussen H, Simonsen K, Patursson Ø (2016) Flow through fish farming sea cages: comparing computational fluid dynamics simulations with scaled and full-scale experimental data. Ocean Eng 124:21–31

Editorial responsibility: Pablo Sánchez Jerez, Alicante, Spain

Submitted: November 16, 2018; Accepted: March 29, 2019
Proofs received from author(s): May 29, 2019

Paper B

Dynamics of dissolved oxygen inside salmon sea-cages with lice shielding skirts at two hydrographically different sites

Jónsdóttir, K. E., Volent, Z., Alfredsen, J.A., 2020. Dynamics of dissolved oxygen inside salmon sea-cages with lice shielding skirts at two hydrographically different sites. Aquaculture Environment Interactions, 12, 559-570

Vol. 12: 559–570, 2020
https://doi.org/10.3354/aei00384

AQUACULTURE ENVIRONMENT INTERACTIONS
Aquacult Environ Interact

Published December 17

Dynamics of dissolved oxygen inside salmon sea-cages with lice shielding skirts at two hydrographically different sites

Kristbjörg Edda Jónsdóttir[1,*], Zsolt Volent[2], Jo Arve Alfredsen[1]

[1]Norwegian University of Science and Technology, Department of Engineering Cybernetics, NO-7491 Trondheim, Norway
[2]SINTEF Ocean, NO-7465 Trondheim, Norway

ABSTRACT: Shielding skirts are widely used as a non-invasive preventive measure against salmon lice *Lepeophtheirus salmonis* infestations on Atlantic salmon *Salmo salar* in sea-cages. Low levels of dissolved oxygen (DO) are reported from some sites, but not others. This disparity is usually explained by local variations in current flow and hydrography. The aim of the present study was to investigate these local variations through vertical mapping of DO and hydrography at 2 hydrographically different sites equipped with shielding skirts. The 2 sites chosen, Fornes and Soløya, are in northern Norway and are equipped with a permeable and a non-permeable skirt, respectively. Over a period of 3 d, current speed and direction were recorded outside the cage, while DO and hydrography were measured both inside and outside the cage, above and below the skirt. At Fornes, the DO inside the cage varied throughout the study period, while DO outside remained stable. The variation in DO inside the cage co-occurred with variations in strength and depth of a present pycnocline that broke down during the study period. At Soløya, DO levels were high throughout the study, and there was no gradient in salinity, temperature or density, indicating good vertical mixing. These data illustrate how the interaction between skirts and local conditions can influence the temporal and spatial variations of DO inside shielded cages and highlight the importance of studying local current conditions and hydrography when applying shielding skirts.

KEY WORDS: Lice shielding skirts · Dissolved oxygen · Pycnocline · Current flow pattern · Atlantic salmon · Salmon lice · Sea-cage environment

1. INTRODUCTION

Shielding skirts are widely used in Norway as a non-invasive preventive measure to reduce salmon lice *Lepeophtheirus salmonis* infestations on Atlantic salmon *Salmo salar* L. in sea-cages. Shielding skirts are a form of barrier technology that attempts to keep the infective copepodids out of the cage by rerouting the upper water column around the cage, which has a higher lice density than the deeper levels due to the preferred swimming depth of the louse (i.e. Huse & Holm 1993, Heuch et al. 1995, Hevrøy et al. 2003, Oppedal et al. 2017, Geitung et al. 2019, Barrett et al. 2020).

The effect of shielding skirts on lice infestation is varied, with some studies finding that skirts reduce lice infestations (Næs et al. 2012, Grøntvedt et al. 2018, Stien et al. 2018, Bui et al. 2020), whereas others find that at certain sites, skirts have little to no effect (Grøntvedt & Kristoffersen 2015, Lien et al. 2015, Grøntvedt et al. 2018). Shielding skirts also affect the environment inside the cage, particularly the dissolved oxygen (DO) concentration (Oldham et al. 2017). Low DO and cyclic hypoxia inside fish cages reduce feed intake and specific growth rates (Remen et al. 2014), while moderate hypoxia can significantly reduce aerobic capacity and swimming

*Corresponding author: kristbjorg.jonsdottir@ntnu.no

Publisher: Inter-Research · www.int-res.com

performance (Oldham et al. 2019). Higher water temperature increases the DO demand of Atlantic salmon (Remen et al. 2013, 2016), and this demand is mainly met by physical transport of sufficient amounts of oxygen-rich water through the cage (Wildish et al. 1993, Johansson et al. 2006). As the skirt diverts the flow around the cage, the natural exchange of water is disrupted and this can result in low DO levels (Stien et al. 2012). However, this effect does not occur at all sites, as some studies have reported sufficient DO inside cages with skirts (Næs et al. 2012, Stien et al. 2018).

One reason for these variations could be differences in the water exchange due to local flow patterns. Farm layout (Rasmussen et al. 2015), local topography (Klebert et al. 2013), cage structure (Klebert et al. 2015), bio-fouling (Gansel et al. 2015), presence of fish (Klebert et al. 2013, Gansel et al. 2014, Klebert & Su 2020) and structures such as shielding skirts (Frank et al. 2015) all influence how the ocean currents flow through and around fish cages. Computational fluid dynamics (CFD) analyses of laminar current flow into a fish cage with a rigid shielding skirt show that part of the incoming current is pressed around the skirt, but a portion is pressed down along the skirt, underneath it and into the sea-cage (Lien & Høy 2011, Lien et al. 2015). The deflection of the current underneath the shielding skirt and into the fish cage was observed in full-scale dye experiments (Frank et al. 2015). However, when repeating the dye experiment with similar ambient current conditions, the amount of dye entering the cage varied significantly (Frank et al. 2015). One variable that influences the current flow pattern, which could explain the observed variance, is density stratification (pycnocline) in the water column caused either by a salinity (halocline) or temperature (thermocline) gradient (Johansson et al. 2007, Gansel et al. 2014).

The density of seawater is predominantly determined by its salinity and temperature, hence a density gradient means that there is a gradient in salinity and/or temperature. Vertical stratification is known to inhibit vertical mixing in the water column (Imberger 2013), and thereby alter the current flow and the distribution of DO in the water column. Stratified sites show lower DO levels than homogeneous sites (Johansson et al. 2007), and haloclines are reported to influence the deflection of the ambient current around empty fish cages (Gansel et al. 2014). As vertical mixing is inhibited at the depth of the stratification, its vertical position is relevant. For instance, in Stien et al. (2012), the combination of relative low salinity and high temperature around the skirt depth is presented as an explanation for the low DO levels inside the fish cage. In addition, by influencing the vertical mixing, stratification can impact the effectiveness of the skirt as a preventive measure against lice (Geitung et al. 2019, Bui et al. 2020), as the vertical position of the salmon lice is influenced by environmental variables such as salinity (Bricknell et al. 2006, Crosbie et al. 2019) and temperature (Crosbie et al. 2020).

Local variations in DO inside fish cages and the varying efficiency of shielding skirts in lice prevention imply that hydrographical conditions at sites should be investigated in more detail. In the present study, 2 hydrographically different sites were monitored using similar equipment to exemplify the differences that can be observed in the field. DO levels and relative water density were measured inside and outside a fish cage at the 2 sites over a period of 3 d to study the dynamics of DO, current conditions and hydrography. The data provide important insight into how shielding skirts in combination with local conditions can influence the temporal and spatial variation of DO inside shielded cages.

2. MATERIALS AND METHODS

2.1. Study sites

The measurement campaigns were performed at the fish farms at Soløya (68.004339 °N, 13.181384 °E) and Fornes (68.410151 °N, 15.435051 °E), located in the Lofoten Islands, Norway (Fig. 1). To achieve continuous measurements unaffected by operational work and feeding, measurements were carried out between the late afternoon, or evening, and the morning. It should be noted that due to the latitudes of the sites, there was continuous daylight through the entire measurement period.

The first campaign was carried out from 21 to 24 May 2019 at Soløya, owned and operated by Ellingsen Seafood AS (Fig. 1). Data were collected over 2 nights between 21–22 May and 23–24 May. The second campaign was carried out at Fornes in Øksfjorden, owned and operated by Nordlaks Oppdrett AS (Fig. 1), with data recorded every night between 2 and 5 July 2019.

The Soløya farm consists of 12 cages in one row, aligned from north to south. Data were collected from the northernmost cage (Fig. 1), which had a circumference of 100 m and was equipped with a cylindrical net. The first 15 m of the cage were cylindrical and kept in place with 16 steel chain weights of 50 kg,

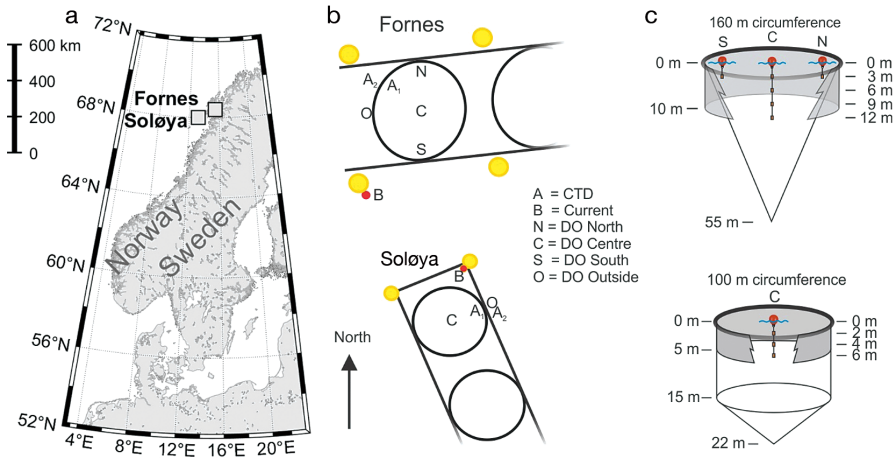

Fig. 1. (a) Locations of sites where measurement campaigns were carried out: Soløya in May 2019, and Fornes in July 2019. (b) Measurement positions of dissolved oxygen (DO), conductivity, temperature and depth (CTD) and current profiles at Fornes and Soløya. (c) Schematic diagram of the sea-cages. DO was measured at position O outside the cage at 3 m depth at Fornes and Soløya. DO was also measured in position C at 3, 6, 9 and 12 m at Fornes and at 2, 4 and 6 m at Soløya. At Fornes, DO was also measured at 3 m depth in positions N and S, 4 m from the floating collar. The CTD profiles were measured manually inside and outside the cage at positions A_1 and A_2, respectively. Current speed and direction profiles were measured at position B

each evenly distributed around the circumference of the cage. The bottom of the cage was formed as a cone from 15 to 22 m depth, with a 50 kg steel chain weight at the tip of the cone. The cage was equipped with a 5 m deep non-permeable tarpaulin shielding skirt (Botngaard), weighted with 4 kg m^{-1} around the bottom of the skirt (Fig. 1). The biomass in the cage during the experiments was 212 t, with 117 500 fish of average weight of 1.8 kg.

There were 9 cages at Fornes, also aligned in one row, but from west to east. Data were collected from the third westernmost cage (Fig. 1), which had a circumference of 160 m and was equipped with a conical net. The net was 55 m deep, with a concrete weight of 2.4 tonnes in water attached to the tip of the cone. The shielding skirt applied was a permeable canvas lice skirt (Norwegian Weather Protection) with a solidity of 51%, mesh size of 350 × 350 µm and a depth of 10 m (Fig. 1). The skirt was weighted with 2 kg m^{-1} lead rope at the bottom. The biomass in the cage during the experiment was 750 t, with 191 310 fish of average weight of 3.8 kg.

2.2. Measurements and sensors

DO was measured every minute at both locations using PME MiniDO_2T oxygen sensors (Kem-En-Tec Nordic). Due to its larger size, Fornes was equipped with 2 additional Aanderaa Optodes 4330 oxygen sensors (Aanderaa Data Instruments). At Soløya, DO was recorded in the cage centre at 2, 4 and 6 m depth, such that measurements were collected both above and below the skirt. Outside the cage, DO was recorded at 3 m depth (Fig. 1). At Fornes, DO was recorded in the cage centre and at 3, 6, 9 and 12 m depth, as the skirt was 10 m long. Measurements outside the cage were made at 3 m depth (Fig. 1). Additional oxygen sensors were deployed at the perimeter at 3 m depth.

Current speed and direction were recorded using an Aanderaa SeaGuard II Doppler current profiler (DCP) measuring continuously with a sampling frequency of 0.67 Hz (Fig. 1). Data were averaged and stored every minute. The DCP was attached to an anchoring buoy at both sites pointing downwards with vertical resolution (cell size) set to 1 m. As buoy-mounted DCPs can experience bias (Mayer et al. 2007), the first depth cell was excluded from the data set.

To measure vertical conductivity and temperature profiles, a SonTek CastAway CTD probe (SonTek/Xylem) was used inside and outside the cage at both sites (Fig. 1). CTD measurements were obtained manually the afternoon before and the morning after each measurement period.

2.3. Statistical analysis

Analyses were performed in MATLAB v. R2018b. A Kolmogorov-Smirnov test revealed that DO data were not normally distributed in any sensor at either location ($p < 0.05$). To test if there was a significant difference in DO levels inside and outside of the fish cage, the non-parametric Kruskal-Wallis test was applied to data from each location for each night. That is, the data from the sensors at 3, 6, 9 and 12 m inside the cage at Fornes were compared with those from the sensor at 3 m outside, while the data from the sensors at 2, 4, 6 and 8 m at Soløya were compared with those from the sensor at 3 m depth outside. All recorded data from the relevant periods were included as there were no outliers. When significant differences were detected, a Tukey-Kramer post hoc test was used to determine significant differences between measurements inside and outside the cage.

3. RESULTS

At both locations, and for all periods, the Kruskal-Wallis test confirmed that at least 2 of the DO sensors gave measurements that came from different distributions ($p < 0.01$). The Tukey-Kramer post hoc test further determined that there was a significant difference between the sensor outside and those inside ($p < 0.01$) at both locations.

3.1. Soløya data

Soløya had no clear tidal pattern and appeared chaotic with relatively low current speed throughout the period, but with some short bursts of 0.2 m s^{-1} in the upper 5 m (Fig. 2). The chaotic pattern at Soløya is also shown in Fig. 3, which shows the current roses for both locations, where the

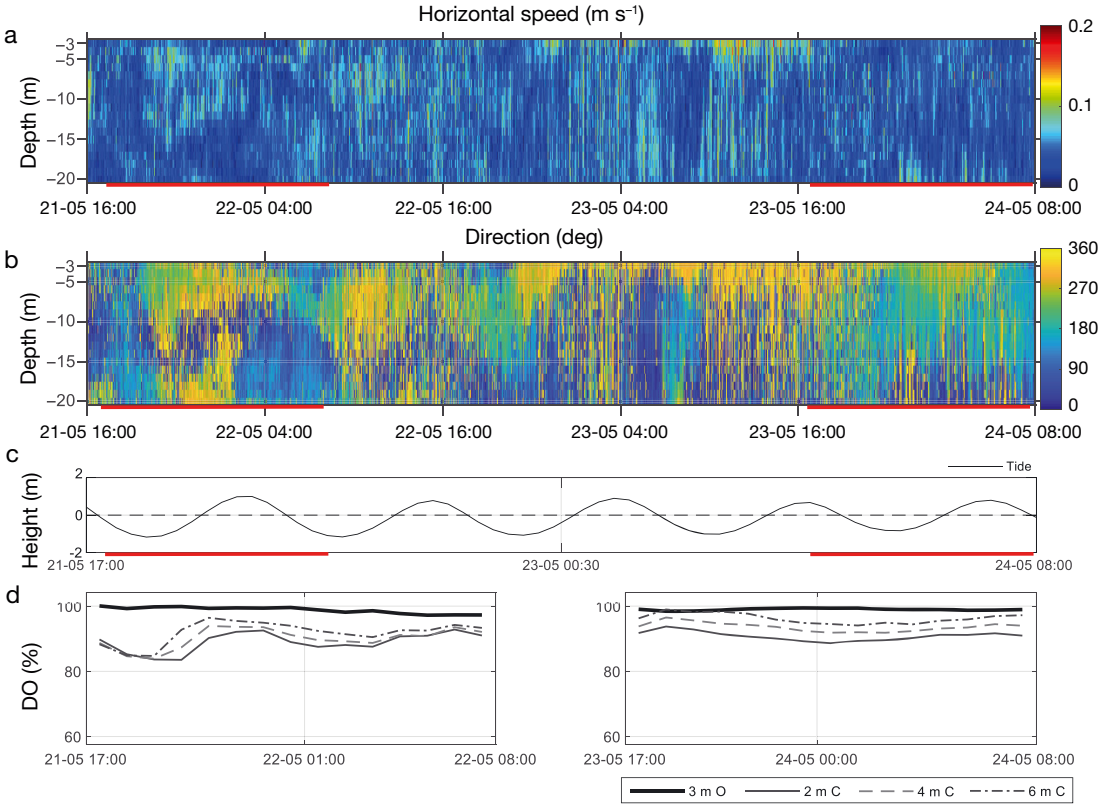

Fig. 2. (a) Current speed and (b) direction at Soløya in the top 20 m of the water column, measured by the Doppler current profiler (DCP) in position B (see Fig. 1) from 21 to 24 May 2019. The red horizontal line along the *x*-axis indicates the periods where DO measurements were taken. (c) Expected tidal height (thin black line). (d) Hourly median DO for all sensors at Soløya, for the periods marked with red in the graphs above. O: outside; C: centre of the cage

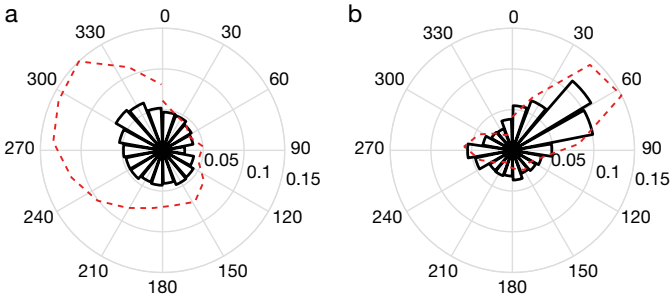

Fig. 3. Current roses showing average current speed and direction measured in the 3rd cell starting at 4 m depth of the DCP at (a) Soløya and (b) Fornes for the entire period the DCP was deployed. North is 0°, and east is 90°. Directions were sorted into bins of 20°, and average current speed for the given bin is shown in the polarplot. The red dashed line shows the direction that had the largest number of measurements, which was normalized based on the direction that had the largest number of measurements

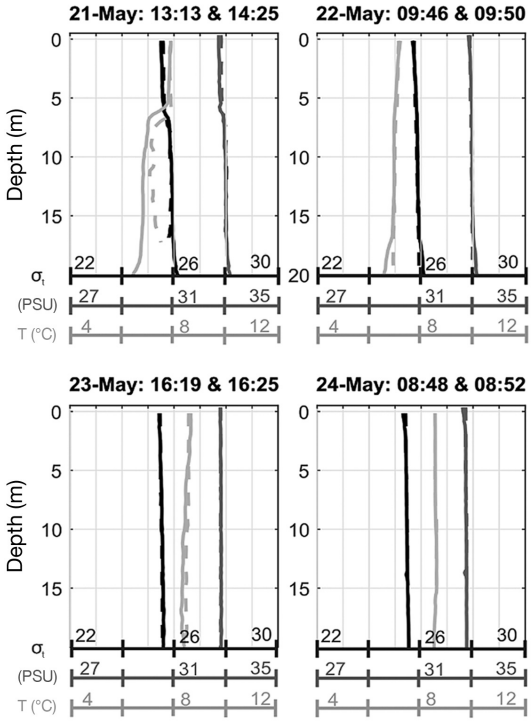

Fig. 4. Water density (σ_t), salinity (PSU) and temperature (°C) measured by the CTD at Soløya outside the fish cage in position A_2 (solid line) (see Fig. 1 for details), and inside the fish cage at position A_1 (dashed line). The time stamps above each graph represent the time the measurement was started outside and inside for each date, respectively

direction of the current at Soløya is more diffuse than that at Fornes, which showed a clear main direction.

The water column at Soløya was homogeneous through the study, with the exception of the data gathered on 21 May; here, there was a weak thermocline at 6 m depth with a difference of 1°C between the water over and underneath the stratification (Fig. 4). This was also the only measurement where there appeared to be a slight difference in temperature between inside and outside the cage, with higher temperatures inside (Fig. 4). Except for this measurement, the water column appeared homogeneous and identical inside and outside the cage.

The DO sensors also had temperature sensors; the minimum and maximum temperatures recorded inside the cage were 6.5 and 8.4°C, respectively. The maximum standard deviation recorded during one of the measurement periods inside the cage was 0.26°C.

The variability in DO, both outside and inside the cage, was greater during the first night than the second (Fig. 5). According to the Tukey-Kramer post hoc test, all sensors had mean ranks significantly different from

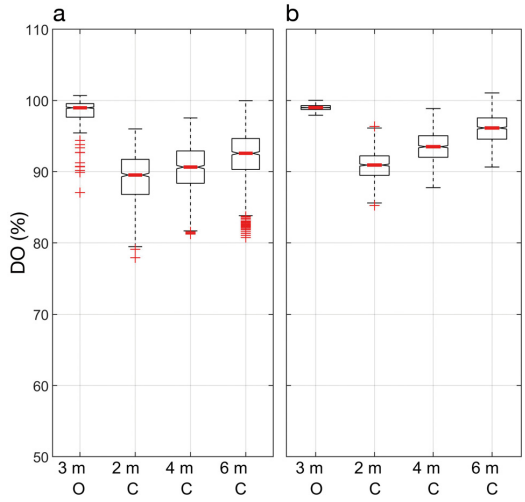

Fig. 5. Boxplot of oxygen levels at Soløya, showing combined oxygen data collected between (a) 21 May 17:00 h and 22 May 08:00 h and (b) 23 May 17:00 h and 24 May 08:00 h (right). The boxplots show the median DO (red line inside box), the lower edge of the box represents the 1st quartile (Q1) and the upper edge the 3rd quartile (Q3). The whiskers extends to Q1 minus 1.5 times the interquartile range (IQR) and to Q3 + 1.5 IQR. Data outside of the whiskers are measurements that exceed these limits (red crosses). The depth of the sensors is given on the *x*-axis with the positions. O: outside; C: centre of the cage

each other ($p < 0.01$). The lowest recorded DO level was 78% inside and 87% outside the cage, while the maximum was 101% both inside and outside. The hourly medians of DO inside the cage varied together, and there was an increase in DO with depth (Fig. 2).

3.2. Fornes data

At Fornes, there was a periodical semi-diurnal tidal pattern with a clear main direction and a maximum current speed of 0.2 m s^{-1} (Figs. 3 & 6). There was a pycnocline present that broke down gradually over the measurement period. In the first measurement, the relative density (σ_t), salinity and temperature inside and outside the cage were identical the entire depth, with a stratification at 8 m depth (Fig. 7). The temperature varied less than the salinity, hence it was mainly the salinity which influenced the density gradient at Fornes. As the difference between inside and outside increased, the inside of the cage had a higher relative density and higher salinity than the water outside (Fig. 7). On 5 July, the water had become more homogeneous,

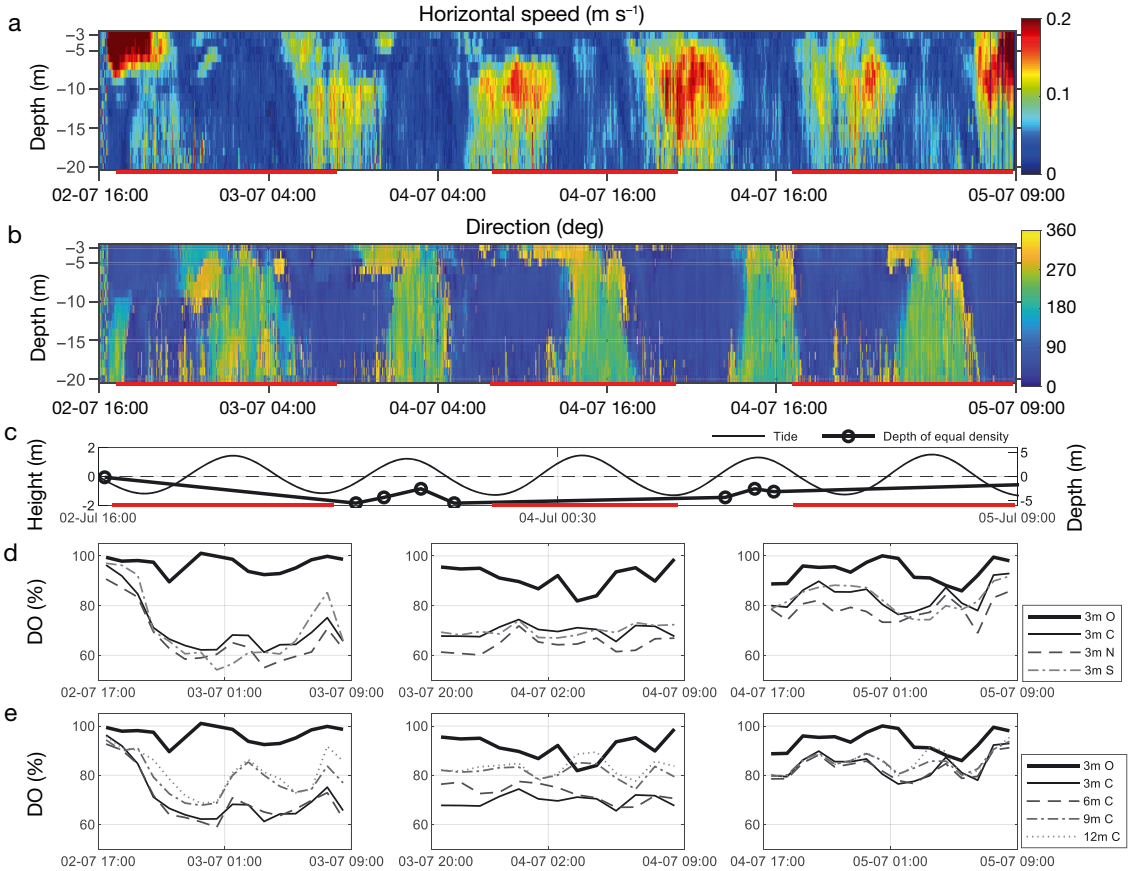

Fig. 6. (a) Current speed and (b) direction at Fornes in the top 20 m of the water column, measured by the DCP in position B (see Fig. 1) from 02 to 05 July 2019. Note that the measurement at 02 July 16:00 h between 3 and 10 m is potentially noise from a nearby boat. The red horizontal line along the *x*-axis indicates the period where DO measurements were taken. (c) Expected tidal height (thin black line) and the depth at which the density inside and outside the cage was equal (see Fig. 7 for density graphs); it should be noted that on 3 and 4 July, 2 and 1 additional CTD measurements, respectively, were included which are not represented in Fig. 7, as they were deemed redundant. (d,e) Hourly median DO for all oxygen sensors at Fornes for the periods marked with red. (d) Median for all sensors placed at 3 m depth, both outside and inside the cage. (e) Median for all sensors placed in the center of the cage, in addition to the one sensor placed outside the cage. O: outside; N: north; S: south; C: centre of the cage

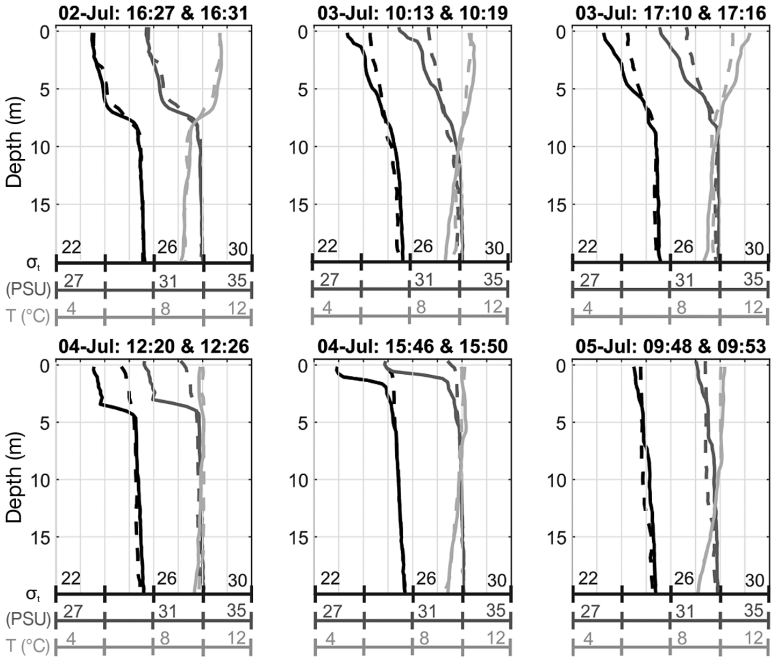

Fig. 7. Water density (σ_t), salinity (PSU) and temperature (°C) measured by the CTD at Fornes outside the fish cage in position A_2 (solid line) (see Fig. 1), and inside the fish cage at position A_1 (dashed line). The time stamps above each figure represent the time the measurement was started outside and inside for each date, respectively

with identical measurements inside and outside the cage (Fig. 7). To give an indication of how the density gradient changed with time, the depth at which the difference between the density outside and inside was less than 0.2 is indicated in Fig. 6. During the study period, this depth varied from 0.14 m on the first day to a maximum of 5.5 m on 3 July, and back up to 1.6 m on 5 July (Fig. 6). The minimum and maximum recorded temperatures at Fornes in the DO sensors inside the cage were 9.0 and 10.9°C, with a maximum standard deviation of 0.3°C in one of the sensors during one of the measurement periods.

There was a larger variance in DO levels at Fornes than at Soløya, with a minimum of 52% and a maximum of 98% DO inside the fish cage, and a minimum of 76% and maximum of 102% DO outside the fish cage (Fig. 8). There was some variation between the DO levels recorded at 3 m depth, with the DO in position N recording the lowest hourly medians (Fig. 6). The mean rank for this sensor was significantly different from all other sensors each night (Tukey-Kramer post hoc, $p > 0.05$). The first and second nights, there was little difference between the sensors at 3 and 6 m depth and between the sensors at 9 and 12 m depth. The first night, the sensor at 6 m depth was not significantly different from the sensors at 3 m in the centre and south in the cage (Tukey-Kramer post hoc, $p > 0.05$). On the second night, only the sensors at 3 m positioned in the centre and south were not significantly different ($p > 0.05$). The third night, variation between depths disappeared inside the cage, with nearly similar DO recorded on all sensors, and the sensors at 3 and 6 m in the centre were not significantly different, nor were the sensors at 9 and 12 m ($p > 0.05$). As with the DO at Soløya, there was an increase in DO with depth (Figs. 6 and 8).

4. DISCUSSION

Comparing the effect of the permeable and non-permeable lice skirt on the internal environment is of limited value due to the differences in topography, hydrography and current flow pattern at the 2 study sites. However, independent of skirt type, the DO improved at both locations with depth inside the cage (Figs. 5 & 8), and both sites had a significant difference in DO between the inside and outside of the cage ($p < 0.01$, Tukey-Kramer post hoc test), with a lower median DO inside the cage.

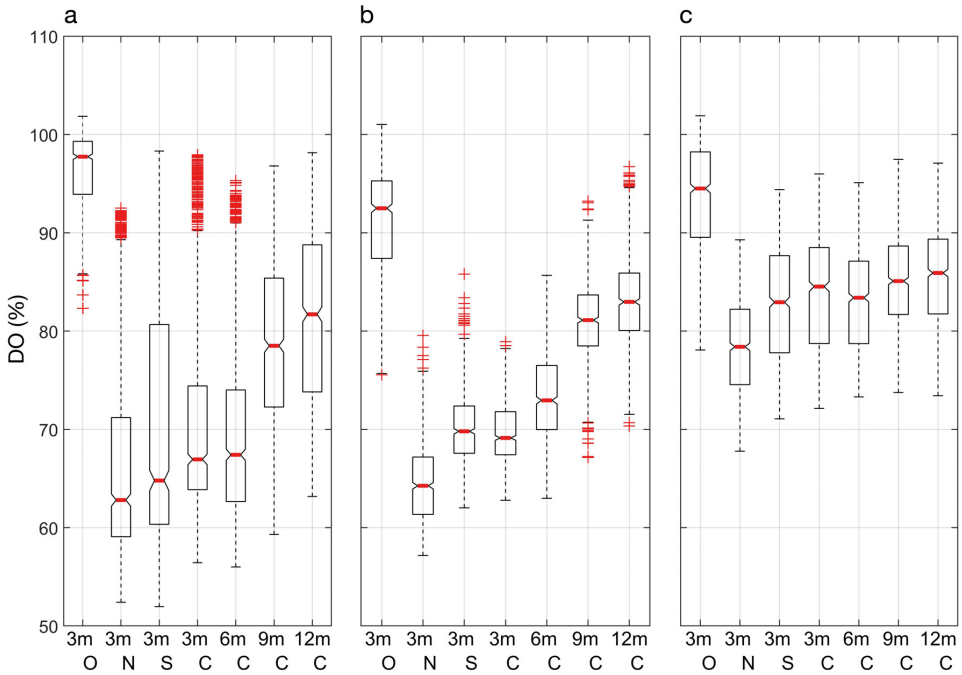

Fig. 8. Boxplot representations of oxygen levels at Fornes, showing the combined oxygen data collected between (a) 02 July 17:00 h and 03 July 09:00 h, (b) 03 July 20:00 h and 04 July 09:00 h and (c) 04 July 17:00 h and 05 July 09:00 h. The boxplots show the median DO (red line inside box), the lower edge of the box represents the 1st quartile (Q1) and the upper edge the 3rd quartile (Q3). The whiskers extends to Q1 minus 1.5 times the interquartile range (IQR), and to Q3 + 1.5 IQR. Data outside of the whiskers are measurements that exceed these limits (red crosses). The depth of the sensors is given on the *x*-axis with their positions. O: outside; N: north; S: south; C: centre of the cage

4.1. Soløya

It was initially assumed that Soløya would have lower DO levels inside the cage than Fornes, as Soløya was equipped with a non-permeable skirt, while Fornes had a permeable one. However, this was not the case; throughout the measurement period, DO was higher at Soløya.

The current at Soløya appeared weak throughout most of the study period, with speeds below 7 cm s^{-1}, and did not show a tidal pattern (Fig. 2). The direction of the current was diffuse, compared to Fornes, with a dominant direction towards the northwest and west (Fig. 3). Soløya is placed in a strait with several small islands to the south, and to the north there is a very narrow strait that leads out to Selfjorden and then to the open Norwegian Sea. The larger variance seen in direction at Soløya could be explained by the local topography and the position of the farm.

This dominant current direction of northwest meant that the cages south of the studied cage could have had a shielding effect on the current flow through the cage and hence DO levels. However, as evidenced by the consistently high DO both inside and outside the cage, the shielding effect was negligible in this instance.

Vertical stratification of the water column, as occurs when a pycnocline is present, is known to inhibit vertical mixing (Imberger 2013). The water column at Soløya was non-stratified with near identical characteristics inside and outside the cage except the first measurement, which showed signs of a weak pycnocline (Fig. 4). The lack of stratification meant that there was no inhibition of vertical mixing at Soløya, and the good DO conditions could be a result of good vertical mixing in the water column.

DO gradients in unshielded cages are reported to increase with depth at some sites (Johansson et al. 2007, Solstorm et al. 2018), while others see a decrease with depth (Johansson et al. 2007, Oldham et al. 2018). The DO at Soløya was lower inside the cage than outside for most of the study period, and the DO had a gradual improvement with depth, with an almost linear relationship (Fig. 5). Increases in DO

with depth are observed in studies using both non-permeable skirts (Stien et al. 2012) and permeable skirts (Stien et al. 2018), similar to those used in the present study. It is therefore likely that the increase with depth when using shielding skirts is due to the shielding skirt itself.

If the homogeneous water at Soløya is caused by vertical mixing, it is uncertain whether the skirt is actually effective in preventing lice from entering the cage, as the vertical mixing could result in the lice being pushed further down in the water column, below the skirt and into the cage. The skirt length of 5 m may not be sufficient if that is the case. However, more environmental data and lice counts are needed to verify this.

4.2. Fornes

The current at Fornes had a clear, dominant southeast–northwest direction and tidal component demonstrated by the semi-diurnal pattern observed in the current speed and direction (Fig. 6). It should be noted that the dominant direction of the current resulted in the DCP's position relative to the cage to be either upstream or downstream of the cage, depending on the phase of the tidal cycle. When upstream of the cage, the DCP recorded the incoming unobstructed current, while downstream measurements were affected by the speed reduction and turbulence caused by the cage structure (Klebert et al. 2015). When the current was moving southwards, the current speed was therefore higher than recorded.

DO at Fornes had a greater variability with a minimum of 52%, and DO levels improved with depth (Figs. 6 & 8). The variability seen between the sensors at 3 m depth can be explained by the current direction and position of the sensors (Fig. 6). As the current travels through the cage, a reduction in speed is expected (Klebert et al. 2015), which can result in a lower water exchange downstream in the cage, as observed by Solstorm et al. (2018). It is therefore possible that the reason that the sensors in positions N and S had a lower median than in the centre of the cage on the first and third nights was due to the current turning and flowing in both directions during the measurement periods (Figs. 6 and 8). On the second night, the stratification appears to have influenced the current in the upper 5 m, which appears to be moving mainly towards the north and north-northwest (Fig. 6), explaining why the lowest median current was recorded by the sensor in position N (Fig. 8).

The improvement in DO with depth was not linear at Fornes. The sensors at 3 and 6 m were more similar than those at 9 and 12 m, indicating that the skirt had a direct impact on the sensors at 3 and 6 m, but not at 9 m depth. This is plausible as the skirt, which was 10 m long, was installed as a cylinder around the conically shaped net. Moderate currents can result in the skirt being pushed into the net and lifted upwards (Lien et al. 2014); it is therefore not unlikely that the sensor at 9 m was not fully shielded, explaining why it is more similar to the sensor at 12 m than to that at 6 m (Figs. 6 & 8).

However, this grouping of the sensors was not always clear. For instance, during the first couple of hours and the last night, all sensors recorded similar DO levels (Fig. 6). The grouping first appeared as the DO dropped at all depths the first night. It is uncertain if this drop also occurred outside of the cage in deeper layers, as the reference sensor was at 3 m depth, and prior to this drop, a pycnocline was recorded at 8 m depth (Fig. 7). A potential cause for the drop is therefore that the water below this pycnocline had lower DO, and it was this water that moved into the cage. Another possibility is that the DO drop occurred due to the high stocking density of 20 kg m^{-3} or an increase in fish activity; however, there were no data recorded regarding the vertical position of the fish. The specific reason for the steep drop the first night cannot be interpreted from the data recorded.

It should be noted that other experiments applying the same type of permeable skirt as used in this study saw no impact on the welfare status of the salmon (Stien et al. 2018, Bui et al. 2020). When using similar skirt with 10 m length, the minimum DO inside the cage was 70% during a 3-mo period (Stien et al. 2018), indicating that the length of the skirt is not the main reason for the low DO inside the cage. A possible reason for the higher DO in Stien et al. (2018) compared with the present study could be the low stocking density of <10 kg m^{-3}. However, the difference in stocking density does not explain the observed temporal variability in DO.

It is uncertain whether the low DO levels recorded in this study had any negative effect on the fish. Moderate hypoxia of 50% DO in water of 16°C significantly reduces aerobic capacity and swimming performance of Atlantic salmon *Salmo salar* (Oldham et al. 2019). The temperature at Fornes never exceeded 11°C, and as required DO increases with temperature, it is uncertain whether the reduced DO posed any real threat to fish welfare or growth. Furthermore, the observations were made over a relatively short period, and as DO was higher at other

locations in the cage (Fig. 6), the fish had the opportunity to avoid the areas with low DO. However, it should be noted that avoidance behaviour is documented for DO <35%, but not for sub-optimal waters with DO <60%, indicating that DO is not a primary driver of behaviour (Oldham et al. 2017, Stehfest et al. 2017).

An explanation for the variation in DO through the study is the hydrography. The current flow at Fornes showed periods where the current speed was faster at deeper layers, indicating a stratification in the water column (Fig. 6). As discussed previously, pycnoclines and haloclines have been observed to impact the DO inside fish cages (Johansson et al. 2006, Stien et al. 2012). The first CTD measurement at Fornes revealed a clear pycnocline, with nearly identical density recorded inside and outside the cage (Fig. 7). The hourly median DO levels inside the cage were nearly equal to DO outside the cage for the first couple of hours (Fig. 6). There was then a sudden drop in DO, which remained throughout the night. During the second and third days, there was a difference in density in the top 6 m of the water column (Fig. 7). The depths at which the density outside and inside the cage were approximately equal varied throughout the period (Fig. 6), and it appeared that as the depth of equal density moved upwards, the DO levels inside the fish cage improved (Figs. 6 & 8). It should be noted that on 4 July, the stratification had moved up to roughly 2 m, hence the pycnocline would be at a higher depth level than the DO sensor at 3 m depth. There are no data for the DO above this depth, and there is a possibility that the DO was lower in this area.

The presence of a density gradient may have influenced the water exchange rate and water flow through the permeable skirt. For the cage at Fornes, water exchange could occur in 2 ways, either from the water passing through the skirt or by the water being pressed down along the skirt and into the cage (Lien & Høy 2011, Lien et al. 2015). When a pycnocline is present and remains above the skirt depth, it could result in the water above the pycnocline being prevented from moving down along the skirt and into the fish cage. However, as the pycnocline moves higher up along the skirt, more of the water below is free to move underneath the skirt and into the cage.

The water above and below the pycnocline is free to pass through the permeable skirt, but how much water actually passed through the permeable skirt was not verified in this study. However, the periods with difference in water density between the inside and outside suggest that the skirt rerouted a large portion of the upper water column around the fish cage and there was not enough water that passed through the skirt to replace the water with low DO inside. This could be due to the size of the cage (as larger cages are reported to have lower DO levels; Oldham et al. 2018), the density of fish, or fouling of the skirt and net, which can reduce water flow (Gansel et al. 2015). It is also possible that the higher density inside the cage created a blocking effect of the water. It has been theorized that the swimming behaviour of the fish can attenuate and redirect the water current (Johansson et al. 2007), and that when the fish are swimming in a torus shape, they produce an area with high pressure inside the cage, which results in the water being pressed outwards (Gansel et al. 2014). The higher density seen in the present study could have resulted in a similar result, with the higher-density water on the inside forcing more of the water around the cage as it blocked the lower-density water from passing through the permeable skirt. This could explain some of the variation seen at Fornes, but more research is needed on this possible effect.

5. CONCLUSIONS

To prevent salmon lice *Lepeophtheirus salmonis* infestations, shielding skirts were used to attempt to reroute the upper layer of the water column around the cage. The effect shielding skirts have on the internal environment of the sea-cage, particularly the DO concentration, varied between sites. In this study, 2 hydrographically different sites were studied. The DO improved with depth at both sites; however, the impact of the shielding skirt varied. The DO levels were higher at Soløya, which was a non-stratified site, while the stratified site Fornes had larger temporal and spatial variance in DO, and this variation appeared to co-occur with the presence and depth of a pycnocline. The local variations exemplified in this study demonstrate the complex relationship between DO, current and stratifications when shielding skirts are used. To verify and document the interaction between shielding skirts, pycnoclines and current flow, and how this influences lice prevention, more data are needed either by studying the underlying mechanisms in a more controlled environment or from long-term studies.

Acknowledgements. This study is part of the project 'Shielding skirt as a method for prevention and control of salmon lice infestation—improving knowledge about environmen-

tal conditions for increase in efficiency and reduction of risk (SKJERMTEK)' (project no. 901396) funded by The Norwegian Seafood Research Fund (FHF). K.E.J. received funding from the RACE research grant program funded by SINTEF Ocean. We are thankful for access to equipment from SINTEF ACE, and to Ellingsen Seafood AS and Nordlaks Oppdrett AS for access to their sites and the help received from their on-site employees.

LITERATURE CITED

Barrett LT, Oppedal F, Robinson N, Dempster T (2020) Prevention not cure: a review of methods to avoid sea lice infestations in salmon aquaculture. Rev Aquacult 12: 2527–2543

Bricknell IR, Dalesman SJ, O'Shea B, Pert CC, Luntz AJM (2006) Effect of environmental salinity on sea lice *Lepeophtheirus salmonis* settlement success. Dis Aquat Org 71:201–212

Bui S, Stien LH, Nilsson J, Trengereid H, Oppedal F (2020) Efficiency and welfare impact of long-term simultaneous in situ management strategies for salmon louse reduction in commercial sea-cages. Aquaculture 520:734934

Crosbie T, Wright DW, Oppedal F, Johnsen IA, Samsing F, Dempster T (2019) Effects of step salinity gradients on salmon lice larvae behaviour and dispersal. Aquacult Environ Interact 11:181–190

Crosbie T, Wright DW, Oppedal F, Dalvin S, Myksvoll MS, Dempster T (2020) Impact of thermoclines on the vertical distribution of salmon lice larvae. Aquacult Environ Interact 12:1–10

Frank K, Gansel LC, Lien AM, Birkevold J (2015) Effects of a shielding skirt for prevention of sea lice on the flow past stocked salmon fish cages. J Offshore Mech Arctic Eng 137:011201

Gansel LC, Rackebrandt S, Oppedal F, McClimans TA (2014) Flow fields inside stocked fish cages and the near environment. J Offshore Mech Arctic Eng 136:031201

Gansel LC, Plew DR, Endresen PC, Olsen AI, Misimi E, Guenther J, Jensen Ø (2015) Drag of clean and fouled net panels–measurements and parameterization of fouling. PLOS ONE 10:e0131051

Geitung L, Oppedal F, Stien LH, Dempster T, Karlsbakk E, Nola V, Wright DW (2019) Snorkel sea-cage technology decreases salmon louse infestation by 75% in a full-cycle commercial test. Int J Parasitol 49:843–846

Grøntvedt RN, Kristoffersen AB (2015) Permaskjørt kan redusere påslag av lakselus-analyse av feltdata. Delrapport Permaskjørt–prosjektet A5. Report 2. Norwegian Veterinary Institute, Oslo, Norway

Grøntvedt RN, Kristoffersen AB, Jansen PA (2018) Reduced exposure of farmed salmon to salmon louse (*Lepeophtheirus salmonis* L.) infestation by use of plankton nets: Estimating the shielding effect. Aquaculture 495: 865–872

Heuch PA, Parsons A, Boxaspen K (1995) Diel vertical migration: a possible host-finding mechanism in salmon louse (*Lepeophtheirus salmonis*) copepodids? Can J Fish Aquat Sci 52:681–689

Hevrøy EM, Boxaspen K, Oppedal F, Taranger GL, Holm JC (2003) The effect of artificial light treatment and depth on the infestation of the sea louse *Lepeophtheirus salmonis* on Atlantic salmon (*Salmo salar* L.) culture. Aquaculture 220:1–14

Huse I, Holm JC (1993) Vertical distribution of Atlantic salmon (*Salmo salar*) as a function of illumination. J Fish Biol 43:147–156

Imberger J (2013) Environmental fluid dynamics: flow processes, scaling, equations of motion, and solutions to environmental flows. Academic Press, Waltham, MA

Johansson D, Ruohonen K, Kiessling A, Oppedal F, Stiansen JE, Kelly M, Juell JE (2006) Effect of environmental factors on swimming depth preferences of Atlantic salmon (*Salmo salar* L.) and temporal and spatial variations in oxygen levels in sea-cages at a fjord site. Aquaculture 254:594–605

Johansson D, Juell JE, Oppedal F, Stiansen JE, Ruohonen K (2007) The influence of the pycnocline and cage resistance on current flow, oxygen flux and swimming behaviour of Atlantic salmon (*Salmo salar* L.) in production cages. Aquaculture 265:271–287

Klebert P, Su B (2020) Turbulence and flow field alterations inside a fish sea cage and its wake. Appl Ocean Res 98: 102113

Klebert P, Lader P, Gansel L, Oppedal F (2013) Hydrodynamic interactions on net panel and aquaculture fish cages: a review. Ocean Eng 58:260–274

Klebert P, Patursson Ø, Endresen PC, Rundtop P, Birkevold J, Rasmussen HW (2015) Three-dimensional deformation of a large circular flexible sea-cage in high currents: Field experiment and modeling. Ocean Eng 104: 511–520

Lien AM, Høy E (2011) Skjørt for Skjerming mot lus i Laksemerd. Rep No A19396, SINTEF Fiskeri og Havbruk, Trondheim

Lien AM, Volent Z, Jensen Ø, Lader P, Sunde LM (2014) Shielding skirt for prevention of salmon lice (*Lepeophtheirus salmonis*) infestation on Atlantic salmon (*Salmo salar* L.) in cages — a scaled model experimental study on net and skirt deformation, total mooring load, and currents. Aquacult Eng 58:1–10

Lien AM, Stien LH, Grøntvedt R, Frank K (2015) Permanent skjørt for redusering av luspåslag på laks. Rep No A26790, SINTEF Fiskeri og Havbruk

Mayer DA, Virmani JI, Weisberg RH (2007) Velocity comparisons from upward and downward acoustic Doppler current profilers on the West Florida Shelf. J Atmos Ocean Technol 24:1950–1960

Næs M, Heuch PA, Mathisen R (2012) Bruk av 'luseskjørt' for å redusere påslag av lakselus *Lepeophtheirus salmonis* (Krøyer) på oppdrettslaks. Vesterålen Fiskehelsetjeneste, Sortland

Oldham T, Dempster T, Fosse JO, Oppedal F (2017) Oxygen gradients affect behaviour of caged Atlantic salmon *Salmo salar*. Aquacult Environ Interact 9:145–153

Oldham T, Oppedal F, Dempster T (2018) Cage size affects dissolved oxygen distribution in salmon aquaculture. Aquacult Environ Interact 10:149–156

Oldham T, Nowak B, Hvas M, Oppedal F (2019) Metabolic and functional impacts of hypoxia vary with size in Atlantic salmon. Comp Biochem Physiol A Mol Integr Physiol 231:30–38

Oppedal F, Samsing F, Dempster T, Wright DW, Bui S, Stien LH (2017) Sea lice infestation levels decrease with deeper 'snorkel' barriers in Atlantic salmon sea-cages. Pest Manag Sci 73:1935–1943

Rasmussen HW, Patursson Ø, Simonsen K (2015) Visualisation of the wake behind fish farming sea-cages. Aquacult Eng 64:25–31

Remen M, Oppedal F, Imsland AK, Olsen RE, Torgersen T (2013) Hypoxia tolerance thresholds for post-smolt Atlantic salmon: dependency of temperature and hypoxia acclimation. Aquaculture 416–417:41–47

Remen M, Aas TS, Vågseth T, Torgersen T, Olsen RE, Imsland A, Oppedal F (2014) Production performance of Atlantic salmon (*Salmo salar* L.) postsmolts in cyclic hypoxia, and following compensatory growth. Aquacult Res 45:1355–1366

Remen M, Sievers M, Torgersen T, Oppedal F (2016) The oxygen threshold for maximal feed intake of Atlantic salmon post-smolts is highly temperature-dependent. Aquaculture 464:582–592

Solstorm D, Oldham T, Solstorm F, Klebert P, Stien LH, Vågseth T, Oppedal F (2018) Dissolved oxygen variability in a commercial sea-cage exposes farmed Atlantic salmon to growth limiting conditions. Aquaculture 486:122–129

Stehfest KM, Carter CG, McAllister JD, Ross JD, Semmens JM (2017) Response of Atlantic salmon *Salmo salar* to temperature and dissolved oxygen extremes established using animal-borne environmental sensors. Sci Rep 7: 4545

Stien LH, Nilsson J, Hevrøy EM, Oppedal F, Kristiansen TS, Lien AM, Folkedal O (2012) Skirt around a salmon sea-cage to reduce infestation of salmon lice resulted in low oxygen levels. Aquacult Eng 51:21–25

Stien LH, Lind MB, Oppedal F, Wright DW, Seternes T (2018) Skirts on salmon production cages reduced salmon lice infestations without affecting fish welfare. Aquaculture 490:281–287

Wildish D, Keizer P, Wilson A, Martin J (1993) Seasonal changes of dissolved oxygen and plant nutrients in seawater near salmonid net pens in the macrotidal Bay of Fundy. Can J Fish Aquat Sci 50:303–311

Editorial responsibility: Tim Dempster, Melbourne, Victoria, Australia

Submitted: September 1, 2020; Accepted: October 19, 2020
Proofs received from author(s): December 5, 2020

Paper C

Current flow and dissolved oxygen in a full-scale stocked fish-cage with and without lice shielding skirts

Jónsdóttir, K. E., Volent, Z., Alfredsen, J.A., 2021. Current flow and dissolved oxygen in a full-scale stocked fish-cage with and without lice shielding skirts. Applied Ocean Research, 108, 102509

Applied Ocean Research 108 (2021) 102509

Contents lists available at ScienceDirect

Applied Ocean Research

journal homepage: www.elsevier.com/locate/apor

Current flow and dissolved oxygen in a full-scale stocked fish-cage with and without lice shielding skirts

Kristbjörg Edda Jónsdóttir [*,a], Zsolt Volent [b], Jo Arve Alfredsen [a]

[a] Norwegian University of Science and Technology, Department of Engineering Cybernetics, Trondheim NO-7491, Norway
[b] Sintef OCEAN, Seafood Technology, Aquaculture Structures, Postboks 4762, Torgarden, Trondheim 7465, Norway

ARTICLE INFO

Keywords:
Salmon aquaculture
Lice shielding skirt
3D velocity field
Stocked fish cage
Current flow reduction
Dissolved oxygen

ABSTRACT

Shielding skirts are widely used on Atlantic Salmon sea-cages as a non-invasive preventive measure against salmon lice infestations. The skirts are however known to impact the current flow and thereby the environment within the cage. As the current is influenced by local factors such as topography, farm layout and stocking density of the cage, it is difficult to compare results from sites that apply skirts with those without. The same high-stocked cage was therefore studied with and without the skirt deployed, including the transition from shielded to unshielded, to investigate the influence the skirt had on the current flow within the cage and dissolved oxygen. When the skirt was deployed the velocity vector in the centre of the cage had a vertical component towards the surface and the reduction in current speed was higher. The dissolved oxygen level inside the cage improved within 30 minutes when the skirt was removed and there was no indication of the skirt influencing the vertical swimming behaviour of the salmon.

1. Introduction

In aquaculture sea-cages a sufficient water exchange is necessary to ensure a healthy environment by supplying dissolved oxygen (DO) and removing waste and nutrient-depleted water. In 2016 the salmon lice challenges were the second highest expense for the industry in Norway (Iversen et al., 2017), and the high cost of delousing treatments (Abolofia et al., 2017; Iversen et al., 2017) has resulted in the use of preventative measures such as the non-invasive lice shielding skirts. As evidence indicates a higher lice density in the upper layers of the water column (Geitung et al., 2019; Heuch et al., 1995; Hevrøy et al., 2003; Huse and Holm, 1993; Oppedal et al., 2017), lice shielding skirts are designed to reroute this layer of the water column around the fish cage, and thereby keep the lice out by altering the current flow.

For empty cages with a shielding skirt, CFD analysis indicate that part of the ocean current is forced underneath the skirt and into the sea cage producing a recirculation pattern, where it meets the skirt in the back and is pressed up and inwards towards the centre of the cage (Lien and Høy, 2011; Lien et al., 2015). This recirculation pattern is seen in full-scale cages with skirt when the cage is empty, but not when stocked (Klebert and Su, 2020).

As the current flows through the fish cage, the current speed is reduced (Frank et al., 2015; Gansel et al., 2014; Johansson et al., 2007; Klebert and Su, 2020; Rasmussen et al., 2015; Winthereig-Rasmussen et al., 2016). The magnitude of current speed reduction as it passes through the cage is determined by the current flow pattern which is influenced by a number of factors such as farm layout (Rasmussen et al., 2015), local flow conditions at the site, local topography (Klebert et al., 2013), shielding skirts (Frank et al., 2015) and the cage structure (Klebert et al., 2015). Furthermore, reduction through plane nets increase with increasing solidity (Bi et al., 2013; Gansel et al., 2015) which can be caused by bio-fouling (Gansel et al., 2015) and increasing inclination angle between the net and the vertical plane (Bi et al., 2013). Most cages used in Norway are gravity nets, which deform as a function of the current speed (Lader et al., 2008). This deformation can alter the inclination angle and hence increase the reduction in flow velocity. The shielding skirt can also deform, and in strong currents the skirt will increasingly be pushed back and up towards the surface, resulting in potentially less obstruction for the current and lice (Lien et al., 2014).

The reduction in current speed is also influenced by the presence of fish (Gansel et al., 2014; Klebert et al., 2013; Klebert and Su, 2020). It is suggested that the swimming pattern of the fish can attenuate and redirect the internal water currents of a cage (Johansson et al., 2007). High fish densities are seen to deflect the ambient current (Gansel et al.,

* Corresponding author.
E-mail address: kristbjorg.jonsdottir@ntnu.no (K.E. Jónsdóttir).

https://doi.org/10.1016/j.apor.2020.102509
Received 24 September 2020; Received in revised form 26 November 2020; Accepted 22 December 2020
Available online 26 January 2021

2014), and it is hypothesized that as the fish swims in a torus shape they push the water outwards at depths of high biomass, resulting in a low pressure area in the centre drawing in water from depths above and below this area (Frank et al., 2015; Gansel et al., 2014). Simulations of fish behaviour on flow dynamics support this notion as a high density of fish swimming in a torus shape increased the maximum velocity in the upwelling flow (Tang et al., 2017). However, in the recent study by Klebert and Su (2020) there was no indication of a recirculation pattern when the cage was stocked, nor was there any evidence that the fish generated a secondary radial or vertical flow (Klebert and Su, 2020).

This reduction can lead to reduced water exchange in the fish cage, which can become problematic with regards to DO levels inside the cage, especially when current speeds are low (Winthereig-Rasmussen et al., 2016). If DO is reduced sufficiently hypoxic conditions can occur, which reduces feed intake, growth rates and fish welfare (Remen et al., 2014). The use of a non-permeable lice shielding skirt increases the blocking effect, and low DO levels inside the fish cages are reported at some locations (Stien et al., 2012).

As lice shielding skirts have a direct impact on how the current flows through the cage, and consequently the internal environment of the cage, it is necessary to investigate how cages with and without skirts differ. The aim of this study was to investigate how a lice shielding skirt influenced the DO and water flow inside a fully stocked cage, specifically the vertical motion and the reduction in current speed from outside to inside the cage. As model-scale experiments can not take into account the presence of fish and their behaviour, and comparing data from different sites with and without skirts may be of limited value due to variable topography, hydrographical conditions and different stocking densities, this study was performed at the same site and measurements were collected from the same fully-stocked fish cage during a three-day period which included the transition from a shielded to an unshielded cage.

2. Material and methods

2.1. Site description

The study took place from the 5–7th of November 2018 on the fish farm Hosnaøyan, located in the county of Trøndelag, Norway (Fig. 1). The Hosnaøyan farm consists of ten cages in a frame mooring (Fig. 2). Cages marked with horizontal and vertical lines contained fish. The cage used for the measurements (shaded cage in Fig. 2), was 157 m in circumference with a 15 m deep cylindrical net with a sinker tube at the bottom with a weight of 60 kg m^{-1}. The bottom of the cage was conical from 15 m to 28 m with a weight of 250 kg at the centre of the cone. The net had a solidity of 0.21 and a mesh opening of 17.5 mm, and was cleaned on the 1st of November, hence there was little bioufouling during this study.

The cage was equipped with a 6.7 m deep non-permeable tarpaulin shielding skirt (Botngaard AS, Oksvoll, Norway), weighted with 4 kg m^{-1} around the bottom of the skirt. The skirt was installed 16:00 on the 4th of November, the day prior to the onset of the study. Due to a sudden drop in dissolved oxygen (DO), the skirt was lifted on the 06.11.2018 09:45. The biomass in the cage during the experiments was 830 tonnes, with 189 200 fish of average weight 4.4 kg.

2.2. Equipment description

2.2.1. ADV and DCP

Current speed and direction outside the cage were recorded using an Aanderaa SeaGuard II doppler current profiler (DCP) measuring continuously with a sampling frequency of 0.5 Hz (see Fig. 2). The velocity accuracy was 0.3 cm s^{-1} or ±1% of full-scale reading, with a velocity resolution of 0.1 cm s^{-1}. The data was averaged and stored every minute. The DCP was attached to the anchoring buoy pointing downwards with vertical resolution (cell size) set to 1 m.

An ADCP Aquadopp Profiler 400kHz produced by Nortek Group was mounted on the oceanographic buoy located roughly 100 m South of the farm (OB, Fig. 2). Its velocity range was ±10 m/s and measurements were made with an accuracy of ± 1% of the measured value or ±0.5 cm s^{-1}. The ADCP had a cell size of 3 m, and a constant sampling rate of 2 Hz during the sample period of 10 min. The acquisition interval was set to 60 min, and the data was averaged over the 10 min sampling period.

The current velocity inside the cage was measured using Nortek Vector Acoustic Doppler Velocimeters (ADV) with a sampling rate of 8Hz, with 60 samples per burst and a burst interval of 60 s. The ADVs have an accuracy of 0.5% of measured value ±1 mm s^{-1}, with velocity precision typical 1% of velocity range (at 16Hz). The ADVs were suspended from a buoy at 2, 6 and 8 m depth.

The ADV-rig had a total of three positions during the study, Pos. 1 was in the centre of the cage, while Pos. 2 was to the N-E end of the cage, and Pos. 3 was to the S-W of the cage. Both Pos. 2 and 3 were roughly 8 m from the floating collar (Fig. 2). Pos. 1 and 2 were used to measure the current flow through the cage, and the reduction in current speed. While Pos. 3 was used when the skirt was lifted, and was positioned just in front of the initial lifting point of the skirt.

Raw data from the ADVs were filtered using the improved phase space filter (Goring and Nikora, 2002) for bubbly flows (Birjandi and Bibeau, 2011) to remove velocity spikes caused by Doppler noise, signal aliasing and disturbances from the fish as the cage was fully stocked. Velocity spikes were not replaced but removed. The ADV data was averaged over 1 min, and if more than 50% of the data in a minute had been removed, the entire minute was excluded from further analyses.

2.2.2. Dissolved oxygen

Dissolved oxygen (DO) was measured every minute using Aanderaa Optode 4330 oxygen sensors (Aanderaa Data Intruments AS, Bergen, Norway). The measurement range was 0 - 1000 μM (0 - 300%) with a calibration range of 0 - 500 μM (0 - 150%), resolution of $<$ 0.5 μM (0.05%) and an accuracy of $<$ 8 μM (5%). DO were measured both inside and outside of the cage at 3 m depth (Fig. 2). The DO sensor inside was suspended from a floating buoy 3 m from the net, while the sensor outside was mounted right outside of the floating collar. DO was sampled every minute throughout the measurement period.

The oceanographic buoy was equipped with an Aanderaa Optode 4531A (Aanderaa Data Intruments AS, Bergen, Norway). The measurement range was 0 - 800 μM (0 - 200%), with a resolution of $<$ 1 μM (0.4%) and an accuracy of $<$ 8 μM (5%). The optode had an averaging cycle of 1 min and acquisition interval of 60 min.

2.2.3. Echosounder

The vertical position of the fish was studied by using a Kongsberg EK15 echosounder mounted from a small buoy facing downwards at about 0.5 m depth and 8 m from the net (see Fig. 2).

3. Results and discussion

3.1. Vertical swimming behaviour and DO conditions

The lice shielding skirt was installed one day prior to this study and was removed on the 6th of November due to welfare concerns for the fish as the gradual decrease in DO during the night became steeper in the morning.

The salmon's swimming depth observed in the echogram did not appear to be influenced by the skirt (Fig. 3). The salmon swam at deeper depths during the day and were more evenly distributed in the water column, while at night they moved closer to the surface and were more clustered. This diurnal pattern is consistent with previous studies of swimming behaviour (Oppedal et al., 2011), but not with the avoidance of the skirt volume observed in (Gentry et al., 2020). One potential reason for this could be the submerged metal halide lamp (OSRAM HQI-T 1000 W/D) which was mounted at 5 m depth, roughly 5 m from

the echogram and 3 m from the net. The light was turned on around sunset at 17:00, and off near sunrise 07:00. Such artificial light are known to attract salmon (Juell and Fosseidengen, 2004; Oppedal et al., 2007), and could therefore have had an effect on the behaviour seen in the echogram after sunset. However, Gentry et al. (2020) also used underwater lighting and unlike in this study, saw a difference in swimming depth in the cage with skirt and those without. It should be noted that in Gentry et al. (2020) a permeable skirt was used and it is possible that this skirt would facilitate different swimming behaviour than a non-permeable one, or that the swimming behaviour was influenced by the combination of local conditions and presence of skirt.

The DO level inside the cage and just outside the cage varied together throughout the period (Fig. 3). The DO at the oceanographic buoy was more consistent, however, it should be noted that it only recorded DO every hour. At some instances, the DO sensor inside the fish cage recorded higher levels than the sensors just outside of the cage. This is probably due to non-optimal placement of the DO-sensor outside of the cage. It is possible that when the current was heading towards N-E that the sensor was positioned in the wake of the cage as it was lowered just outside of the floating ring. The oceanographic buoy may therefore be a better reference point, despite low temporal resolution.

Roughly three hours prior to the lifting of the skirt the fish appear to spread more evenly throughout the cage volume, indicating an increase in activity as the sun rose. The sudden drop in DO from 8 AM could be due to onset of feeding and an increase in swimming activity as swimming speeds are generally higher during the day than at night (Oppedal et al., 2011), and an increase in swimming speed will increase the oxygen consumption (Hvas et al., 2017). Another possible reason for the drop in DO was the weak current during this period as the current appeared to be turning from N-E to S-W (Fig. 3).

A weaker drop in internal DO was seen the 7th of November around 9 AM when there was no skirt deployed (just after Case 2 in Fig. 3). Conditions were similar to the previous drop on the 6th of November, with weak current speed, current direction turning from N-E to S-W and the salmon more evenly spread vertically (Fig. 3). This drop was not as steep nor as severe as the previous day, when the skirt was deployed. It is possible that the combination of the turning current and the increased activity are the main causes for the observed drops in DO.

The results in Fig. 3 indicate that the presence of the skirt intensified the DO drop, but as the skirt had to be removed on the 6th of November, it is uncertain whether DO would have improved with time without the removal of the skirt. The DO just outside had begun to improve prior to the skirt removal, but there was no improvement seen on the sensors inside the cage at this time. The DO dropped to a minimum of 59% when the skirt was on, but did not drop below 69% when the skirt had been lifted. As smaller salmon are more susceptible to hypoxic conditions than large fish (Oldham et al., 2019) and the average water temperature was only 9 °C, it is unlikely that the salmon was harmed by the low DO. However, a DO in the range of 45–55% results in reduced aerobic metabolic capacity and swimming performance also in large salmon (Oldham et al., 2019). Had the DO level continued to decrease it may have posed a threat to the welfare of the salmon.

3.2. Lifting of the skirt

Echogram and DO were recorded during the entire deployment, and thereby also during the transition when the skirt was lifted. The skirt was lifted by use of a crane on a working boat S-W of Pos. 3 (Fig. 2). The skirt removal operation started at 09:48 and was completed by 10:35. During the procedure, the ADV-rig was placed in Pos. 3, and the average current speed in this position and in the DCP during this period are presented in Table 1. As explained previously, the low current speed in the DCP can be explained by the turning current, evident in the direction at the different depths (Table 1) and in the OB (Fig. 3).

When the removal of the skirt was initiated at 09:48 the DO inside the cage was 6.9 Mg/L, equivalent to 59% DO. The DO inside the cage started improving after 9 minutes, and the DO reached 9.5 Mg/L, that is 81%, inside the cage after another 20 minutes. At this point the DO just outside the cage was 84%. It took in total 30 minutes from the lifting was initiated to the DO level inside the cage reaching similar levels as outside and at the OB (Fig. 3).

3.3. Current flow through the cage

The main direction of the current at Hosnaøyan is controlled by the local bathymetry along the North-Easterly isobaths (Fig. 2). To isolate the influence the skirt had on the current flow, it was necessary to find episodes having similar incoming current conditions when the cage was with and without the skirt. Two 3-hour periods were deemed usable for this purpose, one for each condition. The criteria required that the current had to be moving along the depth isobaths (see Fig. 1) and the current had to be reasonably stable and unobstructed by surrounding farm structures. Hence only data where the average hourly current direction was aligned with the depth isobaths towards 45–90 degrees (North-East to East) was included. As an additional requirement the hourly current direction at the DCP had to deviate less than ±25 degrees from the current direction measured at the oceanographic buoy in the same period. The two relevant episodes are arranged into two cases and are listed in Table 2. These cases are used to investigate the current flow through the cage and speed reduction. Average weather conditions during these two cases were recorded at the oceanographic buoy and are listed in Table 3.

As evident from Fig. 3, the current velocity was not homogeneous with depth, and the DCP data indicates that the frame mooring may have been in line of sight of the sensor at 8 m depth. To compare the current outside the cage with the current inside, data from similar depths had to be applied. The reference for the velocity measured by the ADV at 2 m depth was the first cell of the DCP which averages over the depths from 2 to 3 m. While the reference velocity for the ADVs at 6 and 8 m was the average current speed recorded by the DCP from 5 to 6 m and from 6 to 7 m (Cell 4 and 5).

The current data from the DCP and the ADVs for the cases described in Table 2 are shown in Fig. 4 – 5. It is important to note that the ADV in Case 2 was placed in Pos. 2, roughly 8 m from the cage net, while the measurements for Case 1 were taken from the centre of the cage.

For Case 1 the direction of the current measured outside and inside the cage at 6 and 8 m depth were similar. The velocity direction within the skirt volume, recorded at 2 m depth, agreed with the main current direction but was more scattered. There was a weak positive vertical component in the ADVs towards the surface in Case 1. This trend was seen in all of the ADVs, but there was a larger variance for the ADV at 2 m depth (Fig. 4).

For Case 2 there was good agreement regarding direction of the current within the cage and in the DCP outside at all depths. Unlike Case 1, there was a weak downward component in the ADVs at 2 and 8 m depth, while the ADV at 6 m depth did not have a clear vertical component. It should be noted that in Case 2 the ADVs were positioned closer to the cage net, and the downward component could be an effect of its position.

It is unlikely that the positive vertical component in Case 1 was caused by vertical motion in the buoy as the waves were small at the

Table 1
Average horizontal speed and direction in DCP and ADV during lifting of the skirt between 09:48 and 10:55 on the 6th of November.

	DCP		ADV	
	Horizontal Speed [cm/s] (+/- STD)	Direction	Horizontal Speed [cm/s] (+/- STD)	Direction
2m	6.0 (±3.5)	10	6.5 (±2.9)	60
6m	5.3 (±2.8)	273	7.3 (±4.5)	286
8m	6.0 (±2.5)	250	7.8 (±4.7)	270

Table 2
Description of cases including ADV position and time intervals.

Case	ADV Position	Skirt condition	Date	Time interval
1	1	Down	5.11.2018	17:00 - 20:00
2	2	Lifted	7.11.2018	06:00 - 09:00

Table 3
Wave and current conditions measured at oceanographic buoy during cases described in Table 2. Following convention, North is defined as 0°, and East as 90°, with wave direction defined as the direction the wave is coming from, while current direction defined as the direction the current moving towards.

Wave				Current	
Case	Direction (deg)	Period (s)	Height (m)	Speed (m/s)	Direction (deg)
1	290	4.5	0.17	0.21	67
2	22.3	6.8	0.21	0.16	69

oceanographic buoy (Table 3). It is however possible that the high density of the fish in the upper layers during Case 1 (see echogram Fig. 3) could have resulted in the pumping effect, that is, the circular swimming pattern of the fish that causes an area with lower pressure drawing in water from below and above, described by Gansel et al. (2014) and Tang et al. (2017). However, the horizontal swimming behaviour was not observed during this study and it can thus not be confirmed that the fish were swimming in a torus shape. In Klebert and Su (2020) a vertical upwelling was seen in a shielded cage at 1.5 m depth within the skirt volume, but not beneath the skirt volume at 12 m depth. This upwelling was observed in a shielded cage independently if it was stocked or not (Klebert and Su, 2020). Hence the most likely explanation for the positive vertical current component during Case 1 is the skirt itself, and not the biomass.

3.4. Reduction in current speed

For Case 1 and 2, the reduction of the current speed through the cage

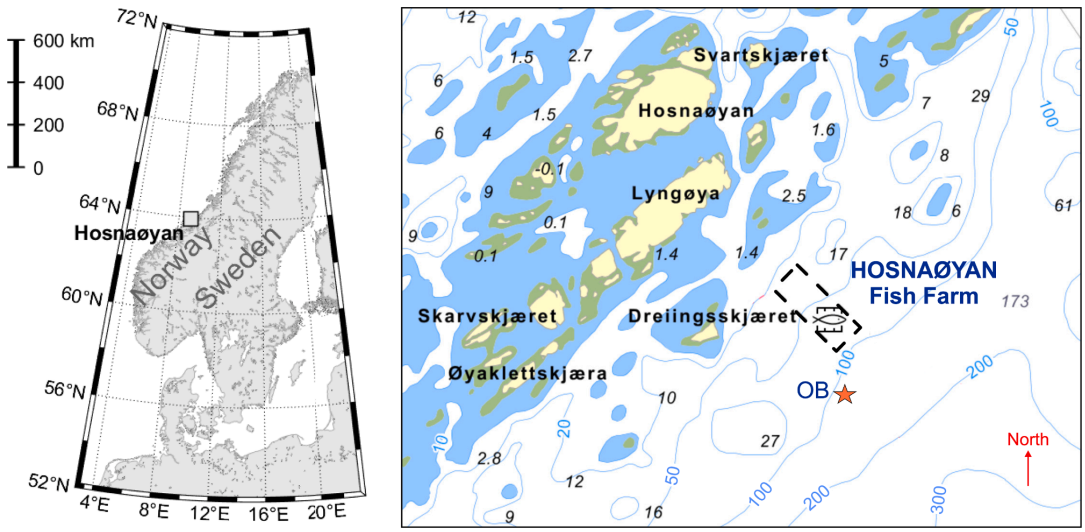

Fig. 1. Location of the fish farm at Hosnaøyan, where the measurement campaign was carried out in November 2018.

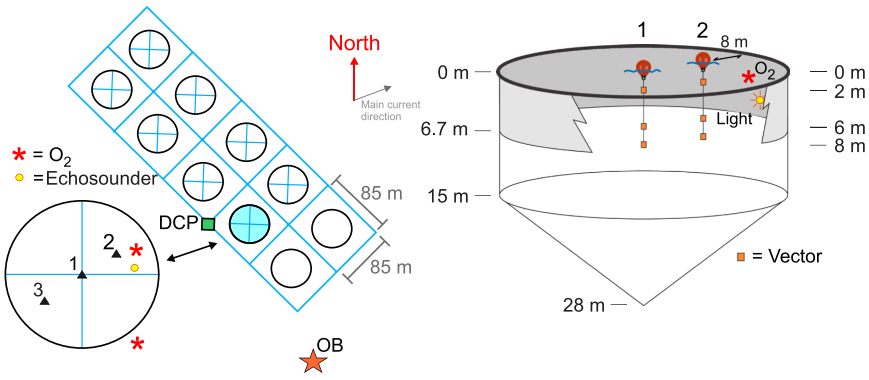

Fig. 2. Instrument placement at Hosnaøyan. The shaded cage was used as the experimental cage. The Aanderaa current profiler (DCP) was placed at the square marked DCP. The vector current meters (ADV) were moved between the two positions 1 and 2. Three ADVs were used, positioned at 2, 6 and 8 m depth suspended from a floater held in place with ropes attached to the cage ring. Two dissolved oxygen (DO) sensors were deployed, one on the inside also suspended from a floater 3 m from the cage ring, and one outside of the cage suspended from the cage ring (marked with *), both at 3 m depth. A light source was mounted at 5 m depth inside the cage. The position of the oceanographic buoy (OB) is marked with a star. The main current direction during Case 1 and 2 described in 3.3 is also marked just beneath the North sign.

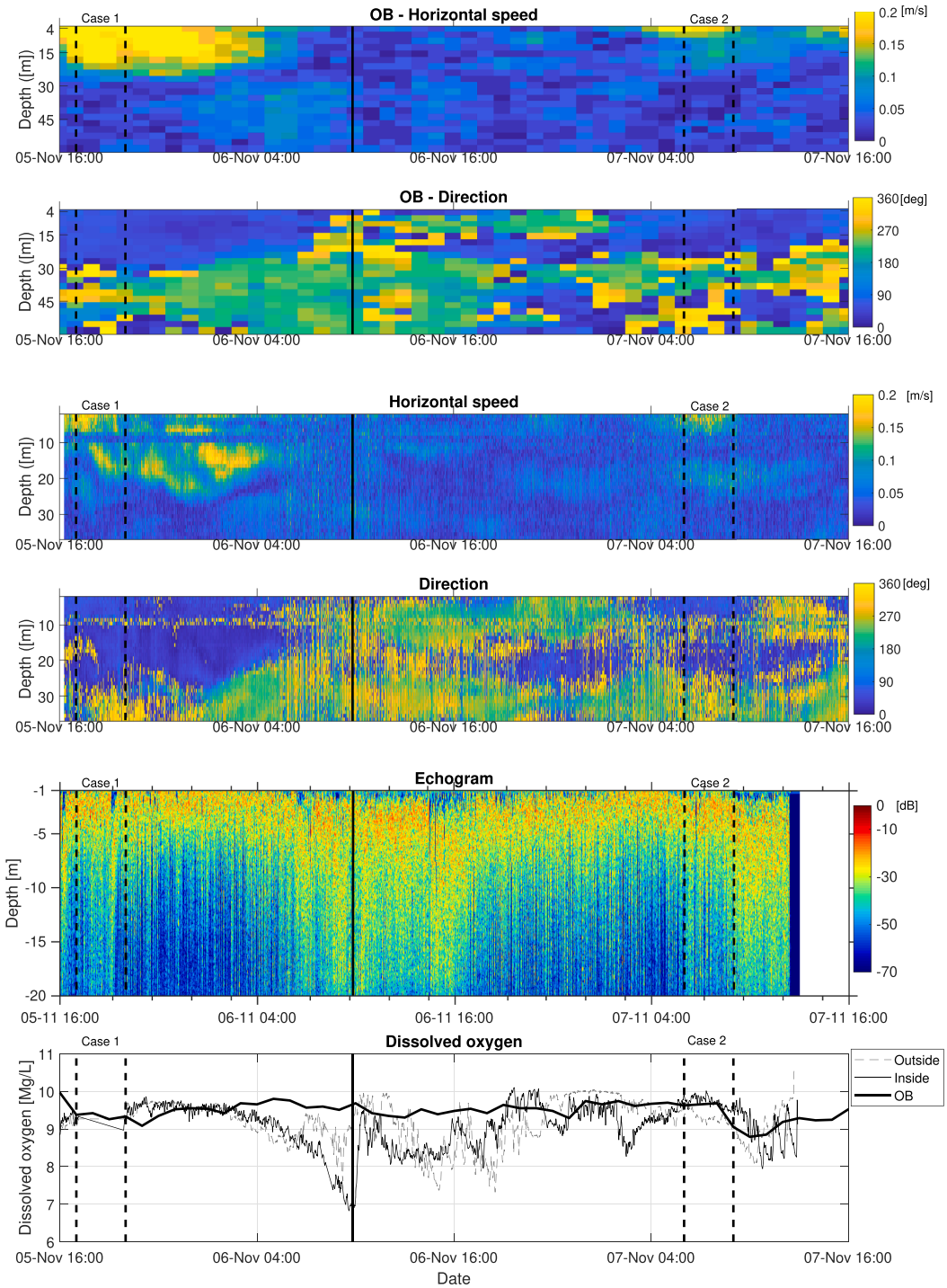

Fig. 3. Horizontal current speed and direction recorded for the entire period in the oceaographic buoy (OB) and in the DCP. Acoustic backscattering strength (S_v) measured in the echosounder. Dissolved oxygen in Mg/L recorded inside and outside of the cage, and at the OB. Case 1 and Case 2 are marked with dotted lines, while the vertical line marks the period where the lifting of the skirt was initiated.

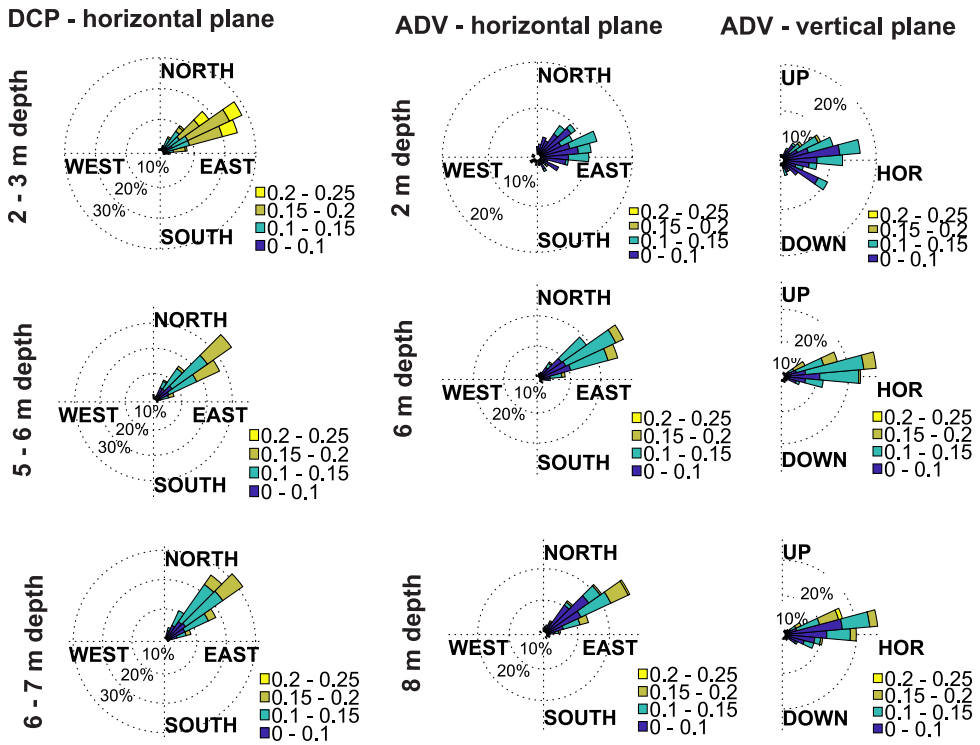

Fig. 4. Polarplots for current data for Case 1: With skirt down. The first column shows the horizontal speed in the DCP outside of the cage in [m/s], while the other two columns show the current data recorded by the ADVs in Pos. 1 inside the cage (centre of the cage, see Fig. 1). The middle column shows the horizontal speed, while the column to the right shows the current speed in the vertical plane inside the cage.

was calculated by comparing the ADVs with the measurements taken by the DCP outside the cage. The mean horizontal speed was calculated over 20-min intervals before the reduction in current speed was calculated. The average reduction in current speed for both cases are listed in Table 4.

The ADV placed at 2 m depth in the shielded cage had the highest mean reduction in current speed compared to the current in the DCP outside (56.9%, Table 4), and recorded the highest reduction of 86% during one of the 20-minute intervals when the current speed outside was 18.6 cm s^{-1}. This is a high reduction rate, but not unheard of for shielded cages. A reduction of 61% is observed downstream of an empty shielded cage (Klebert and Su, 2020). For empty unshielded cages the reduction from upstream to inside the cage is 21.5% (Klebert et al., 2015). This reduction is expected to be higher for stocked cages as in a stocked model-scale cage the reduction was 31%, although it was theorized that this increased reduction was due to biofouling (DeCew et al., 2013). A higher reduction was found in the unshielded stocked cage observed in Johansson et al. (2014), but the reduction varied with current speed, and within the same reference current speed. For instance, the reduction could vary from 0 to 50% when the current speed outside was 20 cm s^{-1} (Johansson et al., 2014). The stocking density in Johansson et al. (2014) was much lower at 6.2 kg m^{-3}, compared to 21.9 kg m^{-3} in this study, hence with the addition of a shielding skirt a reduction of 86% during a 20-minute interval is plausible.

The reduction at 2 m in Case 2 is higher than expected with a maximum reduction of 51% when the current speed was 14 cm s^{-1} outside. The high reduction rate in Case 2 could be influenced by the rig's position, as a near linear reduction in current speed is seen through unshielded and empty cages in experiments and simulations (Klebert et al., 2015; Patursson, 2008; Winthereig-Rasmussen et al., 2016). It is possible that a similar effect has occurred, despite the cage being stocked, hence the reduction for Case 2 might have been lower had the ADV-rig been placed in the centre. This is also valid for the sensors at 6 and 8 m depth. However, this effect does not appear for the sensor at 8 m depth, with Case 2 having a lower reduction rate than Case 1. It is therefore more likely that the high reduction at 2 m in Case 2 is due to the biomass. From the echosounder it appears the highest density of fish during Case 1 and 2 were close to the surface in the top 5 m (Fig. 3). The average reduction in Case 2 at 2 m was also close to that of DeCew et al. (2013) of 32%, however it should be noted that DeCew et al. (2013) used a model-scaled cage with fewer fish.

The reduction at 6 and 8 m in Case 1 and 2 were slightly lower than the reduction of 21.5% in Klebert et al. (2015) despite the cage being stocked. The low reduction at 6 m depth in Case 1 could be explained by the current flow being forced underneath the skirt and into the cage, as seen in dye experiments (Frank et al., 2015) and simulations (Lien et al., 2015). When pressed underneath the skirt, the water accelerates (Lien et al., 2015), which may have caused the lower reduction rate when the skirt was deployed.

The low average reduction rates at 6 and 8 m during Case 2 however could be accounted to the large variation in reduction, as seen by the standard deviation (Table 4), or due to low current speeds outside of the cage. As average current decreased with depth, the strongest currents were those at 2 m depth. This could explain why the reduction in speed decreases with depth for Case 2. It should also be noted that the 21.5% in Klebert et al. (2015) was recorded at the Faroe Islands where the minimum current speed was 0.15 m/s and the maximum over 0.5 m/s. Higher current velocities will result in larger deformations, and thereby

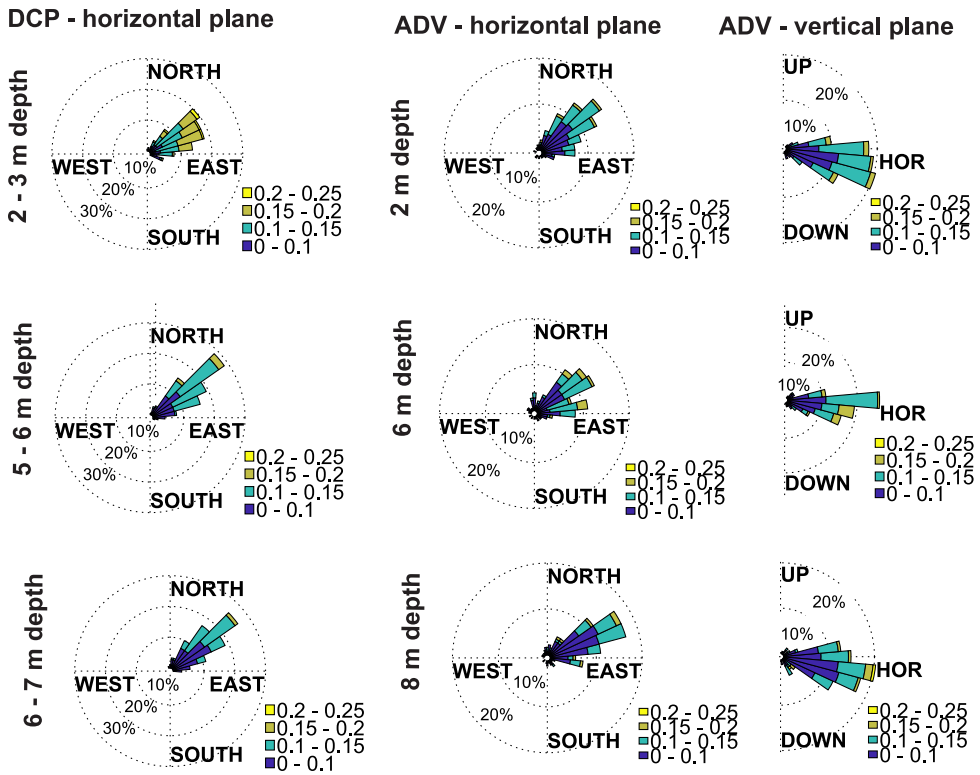

Fig. 5. Polarplots for current data for Case 2: Without skirt. The first column shows the horizontal speed in the DCP outside of the cage in [m/s], while the other two columns show the current data recorded by the ADVs in Pos. 2 inside the cage (see Fig. 1). The middle column shows the horizontal speed, while the column to the right shows the current speed in the vertical plane inside the cage.

Table 4
Mean reduction through cage for each depth for the two cases with and without skirt. Readers should note that the ADV in Case 1 is located in position 1, while it is position 2 in Case 2.

	Mean reduction [%] (± STD)	
Depth	Case 1 (with skirt)	Case 2 (without skirt)
2m	56.9 (± 21.4)	32.0 (± 12.3)
6m	10.4 (± 15.1)	17.9 (± 19.5)
8m	18.6 (± 16.0)	14.6 (± 18.0)

increased solidity of the cage net (Lader et al., 2008). The results from this study may therefore not be applicable at higher velocities.

4. Conclusion

In this study data was collected from a fully stocked cage with high biomass. The current inside the shielded cage had a positive vertical component towards the surface at all depths in the centre of the cage, which was not the case when the skirt was removed and the ADVs were placed closer to the net wall. The reduction in current speed from outside to inside of the cage agree fairly well with previous findings beneath the skirt volume. Only the ADV at 2m depth showed a clear effect of the skirt, with an average reduction of 56.9% when the skirt was deployed in Case 1 compared to 32% when the skirt was removed in Case 2.

There was no clear distinction in behaviour of the salmon during the study when the skirt was deployed. The DO varied throughout the study, however the sudden drop in DO when the skirt was deployed can be explained by the obstruction of the current by the skirt, increased fish activity and low current speed from a non-optimal direction. When the skirt was removed the DO improved from 59% to 81% within 30 minutes despite weak currents, exemplifying the importance of continuous monitoring of DO when using skirts.

CRediT authorship contribution statement

Kristbjörg Edda Jónsdóttir: Conceptualization, Investigation, Data curation, Visualization, Writing - original draft. **Zsolt Volent:** Conceptualization, Investigation, Funding acquisition, Project administration, Writing - original draft. **Jo Arve Alfredsen:** Writing - review & editing.

Declaration of Competing Interest

The authors declare that they have no known competing financial interests or personal relationships that could have appeared to influence the work reported in this paper.

Acknowledgement

This study is part of the project “Shielding skirt as a method for prevention and control of salmon lice infestation - improving knowledge about environmental conditions for increase in efficiency and reduction of risk (SKJERMTEK)” (project number: 901396) funded by The Norwegian Seafood Research Fund (FHF). KEJ received funding from the

RACE research grant program funded by SINTEF Ocean. We are thankful for access to equipment from SINTEF ACE, and SalMar AS for access to their site.

References

Abolofia, J., Asche, F., Wilen, J.E., 2017. The cost of lice: quantifying the impacts of parasitic sea lice on farmed salmon. Mar. Resour. Econ. 32 (3), 329–349.

Bi, C.-W., Zhao, Y.-P., Dong, G.-H., Xu, T.-J., Gui, F.-K., 2013. Experimental investigation of the reduction in flow velocity downstream from a fishing net. Aquacult. Eng. 57, 71–81.

Birjandi, A.H., Bibeau, E.L., 2011. Improvement of acoustic doppler velocimetry in bubbly flow measurements as applied to river characterization for kinetic turbines. Int. J. Multiphase Flow 37 (8), 919–929.

DeCew, J., Fredriksson, D., Lader, P., Chambers, M., Howell, W., Osienki, M., Celikkol, B., Frank, K., Høy, E., 2013. Field measurements of cage deformation using acoustic sensors. Aquacult. Eng. 57, 114–125.

Frank, K., Gansel, L., Lien, A., Birkevold, J., 2015. Effects of a shielding skirt for prevention of sea lice on the flow past stocked salmon fish cages. J. Offshore Mech. Arct. Eng. 137 (1).

Gansel, L.C., Plew, D.R., Endresen, P.C., Olsen, A.I., Misimi, E., Guenther, J., Jensen, Ø., 2015. Drag of clean and fouled net panels–measurements and parameterization of fouling. PLoS ONE 10 (7), e0131051.

Gansel, L.C., Rackebrandt, S., Oppedal, F., McClimans, T.A., 2014. Flow fields inside stocked fish cages and the near environment. J. Offshore Mech. Arct. Eng. 136 (3).

Geitung, L., Oppedal, F., Stien, L.H., Dempster, T., Karlsbakk, E., Nola, V., Wright, D.W., 2019. Snorkel sea-cage technology decreases salmon louse infestation by 75% in a full-cycle commercial test. Int. J. Parasitol. 49 (11), 843–846.

Gentry, K., Bui, S., Oppedal, F., Dempster, T., 2020. Sea lice prevention strategies affect cleaner fish delousing efficacy in commercial atlantic salmon sea cages. Aquac Environ Interact 12, 67–80.

Goring, D.G., Nikora, V.I., 2002. Despiking acoustic doppler velocimeter data. J. Hydraul. Eng. 128 (1), 117–126.

Heuch, P.A., Parsons, A., Boxaspen, K., 1995. Diel vertical migration: a possible host-finding mechanism in salmon louse (Lepeophtheirus salmonis) copepodids? Can. J. Fish. Aquat.Sci. 52 (4), 681–689.

Hevrøy, E., Boxaspen, K., Oppedal, F., Taranger, G., Holm, J., 2003. The effect of artificial light treatment and depth on the infestation of the sea louse lepeophtheirus salmonis on atlantic salmon (Salmo Salar L.) culture. Aquaculture 220 (1–4), 1–14.

Huse, I., Holm, J., 1993. Vertical distribution of atlantic salmon (salmo salar) as a function of illumination. J. Fish Biol. 43, 147–156.

Hvas, M., Folkedal, O., Imsland, A., Oppedal, F., 2017. The effect of thermal acclimation on aerobic scope and critical swimming speed in atlantic salmon, salmo salar. J. Exp. Biol. 220 (15), 2757–2764.

Iversen, A., Hermansen, Ø., Nystøyl, R., Hess, E.J., 2017. Kostnadsutvikling i lakseoppdrett-med fokus på fôr-og lusekostnader. Nofima rapportserie.

Johansson, D., Juell, J.-E., Oppedal, F., Stiansen, J.-E., Ruohonen, K., 2007. The influence of the pycnocline and cage resistance on current flow, oxygen flux and swimming behaviour of atlantic salmon (salmo salar l.) in production cages. Aquaculture 265 (1–4), 271–287.

Johansson, D., Laursen, F., Fernö, A., Fosseidengen, J.E., Klebert, P., Stien, L.H., Vågseth, T., Oppedal, F., 2014. The interaction between water currents and salmon swimming behaviour in sea cages. PLoS ONE 9 (5), e97635.

Juell, J.-E., Fosseidengen, J.E., 2004. Use of artificial light to control swimming depth and fish density of atlantic salmon (salmo salar) in production cages. Aquaculture 233 (1–4), 269–282.

Klebert, P., Lader, P., Gansel, L., Oppedal, F., 2013. Hydrodynamic interactions on net panel and aquaculture fish cages: a review. Ocean Eng. 58, 260–274.

Klebert, P., Patursson, Ø., Endresen, P.C., Rundtop, P., Birkevold, J., Rasmussen, H.W., 2015. Three-dimensional deformation of a large circular flexible sea cage in high currents: field experiment and modeling. Ocean Eng. 104, 511–520.

Klebert, P., Su, B., 2020. Turbulence and flow field alterations inside a fish sea cage and its wake. Appl. Ocean Res. 98, 102113.

Lader, P., Dempster, T., Fredheim, A., Jensen, Ø., 2008. Current induced net deformations in full-scale sea-cages for atlantic salmon (Salmo Salar). Aquacult. Eng. 38 (1), 52–65.

Lien, A.M., Høy, E., 2011. Skjørt for Skjerming mot lus i Laksemerd. Technical Report. SINTEF Fiskeri og Havbruk AS, Brattørkaia 17c, 7010, Trondheim Norway.

Lien, A.M., Stien, L.H., Grøntvedt, R., Frank, K., 2015. Permanent skjørt for redusering av luspåslag på laks. Technical Report. SINTEF Fiskeri og Havbruk AS, Brattørkaia 17c, 7010, Trondheim Norway.

Lien, A.M., Volent, Z., Jensen, Ø., Lader, P., Sunde, L.M., 2014. Shielding skirt for prevention of salmon lice (Lepeophtheirus Salmonis) infestation on atlantic salmon (Salmo Salar L.) in cages–a scaled model experimental study on net and skirt deformation, total mooring load, and currents. Aquacult. Eng. 58, 1–10.

Oldham, T., Nowak, B., Hvas, M., Oppedal, F., 2019. Metabolic and functional impacts of hypoxia vary with size in atlantic salmon. Comparative Biochemistry and Physiology Part A: Molecular & Integrative Physiology 231, 30–38.

Oppedal, F., Dempster, T., Stien, L.H., 2011. Environmental drivers of atlantic salmon behaviour in sea-cages: a review. Aquaculture 311 (1–4), 1–18.

Oppedal, F., Juell, J.-E., Johansson, D., 2007. Thermo-and photoregulatory swimming behaviour of caged atlantic salmon: implications for photoperiod management and fish welfare. Aquaculture 265 (1–4), 70–81.

Oppedal, F., Samsing, F., Dempster, T., Wright, D.W., Bui, S., Stien, L.H., 2017. Sea lice infestation levels decrease with deeper 'snorkel'barriers in atlantic salmon sea-cages. Pest Manag. Sci. 73 (9), 1935–1943.

Patursson, Ø., 2008. Flow through and around fish farming nets. Ocean Engineering, University of New Hampshire, Durham, NH03824, USA.

Rasmussen, H.W., Patursson, Ø., Simonsen, K., 2015. Visualisation of the wake behind fish farming sea cages. Aquacult. Eng. 64, 25–31.

Remen, M., Aas, T.S., Vågseth, T., Torgersen, T., Olsen, R.E., Imsland, A., Oppedal, F., 2014. Production performance of atlantic salmon (Salmo Salar L.) postsmolts in cyclic hypoxia, and following compensatory growth. Aquac. Res. 45 (8), 1355–1366.

Stien, L.H., Nilsson, J., Hevrøy, E.M., Oppedal, F., Kristiansen, T.S., Lien, A.M., Folkedal, O., 2012. Skirt around a salmon sea cage to reduce infestation of salmon lice resulted in low oxygen levels. Aquacult. Eng. 51, 21–25.

Tang, M.-F., Xu, T.-J., Dong, G.-H., Zhao, Y.-P., Guo, W.-J., 2017. Numerical simulation of the effects of fish behavior on flow dynamics around net cage. Appl. Ocean Res. 64, 258–280.

Winthereig-Rasmussen, H., Simonsen, K., Patursson, Ø., 2016. Flow through fish farming sea cages: comparing computational fluid dynamics simulations with scaled and full-scale experimental data. Ocean Eng. 124, 21–31.

Paper D

Characteristic current flow through a stocked conical sea-cage with permeable lice shielding skirt

Jónsdóttir, K. E., Klebert, P., Volent, Z., Alfredsen, J. A., 2021. Characteristic current flow through a stocked conical sea-cage with permeable lice shielding skirt. Ocean Engineering, 223, 108639

Ocean Engineering 223 (2021) 108639

Contents lists available at ScienceDirect

Ocean Engineering

journal homepage: www.elsevier.com/locate/oceaneng

Characteristic current flow through a stocked conical sea-cage with permeable lice shielding skirt

Kristbjörg Edda Jónsdóttir [a,*], Pascal Klebert [b], Zsolt Volent [b], Jo Arve Alfredsen [a]

[a] Norwegian University of Science and Technology, Department of Engineering Cybernetics, NO-7491, Trondheim, Norway
[b] SINTEF Ocean, NO-7465, Trondheim, Norway

ARTICLE INFO

Keywords:
Conical sea cage
Current flow
Atlantic salmon
Permeable lice shielding skirt

ABSTRACT

The characteristic current flow field around a 55 m deep full-scale stocked conical Atlantic salmon sea-cage equipped with a 10 m permeable skirt was studied experimentally using acoustic Doppler velocimeters and profilers. The weakest current speed was inside the cage at 6 m depth and the highest reduction downstream was recorded behind the shielded volume. Downstream of the cage the reduction in speed became little to non-existing at 22 m depth, probably due to the decreasing diameter of the cage with depth. To reduction in current speed through the cage was compared with estimated reduction from theoretical expressions. The results compared reasonably well downstream of the shielded cage, while the reduction inside the cage was higher than the estimates. The difference in current flow field behind a conical cage compared with a cylindrical cage may have implications for the dispersal of waste, feed pellets and microorganisms from the cage influencing the benthic impact of the farm.

1. Introduction

The flow field characteristics around and through a sea cage govern the distribution of feed, waste and dissolved oxygen in the cage, and the sedimentation process that occurs under and behind the cage. How the current flows through and around fish cages is determined by the farm layout (Rasmussen et al., 2015), local topography, flow conditions at the site (Klebert et al., 2013), biomass within the cage (Klebert et al., 2013; Gansel et al., 2014; Klebert and Su, 2020) and the cage structure itself (Klebert et al., 2015). Most cages used in Norway are of the "gravity" type cages, which have a surface collar structure from which a net is suspended. These nets are often weighed down by a sinker ring, resulting in the net having a cylindrical shape above this ring, and a conical shape beneath it.

As the current passes through the net a reduction in current speed occurs (see for example: Løland 1993; Patursson 2008; Klebert et al., 2013). The reduction in current speed in combination with turbulence induced by the net structure has a direct impact on the dispersal of particle and micro-organisms such as pathogens and zooplankton (Klebert and Su, 2020). The reduction in speed increases with solidity which can be due to biofouling (Bi et al., 2013; Gansel et al., 2015), biomass in cage (Klebert and Su, 2020) or increasing inclination angle between the net and vertical direction (Bi et al., 2013; Zhao et al., 2015). This increase in inclination angle can be caused by the cage deformation, as when exposed to strong currents the cage wall upstream and downstream are deformed, and the bottom net is lifted upwards (Fredheim, 2005; Lader et al., 2008; Lien et al., 2014; Klebert et al., 2015).

The reduction in current speed is further enhanced with the use of lice shielding skirts (Frank et al., 2015). The high cost of delousing treatments (Abolofia et al., 2017; Iversen et al., 2017) has led to an increased use of lice shielding skirts as a preventative measure against the salmon lice. Shielding skirts attempt to reroute the upper water column around the cage which has a higher lice density than the deeper levels (i.e. Huse and Holm 1993; Heuch et al., 1995; Hevrøy et al., 2003; Oppedal et al., 2017; Geitung et al., 2019). These skirts are usually made of tarpaulin, which block the current, and some sites experience low DO levels when using such skirts (Stien et al., 2012), which reduces feed intake and specific growth rates (Remen et al., 2014). To counter this, permeable skirts have been introduced. Results from sites applying permeable skirts indicate good DO levels, with a minimum value of 70% DO over a 3-month period (Stien et al., 2018) and no impact on welfare status of the salmon (Bui et al., 2020).

The current flow through normal gravity cages, both with and without skirts, have been studied both through experimental work and

* Corresponding author.
E-mail addresses: kristbjorg.jonsdottir@ntnu.no, kristbjorg.jonsdottir@sintef.no (K.E. Jónsdóttir).

https://doi.org/10.1016/j.oceaneng.2021.108639
Received 1 October 2020; Received in revised form 12 January 2021; Accepted 13 January 2021
Available online 2 February 2021

simulations (i.e. Bi et al., 2013; Zhao et al., 2015; Klebert et al., 2013). However, in recent years there has been an increasing prevalence of conical nets (written communication Dybing, Egersund group, 08.09.2020). Little documentation has been obtained on the current flow around these nets so far, but it is necessary to study the current flow characteristics around these cages to understand the farm's biological footprint, and to ensure that good water quality and fish welfare is maintained. The same holds valid for cages which are equipped with permeable skirts. Therefore, in this study, the current flow field around and through a conical full-scale commercial salmon cage equipped with a permeable shield was studied. Current speed and direction were measured both upstream, downstream and inside the cage. The reduction in current speed from upstream to inside, and from upstream to downstream were also compared with expected reduction when using analytical expressions developed for plane nets.

2. Material and methods

2.1. Site description

The measurement campaign was performed 2–5 July 2019 at Fornes farm owned and operated by Nordlaks Oppdrett AS located in Øksfjorden, Lofoten islands, Norway (68°24′35.5″N, 15°25′44.8″E, Fig. 1), and is placed in a fjord which has a narrow strait to the North leading into a larger basin with depths up to 104 m. The farm consists of nine cages arranged in a single row from West to East, and spans an area with a depth of 100 m. Data were collected from the third westernmost cage, with stocked cages at either sides of the cage.

All cages at Fornes had a circumference of 160 m and were equipped with conical nets (Fig. 1). The net had a solidity of 0.16 and was 55 m deep with a concrete weight of 2.4 tonnes in water attached to the tip of the cone. The shielding skirt applied was a permeable canvas lice skirt (Norwegian Weather Protection, Frekhaug, Norway) with a solidity of 51%, mesh opening of 350 × 350 μm and a depth of 10 m. The skirt was weighted with 2 kg/m lead rope at the bottom and installed as a cylinder around the conical net roughly 10 days prior to measurements were carried out. The skirt is one piece of fabric installed with a 10 m overlap. The biomass in the cage during the experiment was 750 tonnes, with 191 310 fish with an average weight of 3.8 kg.

2.2. Equipment description: ADV and DCP

Current speed and direction outside the cage were recorded using two current profilers attached to anchoring buoys on both sides of the cage, pointing downwards with a vertical resolution (cell size) of 1 m. To the South-West of the cage, in position B (Fig. 1), an Aanderaa SeaGuard II Doppler current profiler (DCP) measured continuously with a sampling frequency of 0.5 Hz. The DCP had a velocity accuracy of 0.3 cm/s or ±1% of reading, with a velocity resolution of 0.1 cm/s. The data were averaged and stored every minute. To the North-East of the cage, in position A (Fig. 1), a Nortek Aquadopp current profiler 400 MHz (ADCP) was used. The ADCP had a velocity accuracy of ±0.5 cm/s or ±1% of measured value, and a horizontal and vertical velocity precision of 0.7 cm/s and 2.2 cm/s, respectively. The data were averaged over every 3rd minute. As buoy mounted DCPs can experience bias (Mayer et al., 2007), the first depth cell was excluded from the data set.

Inside the cage the current velocity was measured using Nortek Vector Acoustic Doppler Velocimeters (ADV) with a sampling rate of 8 Hz, with 120 samples per burst and a burst interval of 60 s. The sampling volume was 0.18 cm^3 placed 0.15 m from the probes, and the sensor had an accuracy ±0.5% of measured value ±1 mm/s, velocity precision typical 1% of velocity range (at 16 Hz). The ADVs were suspended from a buoy at 3, 6, 9 and 12 m depths and placed in the centre of the cage, position C in Fig. 1. Given the depth of the site it is assumed that the influence from bathymetry on the measured current speed is negligible.

2.3. Flow velocity reduction

Different studies have been conducted regarding the velocity reduction behind net panels (reviewed in Klebert et al., 2013) in model cages (Kristiansen and Faltinsen, 2015) or numerically (Lee et al., 2008; Bi et al., 2014; Kim et al., 2014). Only a few are performed at full scale in commercial cage with fish (Johansson et al., 2007; Klebert et al., 2015; Klebert and Su, 2020); the latest being conducted in circular cages with or with skirt. In this study, a more complex conical cage geometry is investigated. With a twine thickness (d) of 2.7 mm and a mesh size (s) of

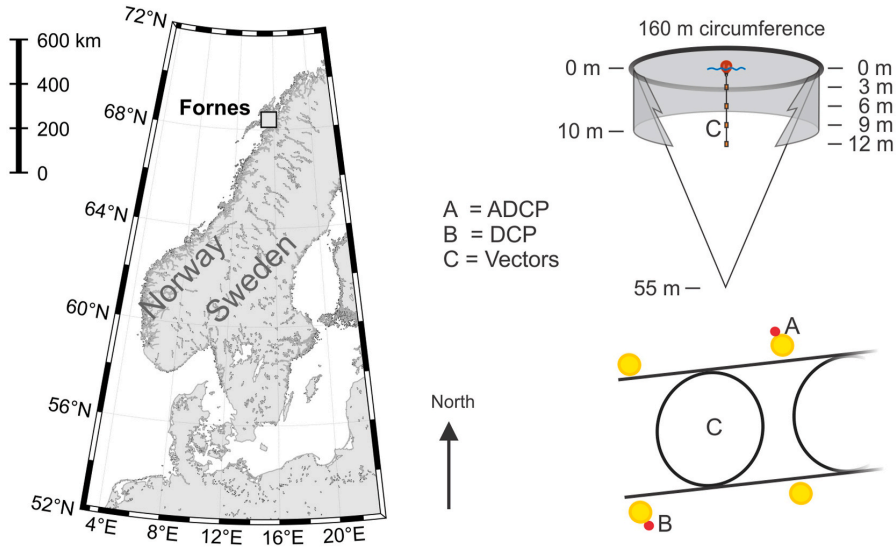

Fig. 1. Left: Location of the fish farm at Fornes were the measurements were carried out. Right: Shape and dimensions of the cage and shielding skirt studied, and the location of sensors.

29 mm, the calculated net solidity ($Sn = 2d/s$) is 0.19. To estimate the velocity flow reduction inside the cage and in its wake the expressions by Løland (1993) and Føre et al. (2020) are used. Løland (1993) proposed a theoretical expression for the non-dimensional velocity reduction factor r behind a net panel based on the solidity (Sn) of the nets: $r = u_w/U_0$ where u_w is the flow velocity in the wake of the cage and U_0 is the free-stream velocity. The velocity reduction factor r is defined as $r = 1 - 0.46C_d$, where C_d is the drag of the netpanel calculated from Sn with the following expression $C_d = 0.04 + (-0.04 + 0.33S_n + 6.54S_n^2 - 4.88S_n^3)$. By performing measurements with net panels with solidity (Sn) ranging from 0.15 to 0.32 Føre et al. (2020) found that an improved expression for r was: $r = 1.02 - 0.84S_n$. In the following the different formulations for the velocity flow reduction are represented together with the measurements data at different location.

3. Results and discussion

3.1. Preprocessing of data

Velocity spikes caused by Doppler noise, signal aliasing and disturbances from the fish as the cage was fully stocked, were removed by filtering the raw data from the ADVs using the improved phase space filter (Goring and Nikora, 2002) for bubbly flows (Birjandi and Bibeau, 2011). Velocity spikes were not replaced, the ADV data were averaged over 1 min and if more than 50% of the data in a minute had been removed, the entire minute was excluded from further analyses.

To establish the characteristic of the flow field around a conical net, a stable incoming current was necessary hence certain critera were set for the incoming current. Previous measurements at the Fornes farm site in accord with NS9415 (Standard Norway, 2009) found that the main current direction was towards North-East (45–60°), and South-West (210–225°), and that the site was influenced by the tidal current. The ADCP and DCP data agreed well with this (see Fig. 2 and Fig. 3). The data from each sensor was therefore averaged over 30 min intervals and if the current direction in the upstream sensor was between 30° and 75° or between 200° and 245°, the sample was categorized as Northward or Southward, respectively.

In addition to these requirements, the standard deviation in the upstream sensor during each 30 min sample could not exceed 30°, the averaged horizontal speed had to be over 0.05 m/s and only dates where there was little to no signs of density stratifications in the water column were considered. The criteria set for the current upstream of the cage are summarised in Table 1.

The current had a clear semi-diurnal tidal pattern (Figs. 2 and 3), with the Nortek ADCPs current direction measurements appearing less structured than the Aanderaa's DCP. This is partially due to the direction fluctuating around 0/360°, but also due to the Aanderaa DCP having a higher temporal resolution and being positioned downstream when the current was moving Southwards making it appear more structured throughout the period (Figs. 2 and 3). The stratification of the water column is evident in Fig. 3 displaying the speed of the Aanderaa's DCP, for instance on the 3rd of July when the top layers had a lower speed than the deeper layers. CTD profiles were also taken irregularly throughout the campaign and showed a clear pycnocline on the 3rd of July at 7.5 m depth that gradually moved up to 3 m depth on the 4th before disappearing on the 5th. CTD data is published in Jónsdóttir et al. (2020). It was therefore only the later periods of the 4th of July and the 5th of July that were relevant for establishing a more or less homogenous current flow field around the conical cage.

The requirements resulted in four data series with the current heading towards the south with a minimum and maximum average direction of 216° and 244°, and seven data series with the current heading towards the north with a minimum and maximum average direction of 32° and 75°. The relevant periods are listed in Table 2.

For the ADVs there was an additional condition for the relevant sampling periods. If more than 16 min of the 30 min averaged over in a period had been removed when using the phase space filter for bubbly flow, the sample was removed from further analysis. This requirement was set to each individual depth, hence some samples have no data from certain depths (see Figs. 4 and 5).

The short duration of this study and the limited number of periods satisfying the criteria should be noted. However, given the depth at Fornes, the clear tidal influence of the site and the farm layout, the results give an clear indication of how the current flow around a conical cage differs from that of a cylindrical cage.

3.2. Current flow during selected periods

The average current speed and direction in all sensors were calculated for the relevant periods listed in Table 2 and are presented in Figs. 4 and 5. The current speed inside the cage at all depths were lower than the speed measured upstream of the cage, but was not necessarily higher than the speed measured downstream of the cage (Figs. 4 and 5).

The maximum average current speed at the inside of the cage was 6 cm/s, while the maximum average current speed outside was 15 cm/s. The current direction inside of the cage did not always agree with the current direction upstream and downstream of the cage. The current downstream and upstream were in relatively good agreement except at 3 m when the current was heading southwards, and a slight disagreement in some of the cases at 3 m and 12 m when heading Northwards. However, this discrepancy could be influenced by the fluctuation around

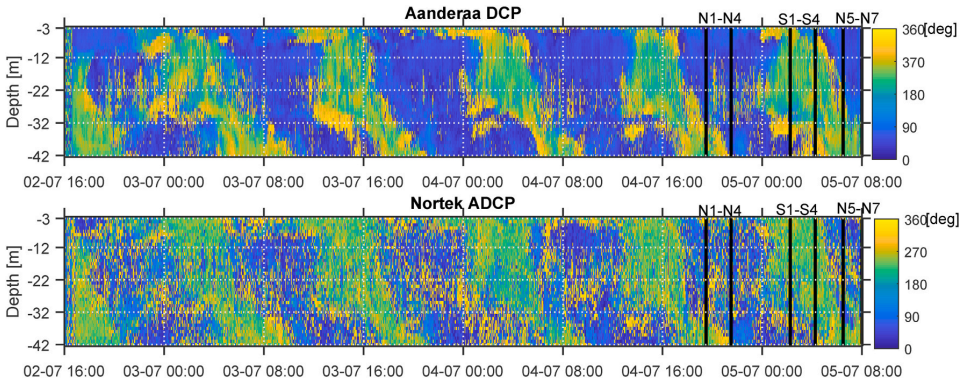

Fig. 2. Current direction recorded by the DCP and ADCP throughout the entire period, respectively. Position of sensors are shown in Fig. 1. Periods described in Table 2 are marked with vertical lines.

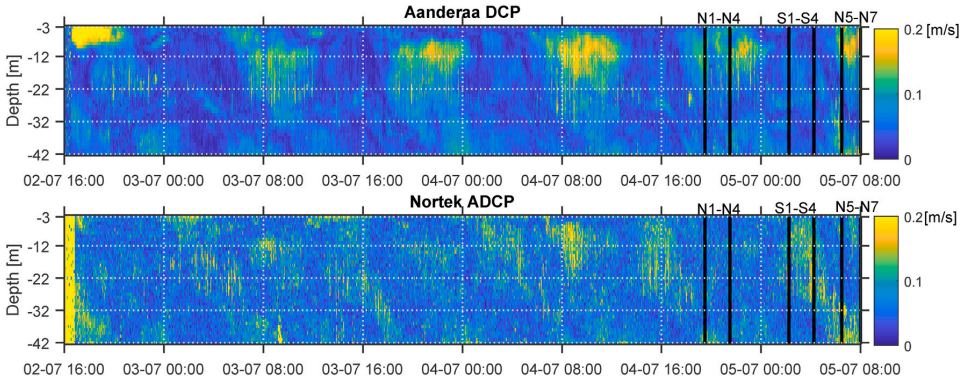

Fig. 3. Horizontal current speed recorded by the DCP and ADCP throughout the entire period, respectively. Position of sensors are shown in Fig. 1. Periods described in Table 2 are marked with vertical lines.

Table 1
Criteria for each 30-min averaged sample current upstream of the cage to be included in further analysis.

	Criteria
Northward	$30° \leq$ direction $\leq 75°$
Southward	$200° \leq$ direction $\leq 245°$
Current speed	> 0.05 m/s
Std. direction	$\leq 30°$

Table 2
Periods where the upstream current has passed the set requirements summarised in Table 1.

Northward		Southward	
Name	Date and Time	Name	Date and Time
N1	04-07-19 19:30–20:00	S1	05-07-19 02:15–02:45
N2	04-07-19 20:00–20:30	S2	05-07-19 02:45–03:15
N3	04-07-19 20:30–21:00	S3	05-07-19 03:15–03:45
N4	04-07-19 21:00–21:30	S4	05-07-19 03:45–04:15
N5	05-07-19 06:30–07:00		
N6	05-07-19 07:00–07:30		
N7	05-07-19 07:30–08:00		

0/360°.

The difference in direction between inside and upstream of the cage could be caused by the recirculation pattern seen in Lien et al. (2014). As this pattern was not observed when fish was present in a shielded cage (Klebert and Su, 2020), it is however more likely that this variation in direction was caused by the very low current speeds inside the cage.

3.3. Flow through cage and net

To compare data from different sensors the characteristic horizontal current speed was established by averaging the horizontal speed in each sensor over all sample periods defined in Table 2 for each depth. To ensure that there were no topographic effects or other effects dependent on the direction of the current, the two groups Northwards and Southwards were preserved. The characteristics horizontal current speed was then normalized using the maximum averaged horizontal current speed recorded upstream independent of depth (Fig. 6).

The results from this study differ from those observed in unshielded cylindrical cages. The current through an unshielded cylindrical cage had a linear reduction from the sensor upstream to the sensor downstream (Klebert et al., 2015). Downstream of the cage there was a reduction in current speed the entire depth of the cage, and below the cage there was an acceleration of the current (Klebert et al., 2015). No such acceleration could be observed in this study due to the spatial limitation of the sensors, but it is unlikely that any such acceleration would have occurred at Fornes due to its conical shape.

In the upper 22 m of the 55 m deep conical cage there was a clear reduction in current speed downstream independently of current direction, similar to that observed for cylindrical cages. Below 22 m however there was no visible blocking effect from the cage (Fig. 6). This is likely due to the tapered shape and smaller diameter of the cage at that depth, which is only 28 m. The reduction in speed downstream was at its highest in the upper 10 m of the cage. This is particularly clear for the current that was heading Southwards, which has an increase in normalized current speed from 9 m depth and deeper. This pattern was not as evident in the downstream current heading Northwards, but the highest reduction rates were still within the top 10 m. These results indicate that the permeable skirt enhanced the reduction of current flow downstream of the cage.

The current flow upstream also appear to be influenced by the skirt with a non-linear response upstream of the skirt volume and a near linear response from 9 m when the current was heading Northward (Fig. 6). The skirt could have influenced the current upstream by decelerating the incoming current flow. As the effect was not constant upstream of the skirt, the slower velocity closer to the surface could have been caused by the stratification at Fornes. The hydrographic conditions at Fornes are detailed in Jónsdóttir et al. (2020), and describe a pycnocline that broke down from the 2nd to the 5th of July. On the 4th of July a weak pycnocline was present at roughly 2 m depth with homogeneous water below, while the water column was homogeneous on the 5th. It was assumed that the pycnocline would have little effect on the characteristic current flow as the normalized current speed was determined by averaging over data from late on 4 th and the 5 th of July. However, given the position of the pycnocline, it is possible that it had some effect on the current speed at 3 m depth.

The increase in current speed downstream of the cage at 9 m when the current was heading southwards could be due to deformations of the skirt. When the current speed is sufficiently high the upstream section of the skirt can creep upwards as it is pushed into the cage, while the downstream section will lift and stand out like a sail (Lien et al., 2014). How the downstream section deforms is dependent on if the skirt is installed as one whole piece or as a long piece of fabric where the ends overlap. At Fornes the skirt was installed as one piece of fabric overlapping at the south side of the cage. At the overlap the skirt was observed to balloon out behind the cage up to several meters at times (Fig. 7). The ballooning in Fig. 7 was probably due to the shorter period of currents close to 20 cm/s just prior to the picture being taken (Fig. 3). A preliminary study at the same site in 2018 observed skirt deformations

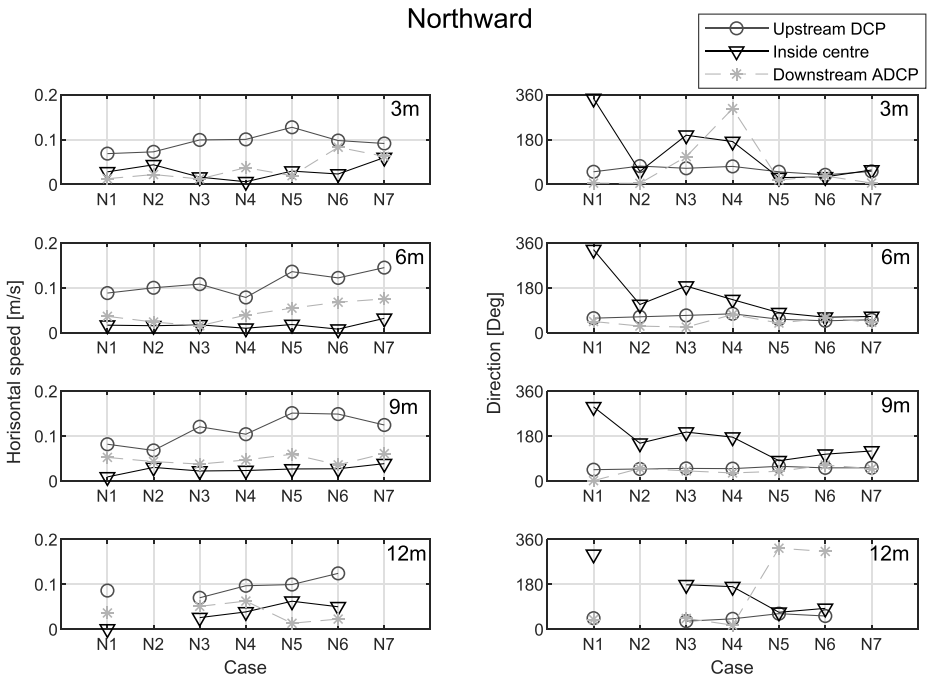

Fig. 4. Horizontal speed and current direction averaged over 30-min for the upstream DCP, downstream ADCP and ADVs inside the cage, for each individual case defined in Table 1 that had a main Northward direction.

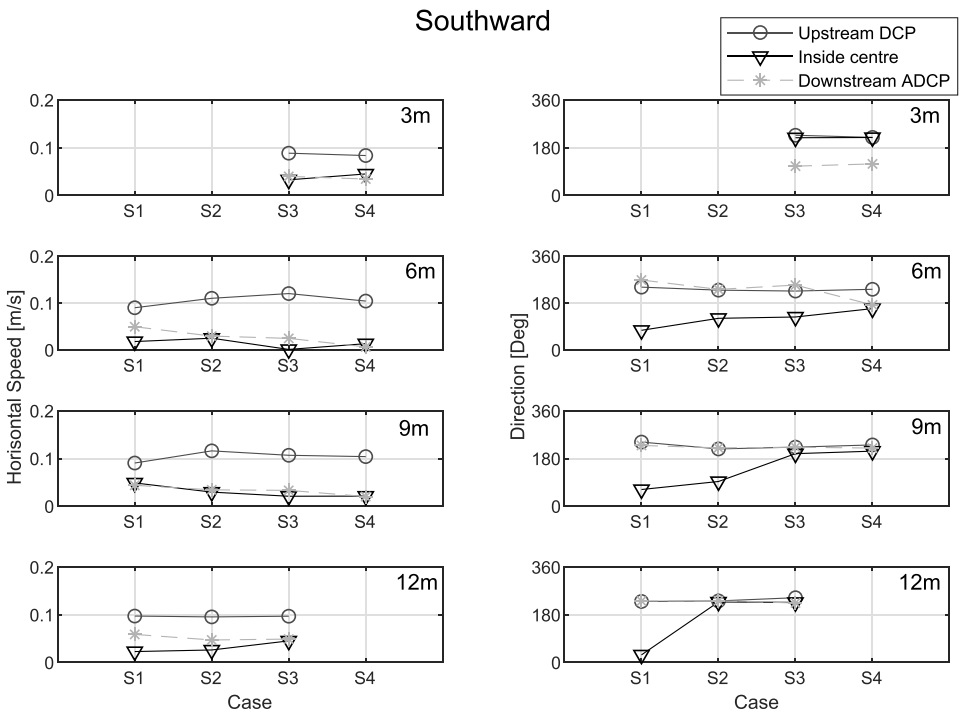

Fig. 5. Horizontal speed and current direction averaged over 30-min for the upstream ADCP, downstream DCP and ADVs inside the cage, for each individual case defined in Table 2 that had a main Southward direction.

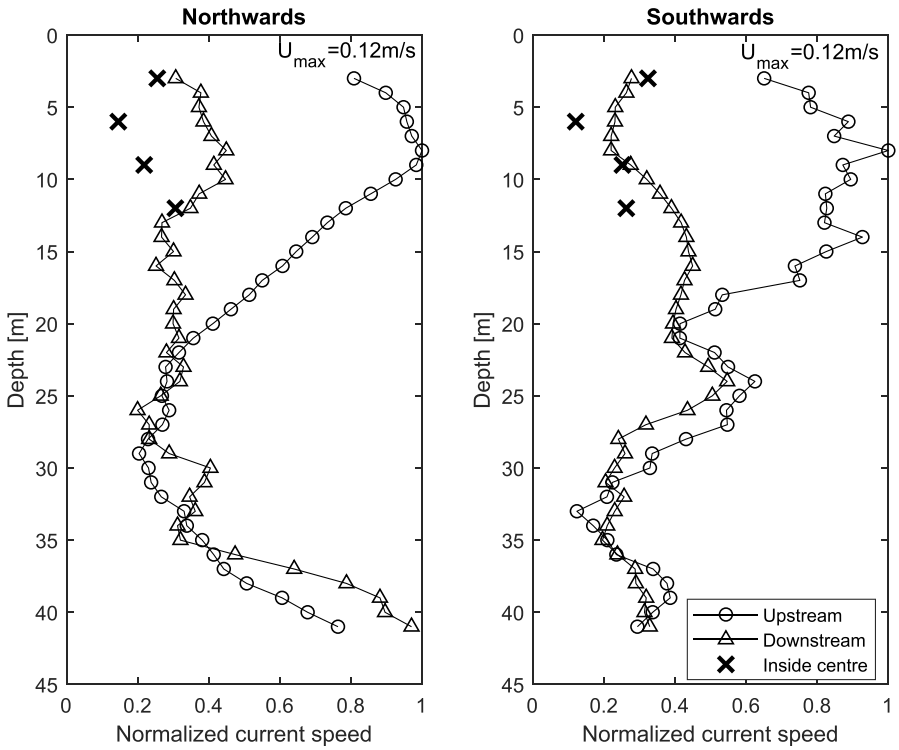

Fig. 6. Average normalized horizontal current speed recorded at each depth in both the upstream, downstream and sensor inside. The maximum average current speed was slightly below 0.12 m/s for both cases.

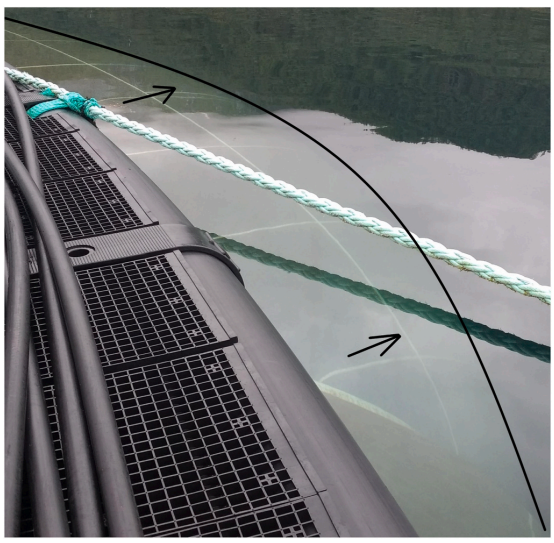

Fig. 7. Black line marks the visible edge of the skirt being lifted due to the current. Black arrows indicate the main current direction (roughly South-West in this image). Image taken the 4th of July at 13:33 local time. The average current upstream (Position A) had a horizontal speed of roughly 8 cm/s at this given time, but had been as high as 20 cm/s only an hour prior, as seen in Fig. 2. The overlap of the skirt is visible just beneath the bottom arrow.

by use of pressure sensors along the bottom of the skirt and registered greater vertical deformation of the skirt downstream than upstream when currents exceeded roughly 13 cm/s (Volent et al., 2020). It should be noted that the horizontal speed inside and downstream of the cage were very low during the selected periods (Figs. 4 and 5) so it's uncertain if the skirt was deforming at all during the chosen periods.

The normalized average current speed on the inside of the cage was lower or equal to the current speed downstream (Fig. 6), thereby not replicating the linear reduction through the cage seen for unshielded cylindrical cages (Klebert et al., 2015). The current speed inside the cage followed a similar pattern independent of current directions with a strong average current speed at 3 m depth, the weakest current speed at 6 m depth, and an increase in current speed from 6 to 12 m depth (Fig. 6). It should also be noted that there were only two samples included in the Southward data group at 3 m depth (see Fig. 5), which could explain why the normalized current speed was at its highest inside the cage at 3 m depth when the current was heading Southwards.

The high reduction at 6 m depth could be due to the vertical positioning of the biomass in the cage as biomass can increase the reduction in speed (Klebert and Su, 2020). During this study the stocking density was 19 kg m^{-3}. Atlantic salmon rarely distributes themselves evenly vertically in the cage and prefer to swim at deeper depths during the day and closer to the surface during night (Oppedal et al., 2011). As this study took place during the summer in Northern Norway the sun never set, and the continuous daylight may have resulted in the salmon swimming in a higher density at 6 m and below, thereby reducing the current speed there more than other layers. Unfortunately, the behaviour of the salmon was not monitored during this study.

3.4. Reduction in current speed

The reduction factor (r) was calculated for 3, 6, 9 and 12 m and compared with the reduction factor found using the expressions by Løland (1993) and Føre et al. (2020) (Fig. 8). The expression by Føre et al. (2020) was better at estimating the current reduction downstream of the skirt (Sn = 0.51) than Løland (1993). This was expected as the expression by Føre et al. (2020) is developed to correctly estimate the current downstream of nets with high solidity.

The reduction from upstream to inside the cage was however higher than expected compared with both expressions. This could be due to the low current speed in this study as the lowest incoming current speed utilised in Føre et al. (2020) was 0.25 m/s, compared to 0.05 m/s in this study. Furthermore, both Løland (1993) and Føre et al. (2020) utilised

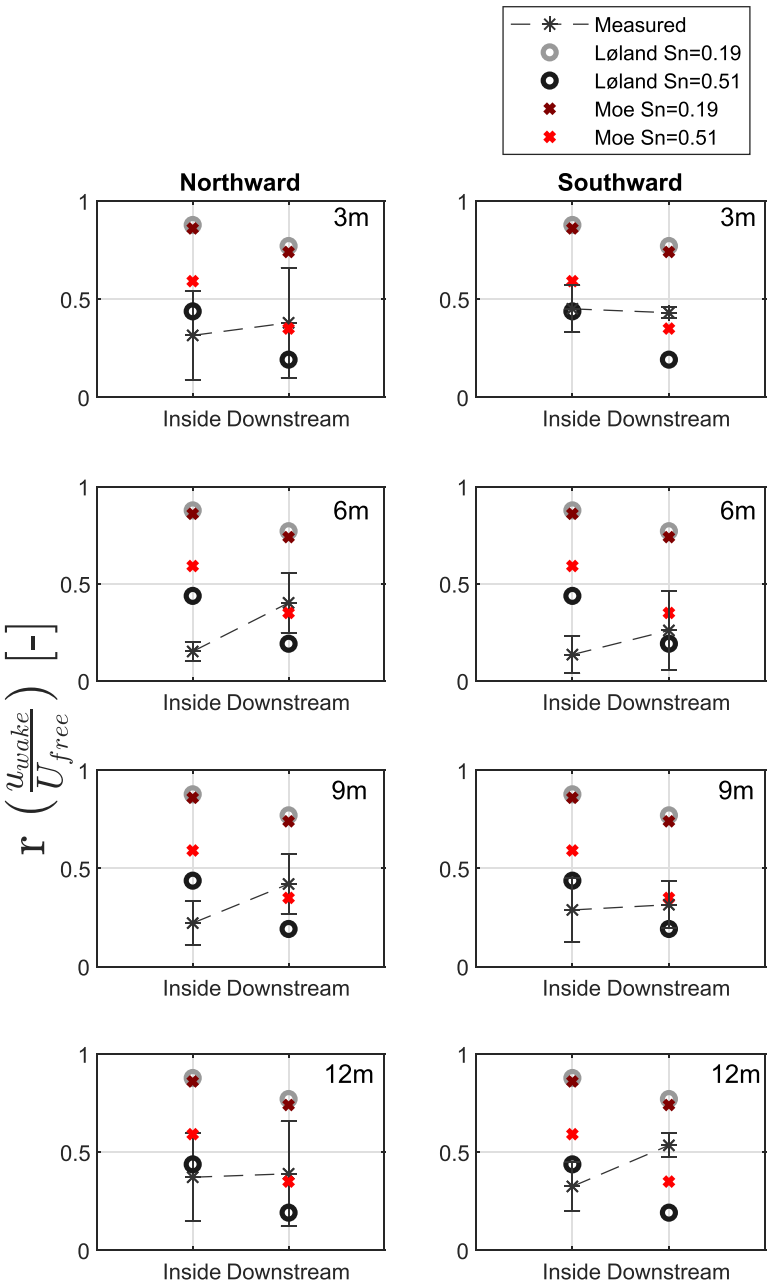

Fig. 8. Average reduction ratio (r) between current speed inside and upstream, and downstream and upstream, measured in this study. Expected reduction ratio behind one net panel and two net panels using Løland (1993) and Føre et al. (2020) are also marked using Sn = 0.19 and Sn = 0.51.

stretched out plane nets. The conical cage in this study had an inclination angle, which would have increased the reduction, but also had the opportunity to deform. There could also have been biofouling on both the net and skirt, which would have increased the solidity and reduction in current speed through the cage. As the estimate by Føre et al. (2020) was good downstream of the cage, but not inside the cage, it could be that the biomass around the ADVs resulted in low current speeds. Another reason is that comparing ADV data with ADCP data is not optimal, as the ADV averages over a very small volume while the ADCP averages over cell sizes of 1 m.

The highest reduction inside the cage was 86% ($r = 0.14$) at 6 m depth. For unshielded cages exposed to currents as strong as 60 cm/s the reduction from outside to inside is 21.5% at 6 m depth (Klebert et al., 2015). In another study by Johansson et al. (2014) the reduction inside a non-shielded cage varied from 0 to 50% when the speed outside was 20 cm/s (Johansson et al., 2014). Given the high biomass in this study, inclination of the cage, the general low current speeds during the relevant periods and the presence of a shielding skirt, a reduction of 86% was deemed reasonable.

4. Conclusion

Current speed upstream, downstream and inside a conical full-scale shielded sea cage were monitored. The velocity measurement inside the cage showed a more complex flow pattern than for a cylindrical cage, probably due to the interaction between the permeable skirt and the conical shape of the cage which could both have affected the distribution of fish in the water column differently than in a cylindrical cage. Speed was generally low inside the cage. The weakest current speed inside the cage was at 6 m depth independently of direction. Current speed increased beneath this depth. There was a clear reduction in current speed downstream of the shielding skirt, with the highest reduction recorded behind the shielded volume. No blocking effect was observed beneath 22 m depth, probably due to the conical shape of the cage. The difference in current flow field behind the conical cage compared with a cylindrical cage may have implications for the dispersal of waste, feed pellets and microorganisms from the cage influencing the benthic impact of the farm, and further work should focus on documenting these differences.

CRediT authorship contribution statement

Kristbjörg Edda Jónsdóttir: Conceptualization, Data curation, Methodology, Visualization, Writing - original draft. **Pascal Klebert:** Conceptualization, Writing - original draft. **Zsolt Volent:** Conceptualization, Data curation, Funding acquisition, Visualization, Writing - original draft. **Jo Arve Alfredsen:** Writing - review & editing.

Declaration of competing interest

The authors declare that they have no known competing financial interests or personal relationships that could have appeared to influence the work reported in this paper.

Acknowledgement

This study is part of the project “Shielding skirt as a method for prevention and control of salmon lice infestation – improving knowledge about environmental conditions for increase in efficiency and reduction of risk (SKJERMTEK)” (project number: 901396) funded by The Norwegian Seafood Research Fund (FHF). KEJ received funding from the RACE research grant program funded by SINTEF Ocean. We are thankful for access to equipment from SINTEF ACE, and to Nordlaks Oppdrett AS for access to their sites and the help received from their on-site employees.

References

Abolofia, J., Asche, F., Wilen, J.E., 2017. The cost of lice: quantifying the impacts of parasitic sea lice on farmed salmon. Mar. Resour. Econ. 32, 329–349.

Bi, C.W., Zhao, Y.P., Dong, G.H., Xu, T.J., Gui, F.K., 2013. Experimental investigation of the reduction in flow velocity downstream from a fishing net. Aquacult. Eng. 57, 71–81. https://doi.org/10.1016/j.aquaeng.2013.08.002. http://www.sciencedirect.com/science/article/pii/S0144860913000691.

Bi, C.W., Zhao, Y.P., Dong, G.H., Zheng, Y.N., Gui, F.K., 2014. A numerical analysis on the hydrodynamic characteristics of net cages using coupled fluid–structure interaction model. Aquacult. Eng. 59, 1–12.

Birjandi, A.H., Bibeau, E.L., 2011. Improvement of acoustic Doppler velocimetry in bubbly flow measurements as applied to river characterization for kinetic turbines. Int. J. Multiphas. Flow 37, 919–929.

Bui, S., Stien, L.H., Nilsson, J., Trengereid, H., Oppedal, F., 2020. Efficiency and welfare impact of long-term simultaneous in situ management strategies for salmon louse reduction in commercial sea cages. Aquaculture 520, 734934.

Føre, H.M., Endresen, P.C., Norvik, C., Lader, P.F., 2020. Hydrodynamic loads on net panels with different solidities. In: Proceedings of 39th International Conference on Ocean, Offshore and Arctic Engineering (OMAE). ASME.

Frank, K., Gansel, L., Lien, A., Birkevold, J., 2015. Effects of a shielding skirt for prevention of sea lice on the flow past stocked salmon fish cages. J. Offshore Mech. Arctic Eng. 137.

Fredheim, A., 2005. Current Forces on Net Structure. Phd Thesis. Norwegian University of Science and Technology.

Gansel, L.C., Rackebrandt, S., Oppedal, F., McClimans, T.A., 2014. Flow fields inside stocked fish cages and the near environment. J. Offshore Mech. Arctic Eng. 136, 31201. https://doi.org/10.1115/1.4027746, 031201.

Gansel, L.C., Plew, D.R., Endresen, P.C., Olsen, A.I., Misimi, E., Guenther, J., Jensen, Ø., 2015. Drag of clean and fouled net panels–measurements and parameterization of fouling. PloS One 10, e0131051.

Geitung, L., Oppedal, F., Stien, L.H., Dempster, T., Karlsbakk, E., Nola, V., Wright, D.W., 2019. Snorkel sea-cage technology decreases salmon louse infestation by 75% in a full-cycle commercial test. Int. J. Parasitol. 49, 843–846.

Goring, D.G., Nikora, V.I., 2002. Despiking acoustic Doppler velocimeter data. J. Hydraul. Eng. 128, 117–126.

Heuch, P.A., Parsons, A., Boxaspen, K., 1995. Diel vertical migration: a possible host-finding mechanism in salmon louse (lepeophtheirus salmonis) copepodids? Can. J. Fish. Aquat. Sci. 52, 681–689.

Hevrøy, E., Boxaspen, K., Oppedal, F., Taranger, G., Holm, J., 2003. The effect of artificial light treatment and depth on the infestation of the sea louse lepeophtheirus salmonis on atlantic salmon (salmo salar l.) culture. Aquaculture 220, 1–14.

Huse, I., Holm, J., 1993. Vertical distribution of atlantic salmon (salmo salar) as a function of illumination. J. Fish. Biol. 43, 147–156.

Iversen, A., Hermansen, Ø., Nystøyl, R., Hess, E.J., 2017. Kostnadsutvikling I Lakseoppdrett–Med Fokus På Fä'r-Og Lusekostnader. Nofima rapportserie.

Johansson, D., Juell, J.E., Oppedal, F., Stiansen, J.E., Ruohonen, K., 2007. The influence of the pycnocline and cage resistance on current flow, oxygen flux and swimming behaviour of atlantic salmon (salmo salar l.) in production cages. Aquaculture 265, 271–287.

Johansson, D., Laursen, F., Fernö, A., Fosseidengen, J.E., Klebert, P., Stien, L.H., Vågseth, T., Oppedal, F., 2014. The interaction between water currents and salmon swimming behaviour in sea cages. PloS One 9, e97635.

Jónsdóttir, K.E., Volent, Z., Alfredsen, J.A., 2020. Dynamics of dissolved oxygen inside salmon sea-cages with lice shielding skirts at two hydrographically different sites. Aquacult. Environ. Interact. 12, 559–570. https://doi.org/10.3354/aei00384.

Kim, T., Lee, J., Fredriksson, D.W., DeCew, J., Drach, A., Moon, K., 2014. Engineering analysis of a submersible abalone aquaculture cage system for deployment in exposed marine environments. Aquacult. Eng. 63, 72–88.

Klebert, P., Su, B., 2020. Turbulence and flow field alterations inside a fish sea cage and its wake. Appl. Ocean Res. 98, 102113.

Klebert, P., Lader, P., Gansel, L., Oppedal, F., 2013. Hydrodynamic interactions on net panel and aquaculture fish cages: a review. Ocean Eng. 58, 260–274.

Klebert, P., Patursson, Ø., Endresen, P.C., Rundtop, P., Birkevold, J., Rasmussen, H.W., 2015. Three-dimensional deformation of a large circular flexible sea cage in high currents: field experiment and modeling. Ocean Eng. 104, 511–520. https://doi.org/10.1016/j.oceaneng.2015.04.045. http://www.sciencedirect.com/science/article/pii/S0029801815001262.

Kristiansen, T., Faltinsen, O.M., 2015. Experimental and numerical study of an aquaculture net cage with floater in waves and current. J. Fluid Struct. 54, 1–26.

Lader, P., Dempster, T., Fredheim, A., Jensen, Ø., 2008. Current induced net deformations in full-scale sea-cages for atlantic salmon (salmo salar). Aquacult. Eng. 38, 52–65. https://doi.org/10.1016/j.aquaeng.2007.11.001. http://www.sciencedirect.com/science/article/pii/S0144860907000957.

Lee, C.W., Kim, Y.B., Lee, G.H., Choe, M.Y., Lee, M.K., Koo, K.Y., 2008. Dynamic simulation of a fish cage system subjected to currents and waves. Ocean Eng. 35, 1521–1532.

Lien, A.M., Volent, Z., Jensen, Ø., Lader, P., Sunde, L.M., 2014. Shielding skirt for prevention of salmon lice (lepeophtheirus salmonis) infestation on atlantic salmon (salmo salar l.) in cages–a scaled model experimental study on net and skirt deformation, total mooring load, and currents. Aquacult. Eng. 58, 1–10.

Løland, G., 1993. Current forces on, and water flow through and around, floating fish farms. Aquacult. Int. 1, 72–89.

Mayer, D.A., Virmani, J.I., Weisberg, R.H., 2007. Velocity comparisons from upward and downward acoustic Doppler current profilers on the west Florida shelf. J. Atmos. Ocean. Technol. 24, 1950–1960.

Norway, Standard, 2009. Marine Fish Farms-Requirements for Site Survey, Risk Analyses, Design, Dimensioning, Production, Installation and Operation. norsk standard ns 9415. E, Norway.
Oppedal, F., Dempster, T., Stien, L.H., 2011. Environmental drivers of atlantic salmon behaviour in sea-cages: a review. Aquaculture 311, 1–18.
Oppedal, F., Samsing, F., Dempster, T., Wright, D.W., Bui, S., Stien, L.H., 2017. Sea lice infestation levels decrease with deeper 'snorkel'barriers in atlantic salmon sea-cages. Pest Manag. Sci. 73, 1935–1943.
Patursson, Ø., 2008. Flow through and Around Fish Farming Nets. Ph.D. thesis. Ocean Engineering, University of New Hampshire, Durham, NH03824, USA.
Rasmussen, H.W., Patursson, Ø., Simonsen, K., 2015. Visualisation of the wake behind fish farming sea cages. Aquacult. Eng. 64, 25–31.
Remen, M., Aas, T.S., Vågseth, T., Torgersen, T., Olsen, R.E., Imsland, A., Oppedal, F., 2014. Production performance of atlantic salmon (salmo salar l.) postsmolts in cyclic hypoxia, and following compensatory growth. Aquacult. Res. 45, 1355–1366.
Stien, L.H., Nilsson, J., Hevrøy, E.M., Oppedal, F., Kristiansen, T.S., Lien, A.M., Folkedal, O., 2012. Skirt around a salmon sea cage to reduce infestation of salmon lice resulted in low oxygen levels. Aquacult. Eng. 51, 21–25.
Stien, L.H., Lind, M.B., Oppedal, F., Wright, D.W., Seternes, T., 2018. Skirts on salmon production cages reduced salmon lice infestations without affecting fish welfare. Aquaculture 490, 281–287.
Volent, Z., Jónsdóttir, K.E., Misund, A., Steinhovden, K.B., Chauton, M.S., Sunde, L.M., 2020. Strategi Lakselus 2017: Luseskjørt Som Ikke-Medikamentell Metode for Forebygging Og Kontroll Av Lakselus – Utvikling Av Kunnskap Om Miljøforhold for Økt Effekt Og Redusert Risiko (SKJERMTEK). SINTEF Ocean. Report 302003409.
Zhao, Y.P., Bi, C.W., Chen, C.P., Li, Y.C., Dong, G.H., 2015. Experimental study on flow velocity and mooring loads for multiple net cages in steady current. Aquacult. Eng. 67, 24–31.

References

Aaen, S.M., Helgesen, K.O., Bakke, M.J., Kaur, K., Horsberg, T.E., 2015. Drug resistance in sea lice: a threat to salmonid aquaculture. Trends in Parasitology 31, 72–81. doi:10.1016/j.pt.2014.12.006.

Abolofia, J., Asche, F., Wilen, J.E., 2017. The cost of lice: Quantifying the impacts of parasitic sea lice on farmed salmon. Marine Resource Economics 32, 329–349. doi:10.1086/691981.

Asche, F., Bjørndal, T., 2011. The Economics of Salmon Aquaculture. Wiley-Blackwell. doi:10.1002/9781119993384.

Balchen, J., 1987. Bridging the gap between aquaculture and the information sciences. IFAC Proceedings Volumes 20, 11–15. doi:10.1016/s1474-6670(17)59150-8.

Barrett, L.T., Oppedal, F., Robinson, N., Dempster, T., 2020. Prevention not cure: a review of methods to avoid sea lice infestations in salmon aquaculture. Reviews in Aquaculture 12, 2527–2543. doi:10.1111/raq.12456.

Beamish, F., 1978. Swimming capacity, in: Fish Physiology. Elsevier, pp. 101–187. doi:10.1016/s1546-5098(08)60164-8.

Bechmann, R.K., Arnberg, M., Bamber, S., Lyng, E., Westerlund, S., Rundberget, J.T., Kringstad, A., Seear, P.J., Burridge, L., 2020. Effects of exposing shrimp larvae (pandalus borealis) to aquaculture pesticides at field relevant concentrations, with and without food limitation. Aquatic Toxicology 222, 105453. doi:10.1016/j.aquatox.2020.105453.

Bechmann, R.K., Arnberg, M., Gomiero, A., Westerlund, S., Lyng, E., Berry, M., Agustsson, T., Jager, T., Burridge, L.E., 2019. Gill damage and delayed mortality of northern shrimp (pandalus borealis) after short time exposure to anti-parasitic veterinary medicine containing hydrogen peroxide. Ecotoxicology and Environmental Safety 180, 473–482. doi:10.1016/j.ecoenv.2019.05.045.

Berglihn, H., 2019. 150.000 cleanerfish die every day. -an unparalleled animal tragedy [in norwegian]. Dagens Næringsliv URL: https://www.dn.no/havbruk/lars-helge-stien/trygve-poppe/mattilsynet/150000-rensefisk-dor-hver-dag-en-dyretragedie-uten-sidestykke/2-1-719477. 09.12.19, [Accessed 16.09.2020].

Bi, C.W., Zhao, Y.P., Dong, G.H., Xu, T.J., Gui, F.K., 2013. Experimental investigation of the reduction in flow velocity downstream from a fishing net. Aquacultural Engineering 57, 71–81. doi:10.1016/j.aquaeng.2013.08.002.

Birjandi, A.H., Bibeau, E.L., 2011. Improvement of acoustic doppler velocimetry in bubbly flow measurements as applied to river characterization for kinetic turbines. International Journal of Multiphase Flow 37, 919–929. doi:10.1016/j.ijmultiphaseflow.2011.05.001.

Bittig, H.C., Körtzinger, A., Neill, C., van Ooijen, E., Plant, J.N., Hahn, J., Johnson, K.S., Yang, B., Emerson, S.R., 2018. Oxygen optode sensors: Principle, characterization, calibration, and application in the ocean. Frontiers in Marine Science 4. doi:10.3389/fmars.2017.00429.

Bjelland, H.V., Føre, M., Lader, P., Kristiansen, D., Holmen, I.M., Fredheim, A., Grøtli, E.I., Fathi, D.E., Oppedal, F., Utne, I.B., Schjølberg, I., 2015. Exposed aquaculture in Norway, in: OCEANS 2015 - MTS/IEEE Washington, IEEE. pp. 1–10. doi:10.23919/oceans.2015.7404486.

Bjordal, A., 1988. Cleaning symbiosis between wrasses (*Labridae*) and lice infested salmon (*Salmo salar*) in mariculture, in: ICES CM documents, ICES. pp. 1–8.

Brett, J.R., 1964. The respiratory metabolism and swimming performance of young sockeye salmon. Journal of the Fisheries Research Board of Canada 21, 1183–1226. doi:10.1139/f64-103.

Broch, O.J., Klebert, P., Michelsen, F.A., Alver, M.O., 2020. Multiscale modelling of cage effects on the transport of effluents from open aquaculture systems. PLOS ONE 15, e0228502. doi:10.1371/journal.pone.0228502.

Broom, D., 1986. Indicators of poor welfare. British Veterinary Journal 142, 524–526. doi:10.1016/0007-1935(86)90109-0.

Broom, D.M., 2017. Animal welfare in the european union. European Parliament Policy Department, Citizen's Rights and Constitutional Affairs, Study for the PETI Committee, Brussels doi:10-2861/891355.

Bui, S., Geitung, L., Oppedal, F., Barrett, L.T., 2020a. Salmon lice survive the straight shooter: A commercial scale sea cage trial of laser delousing. Preventive Veterinary Medicine 181, 105063. doi:10.1016/j.prevetmed.2020.105063.

Bui, S., Stien, L.H., Nilsson, J., Trengereid, H., Oppedal, F., 2020b. Efficiency and welfare impact of long-term simultaneous in situ management strategies for salmon louse reduction in commercial sea cages. Aquaculture 520, 734934. doi:10.1016/j.aquaculture.2020.734934.

Burt, K., Hamoutene, D., Mabrouk, G., Lang, C., Puestow, T., Drover, D., Losier, R., Page, F., 2011. Environmental conditions and occurrence of hypoxia within production cages of atlantic salmon on the south coast of newfoundland. Aquaculture Research 43, 607–620. doi:10.1111/j.1365-2109.2011.02867.x.

Chacon-Torres, A., Ross, L., Beveridge, M., 1988. The effects of fish behaviour on dye dispersion and water exchange in small net cages. Aquaculture 73, 283–293. doi:10.1016/0044-8486(88)90062-2.

Chu, Y., Wang, C., Park, J.C., Lader, P., 2020. Review of cage and containment tank designs for offshore fish farming. Aquaculture 519, 734928. doi:10.1016/j.aquaculture.2020.734928.

Coates, A., Phillips, B.L., Oppedal, F., Bui, S., Overton, K., Dempster, T., 2020. Parasites under pressure: salmon lice have the capacity to adapt to depth-based preventions in aquaculture. International Journal for Parasitology 50, 865–872. doi:10.1016/j.ijpara.2020.05.009.

Conte, F., 2004. Stress and the welfare of cultured fish. Applied Animal Behaviour Science 86, 205–223.

Costello, M.J., 2006. Ecology of sea lice parasitic on farmed and wild fish. Trends in Parasitology 22, 475–483. doi:10.1016/j.pt.2006.08.006.

Crosbie, T., Wright, D., Oppedal, F., Dalvin, S., Myksvoll, M., Dempster, T., 2020. Impact of thermoclines on the vertical distribution of salmon lice larvae. Aquaculture Environment Interactions 12, 1–10. doi:10.3354/aei00344.

Crosbie, T., Wright, D.W., Oppedal, F., Johnsen, I.A., Samsing, F., Dempster, T., 2019. Effects of step salinity gradients on salmon lice larvae behaviour and dispersal. Aquaculture Environment Interactions 11, 181–190. doi:10.3354/aei00303.

DeCew, J., Fredriksson, D., Lader, P., Chambers, M., Howell, W., Osienki, M., Celikkol, B., Frank, K., Høy, E., 2013. Field measurements of cage deformation using acoustic sensors. Aquacultural engineering 57, 114–125. doi:10.1016/j.aquaeng.2013.09.006.

Drucker, E.G., 1996. The use of gait transition speed in comparative studies of fish locomotion. American Zoologist 36, 555–566. doi:10.1093/icb/36.6.555.

Duarte, C.M., Holmer, M., Olsen, Y., Soto, D., Marbà, N., Guiu, J., Black, K., Karakassis, I., 2009. Will the oceans help feed humanity? BioScience 59, 967–976. doi:10.1525/bio.2009.59.11.8.

Eidnes, G., Borge, J., Berstad, A., Reed, J.L., Walaunet, J., 2018. NS 9415 - Strømprosjekt: Fastsettelse av ekstremstrøm. Report 2018:01257. SINTEF Ocean AS.

FAO, 2018. Fishery statistics. URL: http://www.fao.org/fishery/statistics/en. FAO - Food and agriculture organization of the united nations, Fisheries and Aquaculture Department.

FAO, 2020. The state of world fisheries and aquaculture 2020. Sustainability in action, Rome. doi:https://doi.org/10.4060/ca9229en. FAO - Food and agriculture organization of the united nations, Fisheries and Aquaculture Department.

Finstad, B., Bjørn, P., Grimnes, A., Hvidsten, N., 2000. Laboratory and field investigations of salmon lice (*Lepeophtheirus salmonis* (Krøyer)) infestation on atlantic salmon (*Salmo salar L.*) post-smolts. Aquaculture Research 31, 795–803. doi:10.1046/j.1365-2109.2000.00511.x.

Finstad, B., Bjørn, P.A., Todd, C.D., Whoriskey, F., Gargan, P.G., Forde, G., Revie, C.W., 2011. The effect of sea lice on atlantic salmon and other salmonid species, in: Atlantic salmon ecology. Wiley-Blackwell, pp. 253–276. doi:10.1002/9781444327755.ch10.

Folkehelseinstituttet, 2019. 2018: The aquaculture industry is using less and less drugs against salmon lice [in norwegian]. Online. URL: https://www.fhi.no/hn/legemiddelbruk/fisk/2018-oppdrettsnaringen-bruker-stadig-mindre-legemidler-mot-lakselus/. [Accessed 3-11-2020].

Føre, M., Dempster, T., Alfredsen, J.A., Johansen, V., Johansson, D., 2009. Modelling of atlantic salmon (*Salmo salar L.*) behaviour in sea-cages: A lagrangian approach. Aquaculture 288, 196–204. doi:10.1016/j.aquaculture.2008.11.031.

Føre, M., Frank, K., Dempster, T., Alfredsen, J.A., Høy, E., 2017. Biomonitoring using tagged sentinel fish and acoustic telemetry in commercial salmon aquaculture: a feasibility study. Aquacultural Engineering 78, 163–172. doi:10.1016/j.aquaeng.2017.07.004.

Føre, M., Frank, K., Norton, T., Svendsen, E., Alfredsen, J.A., Dempster, T., Eguiraun, H., Watson, W., Stahl, A., Sunde, L.M., 2018. Precision fish farming: A new framework to improve production in aquaculture. Biosystems Engineering 173, 176–193. doi:10.1016/j.biosystemseng.2017.10.014.

Frank, K., Gansel, L., Lien, A., Birkevold, J., 2015. Effects of a shielding skirt for prevention of sea lice on the flow past stocked salmon fish cages. Journal of Offshore Mechanics and Arctic Engineering 137. doi:10.1115/1.4028260.

Fredheim, A., 2005. Current forces on net structure. Thesis. Norwegian University of Science and Technology.

Fredheim, A., Langan, R., 2009. Advances in technology for off-shore and open ocean finfish aquaculture, in: New Technologies in Aquaculture. Elsevier, pp. 914–944. doi:10.1533/9781845696474.6.914.

Føre, H.M., Endresen, P.C., Norvik, C., Lader, P.F., 2020. Hydrodynamic loads on net panels with different solidities. Proceedings of 39th International Conference on Ocean, Offshore and Arctic Engineering (OMAE). ASME .

Gansel, L.C., 2013. Flow past porous cylinders and effects of biofouling and fish behavior on the flow in and around Atlantic salmon net cages. Thesis. Norwegian University of Science and Technology, Faculty of Engineering Science and Technology, Department of Marine Technology.

Gansel, L.C., McClimans, T.A., Myrhaug, D., . The effects of fish cages on ambient currents, in: ASME 2008 27th International Conference on Offshore Mechanics and Arctic Engineering, American Society of Mechanical Engineers. pp. 537–543. doi:10.1115/omae2008-57746.

Gansel, L.C., Oppedal, F., Birkevold, J., Tuene, S.A., 2018. Drag forces and deformation of aquaculture cages—full-scale towing tests in the field. Aquacultural Engineering 81, 46–56. doi:10.1016/j.aquaeng.2018.02.001.

Gansel, L.C., Plew, D.R., Endresen, P.C., Olsen, A.I., Misimi, E., Guenther, J., Jensen, Ø., 2015. Drag of clean and fouled net panels–measurements and parameterization of fouling. PloS one 10, e0131051. doi:10.1371/journal.pone.0131051.

Gansel, L.C., Rackebrandt, S., Oppedal, F., McClimans, T.A., 2014. Flow fields inside stocked fish cages and the near environment. Journal of Offshore Mechanics and Arctic Engineering 136, 031201–031201. doi:10.1115/1.4027746.

Geitung, L., Oppedal, F., Stien, L.H., Dempster, T., Karlsbakk, E., Nola, V., Wright, D.W., 2019. Snorkel sea-cage technology decreases salmon louse infestation by 75% in a full-cycle commercial test. International journal for parasitology 49, 843–846. doi:10.1016/j.ijpara.2019.06.003.

Gentry, K., Bui, S., Oppedal, F., Dempster, T., 2020. Sea lice prevention strategies affect cleaner fish delousing efficacy in commercial atlantic salmon sea cages. Aquaculture Environment Interactions 12, 67–80. doi:10.3354/aei00348.

Gentry, R.R., Froehlich, H.E., Grimm, D., Kareiva, P., Parke, M., Rust, M., Gaines, S.D., Halpern, B.S., 2017. Mapping the global potential for marine aquaculture. Nature Ecology and Evolution 1, 1317–1324. doi:10.1038/s41559-017-0257-9.

Gordon, R.L., Instruments, R., 1996. Principles of operation a practical primer. RD Instruments, San Diego .

Goring, D.G., Nikora, V.I., 2002. Despiking acoustic doppler velocimeter data. Journal of hydraulic engineering 128, 117–126. doi:10.1061/(asce)0733-9429(2002)128:1(117).

Grefserud, E.S., Svåsand, T., Glover, K., Husa, V., Hansen, P.K., Samuelsen, O., Sandlund, N., Stien, L.H., (Eds.), 2019. Risikorapport norsk fiskeoppdrett 2019 - Miljøeffekter av lakseoppdrett. Report. Havforskningsinstituttet.

Grøntvedt, R., Kristoffersen, A., 2015. Permaskjørt kan redusere påslag av lakselus. Norwegian Veterinary Institute's Report Series .

Grøntvedt, R.N., Kristoffersen, A.B., Jansen, P.A., 2018. Reduced exposure of farmed salmon to salmon louse (*Lepeophtheirus salmonis L.*) infestation by use of plankton nets: Estimating the shielding effect. Aquaculture 495, 865–872. doi:10.1016/j.aquaculture.2018.06.069.

Gullestad, P., Bjørgo, S., Eithun, I., Ervik, A., Gudding, R., Hansen, H., Johansen, R., Osland, A., Rødseth, M., Røsvik, I., 2011. Effektiv og bærekraftig arealbruk i havbruksnæringen. The Royal Norwegian Ministry of Fisheries and Coastal Affairs, Oslo, Norway, Technical Report (in Norwegian) .

Harris, P.D., Bachmann, L., Bakke, T.A., 2011. The parasites and pathogens of the atlantic salmon: lessons from gyrodactylus salaris, in: Atlantic Salmon Ecology. Wiley-Blackwell, pp. 221–252. doi:10.1002/9781444327755.ch9.

He, Z., Faltinsen, O.M., Fredheim, A., Kristiansen, T., 2018. The influence of fish on the mooring loads of a floating net cage. Journal of Fluids and Structures 76, 384–395. doi:10.1016/j.jfluidstructs.2017.10.016.

Hesthagen, T., Kleiven, E., 2016. Aurene i Jotunheimen - Når vart han innført, og kor kom han frå?. Portal Kulturhistorisk Museum, Kristiansand. pp. 37–53. doi:https://doi.org/10.23865/noasp.60.

Heuch, P.A., Mo, T.A., 2001. A model of salmon louse production in Norway: effects of increasing salmon production and public management measures. Diseases of aquatic organisms 45, 145–152. doi:10.3354/dao045145.

Heuch, P.A., Parsons, A., Boxaspen, K., 1995. Diel vertical migration: a possible host-finding mechanism in salmon louse (*Lepeophtheirus salmonis*) copepodids? Canadian Journal of Fisheries and Aquatic Sciences 52, 681–689. doi:10.1139/f95-069.

Hevrøy, E., Boxaspen, K., Oppedal, F., Taranger, G., Holm, J., 2003. The effect of artificial light treatment and depth on the infestation of the sea louse lepeophtheirus salmonis on atlantic salmon (*Salmo salar L.*) culture. Aquaculture 220, 1–14. doi:10.1016/s0044-8486(02)00189-8.

Holmer, M., 2010. Environmental issues of fish farming in offshore waters: perspectives, concerns and research needs. Aquaculture Environment Interactions 1, 57–70. doi:10.3354/aei00007.

Holmer, M., Wildish, D., Hargrave, B.T., 2005. Organic enrichment from marine finfish aquaculture and effects on sediment biogeochemical processes, in: Environmental effects of marine finfish aquaculture. Springer. book section 9, pp. 181–206. doi:10.1007/b136010.

Horntvedt, A., 2020. 'Aquabyte har fått gjennomslag fra myndighetene til å bruke kamera og kunstig intelligens til å overvåke lakselus'. Finansavisen URL: https://finansavisen.no/nyheter/sjomat/2020/11/24/7591506/godkjenning-fra-mattilsynet-gjennombrudd-for-aquabyte-med-it-basert-telling-av-lakselus. 24.11.2020.

Huse, I., Holm, J., 1993. Vertical distribution of atlantic salmon (*Salmo salar*) as a function of illumination. Journal of Fish Biology 43, 147–156. doi:10.1111/j.1095-8649.1993.tb01184.x.

Hvas, M., Folkedal, O., Imsland, A., Oppedal, F., 2017a. The effect of thermal acclimation on aerobic scope and critical swimming speed in atlantic salmon, *Salmo salar*. Journal of Experimental Biology 220, 2757–2764. doi:10.1242/jeb.154021.

Hvas, M., Folkedal, O., Imsland, A., Oppedal, F., 2018. Metabolic rates, swimming capabilities, thermal niche and stress response of the lumpfish, *Cyclopterus lumpus*. Biology open 7. doi:10.1242/bio.036079.

Hvas, M., Folkedal, O., Oppedal, F., 2020. Fish welfare in offshore salmon aquaculture. Reviews in Aquaculture doi:10.1111/raq.12501.

Hvas, M., Folkedal, O., Solstorm, D., Vågseth, T., Fosse, J.O., Gansel, L.C., Oppedal, F., 2017b. Assessing swimming capacity and schooling behaviour in farmed atlantic salmon salmo salar with experimental push-cages. Aquaculture 473, 423–429. doi:10.1016/j.aquaculture.2017.03.013.

Hvas, M., Karlsbakk, E., Mæhle, S., Wright, D.W., Oppedal, F., 2017c. The gill parasite paramoeba perurans compromises aerobic scope, swimming capacity and ion balance in atlantic salmon. Conservation physiology 5, cox066. doi:10.1093/conphys/cox066.

Hvas, M., Oppedal, F., 2017. Sustained swimming capacity of atlantic salmon. Aquaculture Environment Interactions 9, 361–369. doi:10.3354/aei00239.

Imberger, J., 2013. Mixing in environmental flows, in: Environmental fluid dynamics: flow processes, scaling, equations of motion, and solutions to environmental flows. Academic Press. book section 7, pp. 305–331. doi:10.1016/b978-0-12-088571-8.00007-3.

Imsland, A.K., Reynolds, P., Eliassen, G., Hangstad, T.A., Foss, A., Vikingstad, E., Elvegård, T.A., 2014. The use of lumpfish (cyclopterus lumpus l.) to control sea lice (lepeophtheirus salmonis krøyer) infestations in intensively farmed atlantic salmon (salmo salar l.). Aquaculture 424, 18–23. doi:10.1016/j.aquaculture.2013.12.033.

Imsland, A.K., Reynolds, P., Nytrø, A.V., Eliassen, G., Hangstad, T.A., Jónsdóttir, Ó.D., Emaus, P.A., Elvegård, T.A., Lemmens, S.C., Rydland, R., 2016. Effects of lumpfish size on foraging behaviour and co-existence with sea lice infected atlantic salmon in sea cages. Aquaculture 465, 19–27. doi:10.1016/j.aquaculture.2016.08.015.

Imsland, A.K.D., Hanssen, A., Nytrø, A.V., Reynolds, P., Jonassen, T.M., Hangstad, T.A., Elvegård, T.A., Urskog, T.C., Mikalsen, B., 2018. It works! lumpfish can significantly lower sea lice infestation in large-scale salmon farming. Biology open 7. doi:10.1242/bio.036301.

Iversen, A., Hermansen, Ø., Nystøyl, R., Hess, E.J., 2017. Kostnadsutvikling i lakseoppdrett–med fokus på fôr-og lusekostnader. Nofima rapportserie .

Johannesen, Á., Patursson, Ø., Kristmundsson, J., Dam, S.P., Klebert, P., 2020. How caged salmon respond to waves depends on time of day and currents. PeerJ 8, e9313. doi:10.7717/peerj.9313.

Johansson, D., Juell, J.E., Oppedal, F., Stiansen, J.E., Ruohonen, K., 2007. The influence of the pycnocline and cage resistance on current flow, oxygen flux and swimming behaviour of atlantic salmon (salmo salar l.) in production cages. Aquaculture 265, 271–287. doi:10.1016/j.aquaculture.2006.12.047.

Johansson, D., Laursen, F., Fern´o, A., Fosseidengen, J.E., Klebert, P., Stien, L.H., Vågseth, T., Oppedal, F., 2014. The interaction between water currents and salmon swimming behaviour in sea cages. PloS one 9, e97635. doi:10.1371/journal.pone.0097635.

Johansson, D., Ruohonen, K., Kiessling, A., Oppedal, F., Stiansen, J.E., Kelly, M., Juell, J.E., 2006. Effect of environmental factors on swimming depth preferences of atlantic salmon (salmo salar l.) and temporal and spatial variations in oxygen levels in sea cages at a fjord site. Aquaculture 254, 594–605. doi:10.1016/j.aquaculture.2005.10.029.

Johnsen, G., Volent, Z., Sakshaug, E., Sigernes, F., Pettersson, L.H., Kovacs, K., 2009. Remote sensing in the Barents Sea. volume 2. book section 6. pp. 139–166.

Juell, J.E., 1995. The behaviour of atlantic salmon in relation to efficient cage-rearing. Reviews in fish biology and fisheries 5, 320–335. doi:10.1007/bf00043005.

Juell, J.E., Westerberg, H., 1993. An ultrasonic telemetric system for automatic positioning of individual fish used to track atlantic salmon (salmo salar l.) in a sea cage. Aquacultural Engineering 12, 1–18. doi:10.1016/0144-8609(93)90023-5.

Klebert, P., Lader, P., Gansel, L., Oppedal, F., 2013. Hydrodynamic interactions on net panel and aquaculture fish cages: A review. Ocean Engineering 58, 260–274. doi:10.1016/j.oceaneng.2012.11.006.

Klebert, P., Patursson, Ø., Endresen, P.C., Rundtop, P., Birkevold, J., Rasmussen, H.W., 2015. Three-dimensional deformation of a large circular flexible sea cage in high currents: Field experiment and modeling. Ocean Engineering 104, 511–520. doi:10.1016/j.oceaneng.2015.04.045.

Klebert, P., Su, B., 2020. Turbulence and flow field alterations inside a fish sea cage and its wake. Applied Ocean Research 98, 102113. doi:10.1016/j.apor.2020.102113.

Kristiansen, T., Faltinsen, O.M., 2012. Modelling of current loads on aquaculture net cages. Journal of Fluids and Structures 34, 218–235. doi:10.1016/j.jfluidstructs.2012.04.001.

Lader, P., Dempster, T., Fredheim, A., Jensen, Ø., 2008. Current induced net deformations in full-scale sea-cages for atlantic salmon (salmo salar). Aquacultural Engineering 38, 52–65. doi:10.1016/j.aquaeng.2007.11.001.

Le Menn, M., 2012. Instrumentation and Metrology in Oceanography. John Wiley and Sons. doi:10.1002/9781118561959.

Lekang, O.I., 2020. Aquaculture Engineering. Newark: John Wiley and Sons, Incorporated, Newark. doi:10.1002/9781118496077.

Lekang, O.I., Salas-Bringas, C., Bostock, J., 2016. Challenges and emerging technical solutions in on-growing salmon farming. Aquaculture International 24, 757–766. doi:10.1007/s10499-016-9994-z.

Lien, A.M., Høy, E., 2011. Skjørt for skjerming mot lus i laksemerd. SINTEF Fiskeri og Havbruk AS, Report .

Lien, A.M., Stien, L.H., Grøntvedt, R., Frank, K., 2015. Permanent skjørt for redusering av luspåslag på laks. Report 8214058732. Sintef Fiskeri og Havbruk.

Lien, A.M., Volent, Z., Jensen, Ø., Lader, P., Sunde, L.M., 2014. Shielding skirt for prevention of salmon lice (lepeophtheirus salmonis) infestation on atlantic salmon (salmo salar l.) in cages–a scaled model experimental study on net and skirt deformation, total mooring load, and currents. Aquacultural Engineering 58, 1–10. doi:10.1016/j.aquaeng.2013.11.003.

Liu, Y., Bjelland, H.V., 2014. Estimating costs of sea lice control strategy in norway. Preventive veterinary medicine 117, 469–477. doi:10.1016/j.prevetmed.2014.08.018.

Liu, Y., Olaussen, J.O., Skonhoft, A., 2011. Wild and farmed salmon in norway—a review. Marine Policy 35, 413–418. doi:10.1016/j.marpol.2010.11.007.

Løland, G., 1993. Current forces on, and water flow through and around, floating fish farms. Aquaculture International 1, 72–89. doi:10.1007/bf00692665.

Marra, J., 2005. When will we tame the oceans? Nature 436, 175–176. doi:10.1038/436175a.

McGinnity, P., Prod'ohl, P., Ferguson, A., Hynes, R., Maoiléidigh, N.O., Baker, N., Cotter, D., O'Hea, B., Cooke, D., Rogan, G., 2003. Fitness reduction and potential extinction of wild populations of atlantic salmon, salmo salar, as a result of interactions with escaped farm salmon. Proceedings of the Royal Society of London. Series B: Biological Sciences 270, 2443–2450. doi:10.1098/rspb.2003.2520.

McKenzie, D.J., Palstra, A.P., Planas, J., MacKenzie, S., Bégout, M.L., Thorarensen, H., Vandeputte, M., Mes, D., Rey, S., De Boeck, G., 2020. Aerobic swimming in intensive finfish aquaculture: applications for production, mitigation and selection. Reviews in Aquaculture doi:10.1111/raq.12467.

Michelsen, F.A., Klebert, P., Broch, O.J., Alver, M.O., 2019. Impacts of fish farm structures with biomass on water currents: A case study from frøya. Journal of Sea Research 154, 101806. doi:10.1016/j.seares.2019.101806.

Misund, A., Volent, Z., Jónsdóttir, K.E., Sunde, L.M., 2020. 'Hvordan forholder oppdrettere seg til skjermingsteknologi mot lakselus?'. Norsk Fiskeoppdrett 9, 2020.

Mori, N., Suzuki, T., Kakuno, S., 2007. Noise of acoustic doppler velocimeter data in bubbly flows. Journal of engineering mechanics 133, 122–125. doi:10.1061/(asce)0733-9399(2007)133:1(122).

Næs, M., Grøntvedt, R., Kristoffersen, A., Johansen, B., 2014. Feltutprøving av planktonduk som skjerming rundt oppdrettsmerder for å redusere påslag av lakselus (lepeophtheirus salmonis). Faglig rapport 4.

Nash, C., 2011. The history of aquaculture. John Wiley and Sons. doi:10.1002/9780470958971.

Noble, C., Gismervik, K., Iversen, M.H., Kolarevic, J., Nilsson, J., Stien, L.H., Turnbull, J.F., (Eds.), 2018. Welfare Indicators for farmed Atlantic salmon: tools for assessing fish welfare. Report. NOFIMA.

Norwegian Directorate of Fisheries, 2020a. Circumstances around escaped farmed fish [in norwegian]. Online. URL: https://www.fiskeridir.no/Akvakultur/Nyheter/2020/0120/Omstendigheter-ved-roemming-av-oppdrettsfisk. [Accessed: 12-11-2020].

Norwegian Directorate of Fisheries, 2020b. Cleanerfish deployed 1998-2019 [in norwegian]. URL: https://www.fiskeridir.no/Akvakultur/Tall-og-analyse/Akvakulturstatistikk-tidsserier/Rensefisk. [Accessed: 13-11-2020].

Norwegian Food and Safety Authority, 2020. National supervision campaign 2018/2019: Welfare of cleaner fish [In Norwegian]. Report. Norwegian Food and Safety Authority. URL: https://www.mattilsynet.no/fisk_og_akvakultur/akvakultur/rensefisk/mattilsynet_sluttrapport_rensefiskkampanje_2018_2019.37769/binary/Mattilsynet%20sluttrapport%20rensefiskkampanje%202018%202019.

Norwegian Ministry of Agriculture and Food, 2009. Animal welfare act. URL: https://www.regjeringen.no/en/dokumenter/animal-welfare-act/id571188/.

Norwegian Ministry of Trade and Industry, 2012. Forskrift om bekjempelse av lakselus i akvakulturanlegg (FOR-2012-12-05-1140). URL: https://lovdata.no/dokument/SF/forskrift/2012-12-05-1140/%C2%A78#%C2%A78.

Norwegian Ministry of Trade and Industry, 2017. Forskrift om produksjonsområder for akvakultur av matfisk i sjø av laks, ørret og regnbueørret (produksjonsområdeforskriften) (FOR-2017-01-16-61). URL: https://lovdata.no/dokument/SF/forskrift/2017-01-16-61.

NTB, 2016. 'massdeath of salmon at fish farm' (in norwegian). NRK URL: https://www.nrk.no/trondelag/massedod-av-laks-pa-oppdrettsanlegg-1.12828610. 1.03.2016.

Oldham, T., Dempster, T., Fosse, J.O., Oppedal, F., 2017. Oxygen gradients affect behaviour of caged atlantic salmon salmo salar. Aquaculture Environment Interactions 9, 145–153. doi:10.3354/aei00219.

Oldham, T., Nowak, B., Hvas, M., Oppedal, F., 2019. Metabolic and functional impacts of hypoxia vary with size in atlantic salmon. Comparative Biochemistry and Physiology Part A: Molecular and Integrative Physiology 231, 30–38. doi:10.1016/j.cbpa.2019.01.012.

Oldham, T., Oppedal, F., Dempster, T., 2018. Cage size affects dissolved oxygen distribution in salmon aquaculture. Aquaculture Environment Interactions 10, 149–156. doi:10.3354/aei00263.

Oppedal, F., Dempster, T., Stien, L.H., 2011. Environmental drivers of atlantic salmon behaviour in sea-cages: a review. Aquaculture 311, 1–18. doi:10.1016/j.aquaculture.2010.11.020.

Oppedal, F., Samsing, F., Dempster, T., Wright, D.W., Bui, S., Stien, L.H., 2017. Sea lice infestation levels decrease with deeper 'snorkel'barriers in atlantic salmon sea-cages. Pest Management Science 73, 1935–1943. doi:10.1002/ps.4560.

Overton, K., Barrett, L.T., Oppedal, F., Kristiansen, T.S., Dempster, T., 2020. Sea lice removal by cleaner fish in salmon aquaculture: a review of the evidence base. Aquaculture Environment Interactions 12, 31–44. doi:10.3354/aei00345.

Overton, K., Dempster, T., Oppedal, F., Kristiansen, T.S., Gismervik, K., Stien, L.H., 2019. Salmon lice treatments and salmon mortality in norwegian aquaculture: a review. Reviews in Aquaculture 11, 1398–1417. doi:10.1111/raq.12299.

Parra, L., Lloret, G., Lloret, J., Rodilla, M., 2018. Physical sensors for precision aquaculture: A review. IEEE Sensors Journal 18, 3915–3923. doi:10.1109/jsen.2018.2817158.

Patursson, O., 2008. Flow through and around fish farming nets. Thesis. University of New Hampshire.

Pike, A., Wadsworth, S., 1999. Sealice on salmonids: Their biology and control, in: Advances in Parasitology. Elsevier, pp. 233–337. doi:10.1016/s0065-308x(08)60233-x.

Plaut, I., 2001. Critical swimming speed: its ecological relevance. Comparative Biochemistry and Physiology Part A: Molecular and Integrative Physiology 131, 41–50. doi:10.1016/s1095-6433(01)00462-7.

Poppe, T., 2017. 'laks og lus: En dyrevelferdsmessig umulighet'. Aftenposten Innsikt URL: http://www.aftenposteninnsikt.no/klimamilj/laks-og-lus-en-dyrevelferdsmessig-umulighet. July/August 2017.

Powell, A., Treasurer, J.W., Pooley, C.L., Keay, A.J., Lloyd, R., Imsland, A.K., Garcia de Leaniz, C., 2018. Use of lumpfish for sea-lice control in salmon farming: Challenges and opportunities. Reviews in aquaculture 10, 683–702. doi:10.1111/raq.12194.

Rasmussen, H.W., Patursson, Ø., Simonsen, K., 2015. Visualisation of the wake behind fish farming sea cages. Aquacultural Engineering 64, 25–31. doi:10.1016/j.aquaeng.2014.12.001.

Remen, M., Aas, T.S., Vågseth, T., Torgersen, T., Olsen, R.E., Imsland, A., Oppedal, F., 2014. Production performance of atlantic salmon (salmo salar l.) postsmolts in cyclic hypoxia, and following compensatory growth. Aquaculture Research 45, 1355–1366. doi:10.1111/are.12082.

Remen, M., Oppedal, F., Imsland, A.K., Olsen, R.E., Torgersen, T., 2013. Hypoxia tolerance thresholds for post-smolt atlantic salmon: dependency of temperature and hypoxia acclimation. Aquaculture 416, 41–47. doi:10.1016/j.aquaculture.2013.08.024.

Remen, M., Sievers, M., Torgersen, T., Oppedal, F., 2016. The oxygen threshold for maximal feed intake of atlantic salmon post-smolts is highly temperature-dependent. Aquaculture 464, 582–592. doi:10.1016/j.aquaculture.2016.07.037.

Roberge, C., Normandeau, E., Einum, S., Guderley, H., Bernatchez, L., 2008. Genetic consequences of interbreeding between farmed and wild atlantic salmon: insights from the transcriptome. Molecular ecology 17, 314–324. doi:10.1111/j.1365-294x.2007.03438.x.

Röcklinsberg, H., 2015. Fish consumption: Choices in the intersection of public concern, fish welfare, food security, human health and climate change. Journal of Agricultural and Environmental Ethics 28, 533–551. doi:10.1007/s10806-014-9506-y.

Ruff, B., Marchant, J., Frost, A., 1995. Fish sizing and monitoring using a stereo image analysis system applied to fish farming. Aquacultural engineering 14, 155–173. doi:10.1016/0144-8609(94)p4433-c.

Sætre, R., 2007. The Norwegian coastal current: oceanography and climate. Tapir Academic Press Institute of Marine Research, Trondheim. doi:10.5860/choice.45-0267.

Sandberg, M.G., Lien, A.M., Sunde, L.M., Størkersen, K.V., Stien, L.H., Kristiansen, T.S., 2012. Erfaringer og analyser fra drift av oppdrettsanlegg på eksponerte lokaliteter. Report 8214054311. SINTEF Fiskeri og Havbruk.

Sigstadstø, E., 2017. Bransjeveileder lakselus: Bruk og hold av leppefisk. Report. FHF. URL: https://lusedata.no/wp-content/uploads/2012/05/Veileder-for-bruk-og-hold-av-leppefisk-oppdatert-v%c3%a5r-2017.pdf.

Simmonds, J., MacLennan, D.N., 2005. Fisheries acoustics: theory and practice. John Wiley and Sons.

Slagstad, D., McClimans, T.A., 2005. Modeling the ecosystem dynamics of the barents sea including the marginal ice zone: I. physical and chemical oceanography. Journal of Marine Systems 58, 1–18. doi:10.1016/j.jmarsys.2005.05.005.

Solstorm, D., Oldham, T., Solstorm, F., Klebert, P., Stien, L.H., Vågseth, T., Oppedal, F., 2018. Dissolved oxygen variability in a commercial sea-cage exposes farmed atlantic salmon to growth limiting conditions. Aquaculture 486, 122–129. doi:10.1016/j.aquaculture.2017.12.008.

Solstorm, F., Solstorm, D., Oppedal, F., Fern´o, A., Fraser, T.W.K., Olsen, R.E., 2015. Fast water currents reduce production performance of post-smolt atlantic salmon salmo salar. Aquaculture Environment Interactions 7, 125–134. doi:10.3354/aei00143.

Solstorm, F., Solstorm, D., Oppedal, F., Olsen, R.E., Stien, L.H., Fern´o, A., 2016. Not too slow, not too fast: water currents affect group structure, aggression and welfare in post-smolt atlantic salmon salmo salar. Aquaculture Environment Interactions 8, 339–347. doi:10.3354/aei00178.

Standards Norway, 2009. Marine fish farms-requirements for site survey, risk analyses, design, dimensioning, production, installation and operation, norsk standard ns 9415. E, Norway .

Stehfest, K.M., Carter, C.G., McAllister, J.D., Ross, J.D., Semmens, J.M., 2017. Response of atlantic salmon salmo salar to temperature and dissolved oxygen extremes established using animal-borne environmental sensors. Scientific Reports 7, 1–10. doi:10.1038/s41598-017-04806-2.

Stien, L.H., Bracke, M.B., Folkedal, O., Nilsson, J., Oppedal, F., Torgersen, T., Kittilsen, S., Midtlyng, P.J., Vindas, M.A., Øverli, Ø., 2013. Salmon welfare index model (swim 1.0): a semantic model for overall welfare assessment of caged atlantic salmon: review of the selected welfare indicators and model presentation. Reviews in Aquaculture 5, 33–57. doi:10.1111/j.1753-5131.2012.01083.x.

Stien, L.H., Lind, M.B., Oppedal, F., Wright, D.W., Seternes, T., 2018. Skirts on salmon production cages reduced salmon lice infestations without affecting fish welfare. Aquaculture 490, 281–287. doi:10.1016/j.aquaculture.2018.02.045.

Stien, L.H., Nilsson, J., Hevrøy, E.M., Oppedal, F., Kristiansen, T.S., Lien, A.M., Folkedal, O., 2012. Skirt around a salmon sea cage to reduce infestation of salmon lice resulted in low oxygen levels. Aquacultural Engineering 51, 21–25. doi:10.1016/j.aquaeng.2012.06.002.

Svåsand, T., Grefserud, E.S., Karlsen, Ø., Kvamme, B.O., Glover, K., Husa, V., Kristiansen, T.S., (Eds.), 2017. Risikorapport norsk fiskeoppdrett 2017. Report. Havforskningsinstituttet.

Svendsen, E., Føre, M., Økland, F., Gräns, A., Hedger, R.D., Alfredsen, J.A., Uglem, I., Rosten, C., Frank, K., Erikson, U., et al., 2020. Heart rate and swimming activity as stress indicators for atlantic salmon (salmo salar). Aquaculture 531, 735804. doi:10.1016/j.aquaculture.2020.735804.

Tang, M.F., Xu, T.J., Dong, G.H., Zhao, Y.P., Guo, W.J., 2017. Numerical simulation of the effects of fish behavior on flow dynamics around net cage. Applied Ocean Research 64, 258–280. doi:10.1016/j.apor.2017.03.006.

Thomson, R.E., Emery, W.J., 2014. Data analysis methods in physical oceanography. Elsevier. doi:10.1016/c2010-0-66362-0.

Thorstad, E.B., Whoriskey, F., Rikardsen, A.H., Aarestrup, K., 2011. Aquatic nomads: the life and migrations of the Atlantic salmon. Wiley-Blackwell. pp. 1–32. doi:10.1002/9781444327755.ch1.

Thorvaldsen, T., Holmen, I.M., Moe, H.K., 2015. The escape of fish from norwegian fish farms: Causes, risks and the influence of organisational aspects. Marine Policy 55, 33–38. doi:10.1016/j.marpol.2015.01.008.

Tilseth, S., Hansen, T., Møller, D., 1991. Historical development of salmon culture. Aquaculture 98, 1–9. doi:10.1016/0044-8486(91)90367-g.

Torrissen, O., Jones, S., Asche, F., Guttormsen, A., Skilbrei, O.T., Nilsen, F., Horsberg, T.E., Jackson, D., 2013. Salmon lice–impact on wild salmonids and salmon aquaculture. Journal of fish diseases 36, 171–194. doi:10.1111/jfd.12061.

Troell, M., Naylor, R.L., Metian, M., Beveridge, M., Tyedmers, P.H., Folke, C., Arrow, K.J., Barrett, S., Crépin, A.S., Ehrlich, P.R., 2014. Does aquaculture add resilience to the global food system? Proceedings of the National Academy of Sciences 111, 13257–13263. doi:10.1073/pnas.1404067111.

Turnbull, J.F., Huntingford, F.A., 2012. Welfare and aquaculture: where benefish fits in. Aquaculture Economics and Management 16, 433–440. doi:10.1080/13657305.2012.729249.

UN, 2019. World Population Prospects 2019: Highlights. Report. United Nations. doi:10.18356/13bf5476-en.

Volent, Z., Jónsdóttir, K.E., Misund, A., Steinhovden, K.B., Chauton, M.S., Sunde, L.M., 2020. Strategi lakselus 2017: Luseskjørt som ikke-medikamentell metode for forebygging og kontroll av lakselus – Utvikling av kunnskap om miljøforhold for økt effekt og redusert risiko (SKJERMTEK). Report 302003409. SINTEF Ocean.

Wildish, D., Keizer, P., Wilson, A., Martin, J., 1993. Seasonal changes of dissolved oxygen and plant nutrients in seawater near salmonid net pens in the macrotidal bay of fundy. Canadian Journal of Fisheries and Aquatic Sciences 50, 303–311. doi:10.1139/f93-035.

Winthereig-Rasmussen, H., Simonsen, K., Patursson, Ø., 2016. Flow through fish farming sea cages: Comparing computational fluid dynamics simulations with scaled and full-scale experimental data. Ocean Engineering 124, 21–31. doi:10.1016/j.oceaneng.2016.07.027.

Xu, Z., Qin, H., 2020. Fluid-structure interactions of cage based aquaculture: From structures to organisms. Ocean Engineering 217, 107961. doi:10.1016/j.oceaneng.2020.107961.

Yuen, J.W., Dempster, T., Oppedal, F., Hvas, M., 2019. Physiological performance of ballan wrasse (labrus bergylta) at different temperatures and its implication for cleaner fish usage in salmon aquaculture. Biological Control 135, 117–123. doi:10.1016/j.biocontrol.2019.05.007.

Zahradnik, J., 1987. Status and perspectives in the instrumentation of aquacultural facilities. IFAC Proceedings Volumes 20, 23–24. doi:10.1016/s1474-6670(17)59152-1.

Zhao, Y.P., Bi, C.W., Chen, C.P., Li, Y.C., Dong, G.H., 2015. Experimental study on flow velocity and mooring loads for multiple net cages in steady current. Aquacultural Engineering 67, 24–31. doi:10.1016/j.aquaeng.2015.05.005.

Zion, B., 2012. The use of computer vision technologies in aquaculture–a review. Computers and electronics in agriculture 88, 125–132. doi:10.1016/j.compag.2012.07.010.